arXiv:astro-ph/9912172v1 8 Dec 1999

TABLE 1
M15 STELLAR VELOCITY RESULTS

ID	RA	DEC	V(km s^{-1})	σ_V	m_V	Prob	ID$_{AC}$
5768	0.006	0.003	–108.2	3.2	15.22	0.312	
5831	0.007	–0.002	–116.5	3.4	15.49	0.448	AC214
5785	0.001	0.007	–115.7	12.0	17.02		
6290	–0.008	–0.010	–103.4	1.0	13.71	0.502	AC216
5933	–0.008	0.010	–79.9	1.1	14.55	0.000	AC215
5364	0.012	0.018	–101.3	2.7	15.87	0.071	AC210
5371	0.018	0.012	–107.9	8.6	15.94		
6541	–0.008	–0.022	–112.5	5.5	17.32		
6475	–0.024	–0.002	–107.3	7.6	16.43		
6498	–0.026	–0.001	–126.7	5.1	17.64		
6174	0.012	–0.024	–142.1	7.0	15.98		
5515	–0.003	0.026	–115.8	5.0	17.24		
6703	–0.022	–0.016	–90.5	4.5	17.98		
5610	0.027	–0.010	–104.8	2.9	16.37		
5469	0.029	–0.004	–123.0	0.8	13.66	0.702	AC212
6772	–0.021	–0.021	–109.3	2.6	14.86	0.020	
6833	–0.020	–0.024	–122.5	4.1	15.84		
5642	–0.014	0.029	–105.0	3.6	17.44	0.159	
5222	0.005	0.033	–106.0	8.2	17.77		
6654	0.000	–0.036	–108.2	4.8	17.83		
5002	0.020	0.031	–93.4	1.8	15.02	0.021	
5619	0.035	–0.018	–104.2	3.6	16.27		
6937	–0.039	–0.010	–123.1	5.6	15.77		
5132	0.042	0.000	–100.7	5.2	16.38		
6841	0.000	–0.045	–131.0	7.0	16.81		
4891	0.013	0.044	–74.9	6.5	17.50		
5389	0.043	–0.015	–121.3	4.8	15.58		
5127	–0.003	0.047	–86.4	3.4	17.09		
4951	0.048	0.006	–104.9	2.6	15.23	0.053	AC155
6127	–0.038	0.029	–107.9	9.3	16.92		
5395	0.046	–0.018	–114.2	2.9	16.58		AC213
4641	0.041	0.029	–117.5	8.2	16.41		
5434	0.046	–0.020	–126.5	10.3	17.53		
7313	–0.034	–0.037	–102.1	3.5	15.40		
7003	–0.002	–0.051	–120.1	5.8	16.48		
6183	–0.041	0.030	–95.8	2.8	16.38	0.206	
4626	0.044	0.027	–110.5	2.7	16.78	0.060	AC206
7185	–0.012	–0.051	–99.8	5.8	18.38		
6904	0.005	–0.053	–120.0	8.7	17.51		
4968	0.054	–0.001	–70.6	13.0	16.87		
6947	–0.053	0.004	–75.1	0.8	13.94	0.065	AC224
7404	–0.029	–0.046	–100.7	6.4	16.40		
4711	0.012	0.055	–119.0	6.5	15.89		
7292	–0.054	–0.015	–87.4	4.7	17.26		
5535	0.051	–0.030	–103.5	4.4	17.39		
5194	0.056	–0.017	–105.9	6.5	17.78		
7438	–0.054	–0.023	–103.5	4.9	15.91		
4862	0.060	–0.002	–73.8	2.2	15.40		AC154
4434	0.028	0.054	–107.1	6.4	18.76		
6928	–0.060	0.011	–107.8	1.0	14.18	0.084	
5819	0.047	–0.041	–78.8	3.6	16.01	0.000	
4841	–0.003	0.062	–100.2	5.4	18.78		
5529	0.054	–0.034	–100.2	3.0	15.69		
7718	–0.040	–0.052	–93.7	1.4	14.23	0.065	AC265
7711	–0.059	–0.033	–120.5	4.3	15.84		
7563	–0.066	–0.017	–137.0	5.7	17.14		

Table 1—*Continued*

ID	RA	DEC	V(km s^{-1})	$\sigma_{\rm V}$	m$_V$	Prob	ID$_{\rm AC}$
5112	0.065	–0.022	–116.7	3.2	15.91		AC153
7656	–0.023	–0.067	–102.3	3.6	17.38		
7783	–0.060	–0.037	–99.5	1.7	15.07	0.000	
7165	0.008	–0.070	–116.6	2.8	15.71	0.193	
4709	–0.004	0.071	–120.9	18.0	17.83		
6226	–0.057	0.044	–109.1	5.1	16.68		
4027	0.045	0.059	–112.2	4.2	16.76		AC205
4113	0.067	0.032	–96.3	0.9	13.33	0.250	AC160
6954	–0.071	0.022	–118.1	3.1	15.88	0.437	AC226
5719	–0.047	0.060	–105.3	3.0	16.32	0.722	
6358	–0.063	0.044	–108.7	2.5	16.71	0.958	
7706	–0.075	–0.016	–102.6	5.3	16.95		
7078	–0.076	0.020	–127.9	6.0	16.91		
4050	0.026	0.077	–125.3	5.3	15.88		
8082	–0.051	–0.062	–107.8	8.2	18.48		
3911	0.039	0.073	–98.4	1.9	15.32	0.113	
5277	0.072	–0.039	–85.8	6.4	15.95		
4440	–0.001	0.083	–119.3	8.1	18.42		
8151	–0.060	–0.058	–97.0	1.5	14.08	0.434	AC260
8090	–0.070	–0.044	–103.3	5.2	16.81		
8194	–0.052	–0.069	–100.7	2.3	15.61		AC261
5773	–0.056	0.066	–76.5	6.4	17.48		
4442	–0.006	0.089	–104.9	6.1	17.88		
4003	0.018	0.089	–121.0	6.2	15.92		
4226	0.090	0.001	–98.9	1.9	15.70		
6944	–0.083	0.035	–130.2	7.4	17.69		
6058	0.061	–0.068	–103.5	1.9	14.80	0.238	AC115
3891	0.089	0.022	–124.5	1.0	14.04	0.022	AC161
4328	–0.004	0.092	–109.5	3.4	16.95	0.038	
5361	0.079	–0.050	–99.1	6.5	18.79		
4975	0.086	–0.035	–112.4	5.6	16.67		
8355	–0.080	–0.049	–99.3	1.5	14.10	0.587	AC254
5844	–0.065	0.071	–105.7	10.5	17.47		
3708	0.029	0.093	–141.1	7.5	16.76		
3593	0.036	0.093	–103.5	4.8	16.51	0.680	
5608	0.079	–0.063	–108.5	2.0	14.87	0.733	AC113
8408	–0.093	–0.040	–117.1	1.3	13.86	0.287	AC255
8496	–0.048	–0.091	–92.0	3.2	16.46	0.807	
7520	–0.100	0.020	–81.5	11.2	17.20		
7610	–0.101	0.015	–112.0	3.1	15.90	0.010	AC269
3982	0.005	0.102	–92.2	1.8	15.35	0.964	AC198
5956	0.073	–0.074	–121.2	1.8	13.92	0.285	AC114
3393	0.047	0.094	–106.7	6.0	15.86		AC202
6962	–0.095	0.046	–100.6	2.7	16.71	0.022	
4965	0.097	–0.045	–112.8	7.6	16.19		AC142
8728	–0.087	–0.065	–108.0	1.4	15.58	0.816	
4683	–0.034	0.103	–134.2	5.1	16.16		
8777	–0.084	–0.070	–115.5	1.7	13.84	0.849	AC253
8369	–0.106	–0.024	–110.6	1.9	14.91	0.986	AC256
7488	0.026	–0.107	–111.8	7.2	16.82		
3200	0.094	0.058	–128.7	2.4	16.21	0.001	
6121	–0.082	0.075	–123.3	3.8	15.54		
8306	–0.109	–0.017	–122.2	3.8	16.76	0.000	
5407	0.091	–0.065	–95.5	1.5	13.97	0.000	AC112
3676	0.112	0.012	–106.1	4.8	17.52		
8429	–0.027	–0.109	–112.8	6.7	16.96		

TABLE 1—*Continued*

ID	RA	DEC	V(km s^{-1})	$\sigma_{\rm V}$	m$_V$	Prob	ID$_{\rm AC}$
5601	0.090	–0.073	–104.4	3.4	16.02		
8760	–0.048	–0.106	–125.6	17.7	17.72		
8655	–0.109	–0.038	–100.0	3.0	16.34		
6041	–0.085	0.081	–98.3	0.9	13.32	0.142	AC3
6990	–0.105	0.054	–128.9	3.8	15.99		
7823	0.016	–0.117	–111.4	3.3	16.29		
8578	–0.114	–0.028	–108.1	4.9	15.86		
4658	–0.041	0.112	–102.7	1.8	15.39	0.969	
3356	0.118	0.023	–124.1	5.9	17.30		
4215	0.118	–0.026	–129.5	5.2	16.75		
8417	–0.015	–0.120	–114.0	2.4	16.02		
9044	–0.083	–0.090	–113.5	5.2	18.43		
3371	0.021	0.122	–94.2	3.6	16.27		
2883	0.093	0.080	–104.5	2.0	15.38	0.486	AC165
3693	–0.001	0.125	–103.5	4.5	16.55		
4607	–0.043	0.117	–112.8	5.7	15.53		
5012	–0.060	0.111	–94.0	9.0	17.22		
2989	0.117	0.048	–110.2	1.9	14.76		AC163
4847	–0.054	0.114	–124.0	6.1	16.13		
7802	–0.124	0.027	–80.2	3.9	14.59		
3987	0.128	–0.023	–102.4	2.1	15.48		AC158
3809	–0.015	0.132	–95.3	1.5	14.80	0.157	AC185
2670	0.089	0.100	–97.7	3.4	16.26		
3159	0.133	0.021	–100.8	1.9	15.52		AC169
7830	0.031	–0.132	–109.5	2.2	15.50		
2688	0.073	0.115	–119.3	4.6	16.35		
5166	0.114	–0.075	–117.5	0.6	13.57	0.000	AC111
4551	–0.050	0.127	–117.8	4.7	16.31		
3199	0.018	0.136	–116.1	2.2	15.64	0.049	AC181
2703	0.066	0.121	–90.9	0.9	13.51	0.033	AC178
2687	0.121	0.066	–92.4	1.7	14.49	0.366	AC166
2945	0.135	0.033	–114.2	2.5	16.33		
9387	–0.096	–0.100	–108.6	3.8	17.11		
3316	0.006	0.140	–116.8	2.8	16.15	0.051	
2976	0.030	0.137	–110.7	1.9	15.43	0.251	AC179
2576	0.114	0.081	–120.3	3.9	17.03		
5687	–0.094	0.109	–95.2	6.1	17.85		
2774	0.044	0.139	–104.2	6.0	17.74		
2461	0.096	0.108	–123.2	5.4	16.56		
2683	0.135	0.052	–121.5	3.7	17.11		
4065	0.141	–0.041	–95.8	3.5	16.02		
7473	–0.135	0.058	–109.5	4.5	15.83		
2937	0.147	0.021	–104.9	6.3	16.54		
6023	0.103	–0.109	–99.1	2.4	14.71		AC117
4872	0.130	–0.074	–125.2	4.4	17.12		
8380	0.016	–0.149	–120.6	2.4	15.56		
4295	0.140	–0.053	–80.6	1.9	15.17		AC107
3962	–0.036	0.146	–92.7	5.3	15.96		
7583	0.054	–0.141	–112.5	7.2	16.40		
3084	0.151	0.007	–97.2	1.8	15.31	0.000	AC171
8991	–0.150	–0.018	–112.4	2.2	15.72	0.321	
2392	0.129	0.081	–129.0	6.1	16.64		
8321	–0.150	0.024	–102.7	1.8	14.93	0.432	AC233
2997	0.014	0.153	–110.4	5.5	15.78		
5089	0.127	–0.084	–102.9	1.2	14.15	0.182	AC110
7638	–0.145	0.059	–114.9	5.0	16.81		

TABLE 1—*Continued*

ID	RA	DEC	V(km s^{-1})	σ_V	m$_V$	Prob	ID$_{AC}$
2777	0.155	0.025	–99.9	3.9	15.99		
3308	0.157	–0.013	–105.1	5.3	16.57		
6525	–0.124	0.098	–125.8	13.0	17.07		
8700	–0.158	0.009	–91.5	4.6	15.91		
2357	0.072	0.142	–102.6	1.6	14.99	0.914	
7669	0.058	–0.150	–92.5	2.2	15.44		
7593	–0.147	0.064	–99.0	10.7	18.77		
2769	0.160	0.020	–117.4	2.0	15.28		
8767	0.007	–0.162	–115.9	3.8	15.70		
8998	–0.162	–0.006	–92.5	1.6	14.54	0.916	
6313	–0.124	0.108	–100.0	1.7	14.74	0.908	AC292
9355	–0.161	–0.032	–114.4	4.7	15.93		
7135	0.083	–0.145	–113.1	7.7	16.99		
6440	0.104	–0.131	–99.5	2.9	16.51		
9936	–0.107	–0.128	–110.1	0.8	13.44	0.026	AC6
4915	0.143	–0.090	–109.4	3.1	15.93		AC109
2009	0.114	0.126	–88.6	7.0	15.98		
5681	0.126	–0.115	–105.1	2.0	15.56		
9180	–0.014	–0.169	–114.1	4.0	17.67		
7384	–0.151	0.079	–104.6	2.1	15.60	0.508	AC296
9281	–0.169	–0.019	–98.7	1.9	15.34	0.183	
3921	0.163	–0.054	–102.3	1.8	14.47		AC106
5836	–0.117	0.125	–99.2	1.5	15.30	0.022	AC291
2017	0.141	0.097	–96.2	2.9	15.43		AC769
6474	–0.134	0.110	–126.7	3.1	15.90	0.170	
2657	0.017	0.174	–107.0	3.3	15.58		AC184
8977	–0.174	0.007	–115.5	3.8	16.04	0.114	
7695	0.068	–0.161	–109.4	4.3	16.01		
3724	–0.046	0.169	–116.0	3.4	18.24		
6898	–0.145	0.100	–108.0	2.3	15.81	0.609	AC293
9882	–0.163	–0.067	–87.6	5.1	16.80		
4176	0.163	–0.070	–96.8	0.8	13.59	0.023	AC104
8374	0.041	–0.174	–111.6	2.3	15.75		AC125
1897	0.148	0.099	–105.4	4.7	17.02		
9546	–0.033	–0.175	–88.1	9.8	17.45		
9234	–0.177	–0.006	–116.1	3.7	16.00	0.764	AC238
3077	0.178	–0.020	–104.2	4.3	16.67		
2173	0.171	0.056	–121.2	5.6	15.89		AC175
6212	0.120	–0.136	–94.8	5.8	16.89		
4341	–0.076	0.164	–111.9	1.9	15.06	0.157	AC189
2363	0.181	0.031	–109.7	10.0	17.72		
3592	–0.046	0.177	–111.7	1.8	15.07	0.775	AC188
8107	–0.174	0.061	–110.8	3.1	15.01	0.000	AC297
7429	0.086	–0.164	–117.3	4.3	16.84		
9452	–0.018	–0.184	–88.1	2.7	15.51		
4286	0.169	–0.081	–104.8	2.8	16.26		
1948	0.176	0.067	–113.0	3.6	17.65		
3783	0.178	–0.063	–111.4	1.7	14.59		AC105
4456	–0.086	0.169	–100.0	1.7	14.77	0.352	
5497	–0.120	0.146	–122.3	3.2	16.08	0.228	
9834	–0.044	–0.184	–103.4	9.8	18.67		
10311	–0.120	–0.148	–82.8	2.3	15.74		
2560	0.191	0.004	–119.3	2.2	15.25	0.019	AC100
10353	–0.132	–0.139	–111.5	3.2	16.12		
6670	–0.151	0.118	–80.5	6.6	18.54		
1644	0.124	0.148	–117.4	6.3	16.48		

TABLE 1—*Continued*

ID	RA	DEC	V(km s^{-1})	σ_V	m_V	Prob	ID_{AC}
2073	0.050	0.187	–96.0	4.3	17.45	0.015	
4575	0.168	–0.096	–109.3	8.2	17.15		
10077	–0.183	–0.063	–101.2	2.2	15.62	0.991	AC246
9928	–0.190	–0.043	–105.5	3.0	16.39		
9228	0.009	–0.196	–85.7	9.0	17.92		
8944	–0.194	0.030	–105.6	1.8	15.10	0.901	AC298
8808	0.036	–0.194	–102.6	3.6	15.92		
1797	0.074	0.182	–97.1	5.6	15.92		
3950	0.182	–0.076	–95.4	7.2	18.29		
1740	0.183	0.077	–106.8	1.7	15.54	0.000	
4190	0.180	–0.087	–89.5	6.1	17.17		
8737	0.042	–0.196	–108.3	3.0	15.87		AC127
9039	0.026	–0.200	–110.9	5.5	17.31		
1511	0.124	0.159	–98.6	6.7	17.50		
1868	0.056	0.195	–109.2	7.8	18.17		
10399	–0.180	–0.094	–95.7	0.8	13.37	0.912	AC247
10149	–0.195	–0.057	–73.7	7.0	16.83		
8366	0.062	–0.194	–107.6	5.2	18.02		
1585	0.184	0.092	–111.2	4.0	17.42		
10361	–0.086	–0.186	–98.4	3.8	15.91		
6992	0.115	–0.170	–100.2	4.5	16.64		
2011	0.205	0.033	–104.4	6.2	17.07		
10075	–0.046	–0.202	–96.2	6.7	18.61		
7001	–0.170	0.120	–116.3	2.3	15.57	0.716	
4843	0.173	–0.117	–108.2	1.4	13.85	0.150	AC616
1361	0.144	0.153	–105.8	7.3	17.35		
1990	0.035	0.208	–106.1	5.8	17.75		
1581	0.195	0.081	–102.1	2.0	15.52		AC706
10331	–0.069	–0.201	–92.3	1.9	15.18		AC442
1543	0.085	0.196	–90.5	3.2	16.56		
10097	–0.038	–0.212	–114.2	3.5	16.05		AC413
10602	–0.112	–0.185	–106.7	2.0	15.39		
6082	–0.155	0.151	–104.6	2.0	15.57		
10534	–0.197	–0.091	–86.4	2.1	15.47		
10451	–0.202	–0.076	–115.6	4.5	16.89		
8749	–0.209	0.060	–100.3	5.3	17.30		
4421	0.189	–0.109	–107.6	3.3	15.86		AC617
10356	–0.063	–0.209	–110.2	6.2	15.60		
1222	0.172	0.136	–124.3	1.4	14.77	0.043	AC768
3315	–0.062	0.210	–109.4	3.4	15.73		AC270
5241	–0.134	0.173	–115.8	1.1	14.29	0.000	AC279
9496	–0.219	0.018	–93.1	5.1	17.83		
9258	–0.217	0.033	–93.4	2.8	16.17		
2101	0.015	0.221	–103.8	2.9	16.95		
1507	0.070	0.214	–111.7	2.8	16.23		
5615	0.166	–0.152	–94.1	2.1	15.61		
1254	0.199	0.106	–106.3	1.4	12.92	0.000	AC5
1563	0.217	0.060	–99.8	3.5	15.95		
1352	0.094	0.206	–106.6	4.6	15.95		
2092	0.228	0.005	–116.8	5.6	15.94		AC621
1082	0.165	0.158	–112.0	5.3	17.63		
9945	–0.009	–0.229	–102.2	2.1	15.35		AC412
2606	–0.032	0.227	–117.8	6.7	17.17		
5327	–0.144	0.180	–89.1	7.5	15.92		AC280
5613	–0.153	0.173	–111.7	8.1	17.39		
1057	0.148	0.178	–112.1	6.5	17.16		

Table 1—*Continued*

ID	RA	DEC	V(km s^{-1})	σ_{V}	m$_V$	Prob	ID$_{\mathrm{AC}}$
4756	0.192	–0.131	–90.2	0.9	13.49	0.001	AC615
10749	–0.211	–0.097	–115.6	3.0	16.78		
7363	0.123	–0.199	–119.7	5.1	16.69		
10910	–0.135	–0.192	–98.6	6.5	17.12		
10494	–0.228	–0.054	–113.0	6.0	17.73		
1056	0.199	0.126	–102.8	3.5	16.56		
1227	0.089	0.220	–116.7	4.6	16.64		
2299	–0.016	0.237	–93.5	2.1	15.35		
1732	0.028	0.237	–96.2	2.1	15.40		AC779
8585	0.079	–0.225	–110.2	2.1	15.79		
942	0.185	0.150	–109.0	3.2	16.48		
10923	–0.125	–0.203	–94.6	2.4	15.94		
5892	–0.165	0.172	–113.8	2.0	15.56		
1288	0.228	0.073	–98.9	4.8	16.68		
1572	0.236	0.040	–98.8	2.2	15.62		AC624
2319	0.238	–0.023	–125.5	2.2	15.23		AC620
10464	–0.048	–0.234	–96.7	0.8	13.04	0.278	AC414
6653	–0.184	0.152	–79.7	2.4	15.73		
10373	–0.237	–0.034	–81.0	3.0	16.54		
6261	0.160	–0.179	–92.9	2.7	16.52		
897	0.172	0.168	–103.8	3.0	16.41		
1902	0.009	0.241	–102.5	2.6	15.86		
1051	0.213	0.112	–108.2	6.3	17.19		
10881	–0.110	–0.215	–96.3	4.1	15.96		AC447
11031	–0.144	–0.194	–107.2	2.4	16.27		
40001	0.127	–0.206	–111.7	4.8	16.50		
906	0.194	0.144	–109.4	6.7	17.73		
3748	0.219	–0.103	–108.6	2.0	15.27		AC618
1174	0.227	0.085	–106.1	9.4	18.57		
8845	–0.231	0.076	–101.8	2.5	16.15		
9158	–0.237	0.060	–111.3	1.8	14.94	0.008	AC303
11095	–0.200	–0.143	–91.1	5.7	16.94		
10012	0.004	–0.247	–84.6	0.6	12.81	0.037	AC411
889	0.135	0.206	–110.9	8.0	18.50		
2122	0.246	–0.016	–122.7	3.1	16.38		
1761	0.014	0.247	–114.5	0.9	13.89	0.848	AC780
2984	0.237	–0.074	–113.1	4.9	17.41		
7641	0.125	–0.215	–106.3	2.1	15.85		
860	0.215	0.127	–108.2	4.6	17.85		
25783	0.180	–0.176	–121.0	1.1	14.18	0.524	AC9
3172	–0.081	0.237	–81.8	1.0	13.94	0.119	AC271
733	0.160	0.195	–105.8	3.2	15.68		AC764
2431	–0.040	0.249	–91.3	8.1	18.12		
1422	0.251	0.037	–100.4	0.7	13.58	0.796	AC623
687	0.185	0.175	–115.2	2.5	16.15		
1548	0.253	0.024	–117.5	3.0	15.67		
10902	–0.089	–0.238	–104.4	6.6	16.88		
752	0.215	0.138	–116.5	2.1	15.74		AC708
11081	–0.229	–0.113	–111.4	0.8	13.76	0.600	AC488
701	0.207	0.151	–84.7	8.0	17.25		
2127	–0.020	0.255	–107.4	3.3	15.15		
824	0.115	0.232	–99.1	7.3	17.83		
10475	–0.025	–0.258	–99.0	4.3	17.43		
3696	–0.109	0.235	–101.4	5.3	17.83		
4454	–0.137	0.220	–104.8	4.2	16.46		
10507	–0.260	–0.023	–92.3	6.6	17.35		

TABLE 1—*Continued*

ID	RA	DEC	V(km s^{-1})	σ_V	m_V	Prob	ID$_{AC}$
8409	0.104	–0.240	–95.8	1.9	15.44	0.001	AC604
2103	–0.024	0.261	–119.7	1.5	14.37	0.623	AC783
10861	–0.253	–0.066	–106.3	3.4	16.90		
40002	–0.203	–0.167	–81.6	1.6	15.31	0.676	AC484
9934	0.026	–0.263	–92.8	3.9	17.80		
6217	–0.192	0.182	–92.1	2.6	16.05		
9923	–0.262	0.031	–106.8	6.8	17.42		
40003	–0.139	–0.226	–108.6	4.1	17.42		
40004	0.133	–0.231	–91.2	1.7	15.65	0.486	
1619	0.266	0.005	–107.8	4.0	17.33		
5069	–0.161	0.211	–108.4	1.5	14.73	0.046	AC281
10197	–0.265	0.011	–102.4	5.5	17.28		
40005	–0.166	–0.209	–119.0	2.2	16.19		
1617	0.008	0.268	–97.4	6.7	17.53		
2528	–0.060	0.262	–120.5	7.6	16.09		
3801	–0.120	0.240	–92.0	2.6	16.45		
40006	–0.225	–0.148	–117.7	5.2	17.24		
9181	0.076	–0.259	–96.3	4.9	18.35		
40007	0.103	–0.250	–99.7	5.6	18.05		
40008	0.169	–0.212	–105.4	4.6	17.90		
5293	–0.172	0.210	–111.9	2.5	16.16		
40009	–0.220	–0.158	–117.2	5.2	17.76		
2156	0.270	–0.044	–112.6	7.4	17.41		
11087	–0.085	–0.260	–126.2	1.2	14.09	0.211	AC8
515	0.236	0.140	–120.1	4.9	16.88		
8886	–0.256	0.099	–105.7	3.1	15.84		
10873	–0.269	–0.051	–110.0	8.8	17.63		
10635	–0.028	–0.273	–115.4	2.3	15.11		AC415
2787	–0.080	0.263	–108.7	1.9	15.32		
5680	–0.185	0.203	–112.2	9.6	17.56		
24827	0.232	–0.150	–99.1	6.8	17.27		
4411	–0.147	0.234	–114.0	2.8	16.05		
10515	–0.276	–0.007	–98.6	1.7	15.07	0.227	
819	0.085	0.263	–118.6	3.4	16.11		AC760
2515	–0.066	0.269	–117.5	1.0	14.27	0.011	AC787
9149	0.083	–0.265	–99.7	6.3	17.76		
505	0.244	0.132	–84.0	3.2	16.28		AC709
8754	–0.256	0.107	–89.2	1.9	15.30	0.120	
10256	–0.278	0.018	–118.5	6.1	17.26		
24937	0.218	–0.177	–114.1	10.0	18.27		
10983	–0.061	–0.273	–122.6	8.9	17.53		
10470	–0.002	–0.281	–112.1	2.0	15.27		AC416
24834	0.247	–0.136	–103.9	1.4	15.05	0.592	AC614
40010	–0.192	–0.206	–101.7	5.9	17.23		
3129	–0.103	0.263	–116.0	0.8	13.23	0.117	AC1
9714	–0.276	0.062	–89.7	3.9	16.31		
736	0.273	0.080	–91.1	2.0	15.38		AC701
402	0.249	0.140	–87.4	5.1	17.02		
1748	0.285	–0.027	–106.9	3.7	16.70		
4894	–0.170	0.230	–94.4	2.8	15.96		
40011	–0.211	–0.192	–98.6	8.3	17.50		
9528	–0.276	0.074	–121.2	2.5	15.67		
40012	–0.222	–0.181	–110.1	4.8	17.31		
40013	0.072	–0.279	–117.6	3.5	16.42		
40014	–0.170	–0.233	–109.8	4.0	17.26		
40015	–0.083	–0.277	–113.0	2.0	15.81		AC440

TABLE 1—*Continued*

ID	RA	DEC	V(km s^{-1})	σ_{V}	m$_V$	Prob	ID$_{\mathrm{AC}}$
702	0.082	0.278	–109.0	4.5	15.97		
615	0.094	0.274	–97.7	6.4	18.42		
1323	0.290	0.007	–103.1	5.2	17.89		
905	0.286	0.050	–103.5	6.4	18.62		
8102	–0.253	0.143	–104.8	8.0	17.58		
25045	0.239	–0.167	–89.9	3.0	16.49		
10868	–0.290	–0.029	–98.1	8.3	17.87		
2619	0.281	–0.084	–91.2	2.0	16.06		
10163	–0.290	0.040	–121.5	2.8	15.72		AC314
24847	0.107	–0.273	–109.8	6.5	17.79		
716	0.072	0.286	–120.0	1.7	14.94	0.247	AC759
412	0.271	0.117	–108.8	4.8	16.08		AC700
1400	–0.001	0.296	–94.7	3.5	16.71		
40016	–0.133	–0.265	–118.4	1.4	14.42	0.262	AC451
40017	–0.227	–0.190	–116.6	5.5	17.21		
24941	0.270	–0.127	–114.4	3.6	16.41		
1481	0.298	–0.017	–94.3	3.4	16.92		
24989	0.122	–0.273	–103.0	7.9	17.41		
40018	–0.259	–0.153	–110.5	3.7	17.37		
204	0.159	0.257	–102.9	5.2	17.24		
1084	0.301	0.019	–107.7	1.2	14.37	0.977	AC7
2720	–0.098	0.286	–120.9	2.0	15.65		
10026	–0.296	0.059	–125.5	0.7	13.44	0.388	AC4
332	0.124	0.276	–109.6	0.6	13.27	0.685	AC761
25188	0.163	–0.255	–116.4	3.0	16.55	0.621	
25124	0.264	–0.152	–105.4	3.3	16.72	0.532	
3480	–0.135	0.273	–108.4	2.8	16.69		
40019	–0.114	–0.284	–82.1	5.3	17.18		AC452
405	0.102	0.289	–116.2	1.6	14.33	0.379	AC758
122	0.256	0.170	–100.6	2.9	16.70		
25255	0.252	–0.177	–98.9	5.3	17.87		
1685	0.306	–0.042	–123.6	1.2	14.11	0.795	AC576
40020	–0.143	–0.277	–98.1	3.9	17.63		
3849	–0.153	0.271	–96.6	5.5	17.23		
40021	–0.297	–0.091	–117.0	2.2	16.19	0.231	
40022	–0.169	–0.262	–92.2	3.4	17.01	0.592	AC455
8390	–0.274	0.148	–111.5	7.4	17.78		
36	0.189	0.249	–122.2	1.4	14.51	0.908	AC715
25419	0.225	–0.219	–119.5	3.4	15.89	0.707	
2763	–0.109	0.294	–119.7	7.4	17.75		
40023	–0.126	–0.287	–98.6	9.5	17.88		
40024	–0.280	0.143	–120.3	5.5	17.67		
9029	–0.289	0.122	–113.1	4.7	17.48		
25086	0.112	–0.294	–96.4	4.0	17.11		
40025	0.198	0.245	–94.9	1.4	14.62	0.005	AC716
25424	0.205	–0.239	–117.1	2.9	16.90		
30	0.262	0.175	–119.2	1.3	14.43	0.000	AC710
40026	–0.252	–0.191	–115.4	2.0	16.30	0.079	
25155	0.289	–0.131	–96.1	6.6	17.50		
40027	–0.278	–0.152	–131.8	7.1	17.00		
393	0.087	0.306	–128.3	5.7	17.54		
1506	0.316	–0.037	–106.9	5.4	17.90		
40028	–0.252	0.194	–113.6	7.1	18.13		
1723	–0.050	0.316	–105.1	3.8	15.97		
9956	–0.311	0.079	–111.3	3.3	16.41		
25508	0.242	–0.212	–114.1	1.6	14.91	0.592	AC590

TABLE 1—*Continued*

ID	RA	DEC	V(km s^{-1})	σ_V	m_V	Prob	ID_{AC}
25068	0.094	–0.309	–106.5	8.5	17.51		
40029	–0.153	–0.285	–101.9	5.4	17.31		
40030	0.257	0.198	–121.7	9.5	17.40		
40031	–0.292	0.141	–103.6	3.8	15.20		
40032	–0.307	–0.102	–102.4	1.3	14.61	0.155	AC493
25376	0.287	–0.156	–89.7	2.4	16.25	0.252	
40033	–0.243	–0.217	–96.2	6.8	17.84		
25354	0.136	–0.298	–124.9	3.8	16.98	0.890	
48	0.138	0.297	–105.4	4.0	17.75		
40034	–0.138	–0.298	–122.4	7.6	17.36		
40035	–0.278	0.173	–98.4	6.5	17.75		
40036	–0.297	0.143	–100.6	1.6	15.50	0.447	AC327
10339	–0.325	0.061	–98.9	1.9	15.26		
25323	0.303	–0.135	–89.7	2.9	16.15		
40037	–0.246	0.221	–116.1	1.4	15.75	0.045	
10491	–0.327	0.049	–109.2	5.4	15.88		AC315
40038	–0.329	–0.036	–96.2	7.0	18.54		
40039	0.196	0.268	–111.2	3.7	17.84	0.312	
133	0.314	0.108	–96.6	2.7	16.46		
40040	–0.176	–0.282	–109.9	0.8	13.22	0.433	AC456
25096	0.082	–0.324	–115.0	1.9	15.61	0.521	
25650	0.192	–0.276	–101.7	4.7	16.89		
40041	0.335	–0.017	–111.7	8.3	17.87		
25715	0.237	–0.240	–93.6	9.7	17.21		
638	0.336	0.025	–121.0	1.9	15.21		AC698
40042	–0.023	–0.336	–114.5	0.7	13.65	0.715	AC417
26	0.125	0.315	–121.7	3.6	15.86		AC757
40043	0.151	0.305	–94.5	6.2	18.30		
40044	–0.314	–0.130	–125.1	1.6	15.73	0.502	
225	0.332	0.078	–98.5	2.4	16.13		
40045	–0.279	–0.196	–124.8	5.7	17.38		
13611	0.213	0.268	–102.3	3.9	17.13		
40046	0.160	0.305	–124.0	0.7	13.59	0.728	AC2
25640	0.295	–0.175	–136.8	3.7	16.28		
40047	–0.201	–0.280	–124.6	0.9	13.47	0.018	AC457
40048	0.130	0.320	–98.6	5.6	17.71		
25814	0.248	–0.240	–105.3	10.1	16.62		
25693	0.292	–0.185	–92.1	6.6	15.76		AC586
1883	–0.083	0.335	–98.4	4.3	16.93		
13449	0.230	0.259	–113.5	3.0	16.26	0.627	
40049	–0.234	–0.255	–103.4	9.4	18.75		
40050	–0.323	0.124	–104.4	2.1	16.24	0.190	
40051	0.347	–0.016	–118.2	1.4	15.51	0.000	AC573
14001	0.182	0.297	–111.1	1.8	15.56	0.152	
25838	0.266	–0.225	–98.0	2.1	15.98		
208	0.341	0.071	–107.3	5.4	17.12		
40052	–0.322	0.139	–100.4	1.2	14.43	0.593	AC328
25518	0.121	–0.331	–102.0	3.3	16.58	0.403	
25313	0.087	–0.342	–98.4	2.0	15.61	0.929	AC392
13411	0.237	0.261	–103.7	2.2	16.06		
1864	–0.089	0.342	–109.2	5.8	17.32		
40053	–0.138	0.325	–100.3	4.1	16.66		AC837
40054	–0.335	0.112	–97.7	7.4	17.96		
11007	–0.352	0.022	–92.6	6.5	16.10		
12959	0.274	0.227	–106.5	4.5	17.23		
40055	0.356	–0.020	–118.1	3.8	17.21		

TABLE 1—*Continued*

ID	RA	DEC	V(km s^{-1})	σ_{V}	m_V	Prob	ID$_{\mathrm{AC}}$
25974	0.227	–0.277	–96.5	4.2	17.51		
40056	–0.291	–0.210	–117.7	3.3	17.24	0.837	
40057	–0.013	–0.361	–135.8	1.9	15.16	0.819	AC418
40058	–0.238	0.272	–97.4	8.1	18.43		
261	0.359	0.044	–117.2	2.6	15.86		AC696
40059	–0.293	–0.214	–107.8	1.8	15.69	0.576	AC473
25828	0.158	–0.329	–111.2	5.9	17.27		
40060	0.347	0.112	–86.2	4.8	17.60		
40061	–0.253	0.263	–117.1	3.8	17.17		
12109	0.335	0.149	–100.9	1.7	15.42	0.838	
40062	–0.039	–0.364	–116.6	3.7	17.20		
40063	–0.271	0.247	–130.5	2.1	16.70	0.405	
26029	0.299	–0.213	–118.3	1.6	15.18	0.306	AC587
40064	–0.344	–0.130	–110.4	1.7	15.65	0.353	
13828	0.211	0.302	–119.3	3.7	16.78		
40065	–0.223	–0.293	–100.4	2.8	16.50		
40066	0.369	–0.003	–125.8	3.9	16.95	0.848	
25703	0.345	–0.135	–109.9	1.6	15.91	0.000	
1002	–0.035	0.368	–114.1	7.4	18.15		
40067	0.118	0.351	–132.1	5.3	17.79		
40068	0.354	0.110	–110.3	6.6	18.09		
40069	–0.233	0.290	–112.1	8.0	17.90		
26178	0.244	–0.282	–101.4	4.0	16.82		
351	0.373	0.020	–108.7	10.0	18.01		
1128	–0.048	0.369	–119.8	8.6	17.71		
40070	–0.065	–0.367	–113.2	3.4	17.42	0.061	
102	0.372	0.052	–93.6	4.6	16.07		AC697
13340	0.259	0.272	–98.2	4.1	16.40	0.098	
14100	0.192	0.324	–103.0	5.8	17.28		
40071	–0.141	0.350	–107.5	4.5	17.27	0.788	AC836
40072	0.095	0.365	–131.1	6.0	17.56		
25724	0.112	–0.361	–119.8	8.4	17.59		
14365	0.163	0.341	–97.6	5.2	16.98		
40073	–0.236	–0.296	–107.1	6.9	17.59		
26245	0.255	–0.281	–111.6	2.3	15.22	0.688	AC594
40074	–0.149	–0.349	–111.8	3.2	17.10		
40075	–0.375	–0.053	–78.1	2.2	16.65		
40076	–0.080	–0.372	–102.3	2.1	16.41	0.715	
40077	–0.085	0.371	–107.9	6.0	17.07		
13314	0.266	0.275	–102.0	3.5	16.69	0.131	
25929	0.353	–0.151	–106.1	3.4	15.86		
40078	0.374	0.089	–135.7	4.7	17.08	0.770	
40079	–0.332	–0.193	–117.4	6.3	17.37		
25964	0.141	–0.359	–100.9	8.9	17.47		
26261	0.209	–0.327	–93.3	3.4	15.22		AC598
25505	0.380	–0.080	–114.7	2.4	16.25	0.856	
40080	–0.211	0.326	–111.7	2.5	16.62	0.715	
40081	–0.388	–0.039	–98.8	4.9	17.51		
40082	–0.293	–0.258	–82.7	2.1	16.43	0.665	
40083	–0.330	0.209	–118.7	4.6	17.21		
40084	–0.190	–0.343	–97.5	2.7	16.58		
501	–0.012	0.393	–125.0	6.3	17.05		
12316	0.344	0.192	–85.0	4.5	17.23		
40085	–0.386	0.084	–106.0	7.4	17.96		
26116	–0.041	–0.394	–126.0	6.2	17.91		
40086	–0.285	0.275	–95.3	4.4	17.18		AC355

Table 1—*Continued*

ID	RA	DEC	V(km s^{-1})	σ_V	m_V	Prob	ID_{AC}
40087	–0.365	–0.152	–109.8	4.9	17.33		
26453	0.278	–0.284	–93.9	1.6	14.93	0.000	AC595
40088	–0.397	–0.006	–109.4	3.6	16.64	0.412	AC517
13717	0.244	0.315	–96.7	7.4	18.17		
25951	0.377	–0.130	–101.6	9.5	17.47		
95	0.032	0.400	–102.6	5.0	18.66		
11609	0.385	0.112	–115.2	1.9	15.33	0.674	AC689
12476	0.340	0.214	–138.6	4.6	17.05		
11529	0.389	0.101	–122.2	2.1	15.84	0.776	
40089	–0.263	0.304	–121.7	1.7	15.67	0.166	
25101	0.000	–0.404	–102.5	2.5	16.23	0.671	
26546	0.303	–0.270	–95.4	4.8	16.43		
24828	–0.032	–0.405	–100.0	7.6	17.76		
40090	–0.326	0.242	–96.9	1.2	14.43	0.911	AC349
15012	0.105	0.393	–109.3	1.7	15.43	0.698	AC750
26549	0.259	–0.315	–103.3	1.5	15.13	0.461	AC596
40091	–0.313	–0.261	–106.6	2.4	16.65	0.367	
40092	–0.399	0.085	–98.6	3.7	17.37		
40093	–0.407	0.042	–107.3	5.1	17.61		
26422	0.193	–0.362	–120.4	2.1	15.92	0.433	
26284	0.371	–0.174	–110.4	3.9	16.77		
40094	–0.111	–0.395	–115.3	1.6	14.81	0.557	AC423
40095	–0.126	–0.391	–118.1	10.0	18.26		
40096	–0.211	0.353	–103.1	2.0	15.97	0.603	AC832
26056	0.109	–0.399	–119.0	5.8	16.95		
40097	–0.063	0.411	–124.7	2.9	17.15	0.559	
40098	–0.237	–0.341	–100.1	1.6	15.60	0.996	
40099	–0.401	0.108	–102.3	1.8	15.79	0.854	AC334
40100	–0.404	–0.098	–117.7	8.6	17.37		
40101	–0.406	–0.089	–76.7	4.4	16.65		
26586	0.337	–0.244	–102.3	3.1	16.43	0.917	
26311	0.380	–0.168	–101.5	2.8	17.33		AC566
24953	0.416	0.012	–117.9	4.0	15.86		
40102	–0.209	0.361	–112.9	3.1	16.73		
24857	0.417	0.023	–113.0	1.8	15.57	0.321	
26338	0.155	–0.389	–103.2	3.2	15.66		
40103	–0.336	–0.250	–110.0	5.5	17.51		
26366	0.383	–0.173	–108.8	5.3	15.83		
26425	0.169	–0.386	–112.5	3.7	16.66	0.471	
40104	–0.188	–0.377	–100.9	7.9	18.12		
40105	–0.293	–0.304	–126.1	2.2	15.37	0.225	AC466
40106	–0.404	0.123	–109.1	7.3	18.19		
14013	0.235	0.352	–114.8	1.1	13.97	0.414	AC739
25333	0.422	–0.022	–94.9	5.5	15.91		AC634
40107	–0.375	–0.198	–106.8	9.7	18.10		
26657	0.223	–0.362	–108.3	5.4	17.33		
25444	0.424	–0.031	–126.5	3.9	16.81		
40108	–0.074	0.419	–104.7	2.9	16.53	0.760	
40109	–0.199	–0.378	–107.9	7.1	17.88		
40110	–0.338	–0.260	–105.0	3.5	16.92	0.131	
40111	–0.367	–0.220	–85.3	6.3	17.74		
15326	0.081	0.421	–94.6	4.2	15.90		
40112	–0.368	0.221	–103.5	1.7	15.76	0.441	
40113	–0.350	0.250	–122.4	2.0	15.99	0.081	
25689	0.038	–0.430	–81.2	3.9	16.89		
13234	0.306	0.303	–95.7	3.3	16.65		

TABLE 1—*Continued*

ID	RA	DEC	V(km s^{-1})	σ_V	m$_V$	Prob	ID$_{AC}$
25960	0.422	–0.088	–101.9	5.6	17.97		
40114	–0.076	0.424	–105.7	3.0	16.89	0.468	
11977	0.391	0.184	–124.4	1.4	14.71	0.354	AC681
40115	–0.283	–0.326	–101.3	3.2	16.76		
40116	–0.425	0.078	–83.7	3.5	17.30	0.934	
40117	–0.308	0.306	–110.3	9.1	17.75		
26870	0.318	–0.297	–109.5	8.5	17.62		
26619	0.385	–0.201	–83.0	8.1	15.62		
40118	–0.281	–0.332	–112.6	6.8	16.84		
14667	0.169	0.401	–94.3	1.3	14.37	0.545	AC736
40119	–0.126	–0.417	–122.2	8.1	17.05		
40120	–0.303	–0.314	–85.8	9.3	18.23		
40121	–0.110	0.423	–100.9	6.6	18.17		
13205	0.314	0.306	–122.4	4.4	17.12		
40122	–0.389	–0.203	–100.4	2.3	16.72	0.917	
26860	0.249	–0.362	–133.6	2.7	16.20	0.447	
40123	–0.121	–0.423	–110.6	1.8	15.51	0.451	AC424
14225	0.224	0.379	–103.7	1.8	15.06	0.334	AC738
12467	0.369	0.242	–105.7	6.0	17.24		
40124	–0.415	–0.155	–97.2	2.2	15.89	0.792	AC508
25971	0.058	–0.439	–97.6	3.4	15.84		
26796	0.385	–0.222	–103.7	1.5	15.07	0.799	AC564
26735	0.392	–0.208	–118.8	1.5	15.05	0.056	AC565
26575	0.408	–0.174	–127.1	8.7	17.33		
40125	–0.437	–0.081	–87.8	5.2	17.89		
26674	0.404	–0.189	–108.4	8.6	17.79		
40126	–0.409	0.180	–97.8	1.7	15.90	0.403	
25544	0.002	–0.448	–99.0	3.7	16.07	0.286	
19763	0.446	0.033	–111.9	7.6	17.37		
11543	0.427	0.141	–117.4	3.7	15.90		
40127	–0.082	0.442	–115.0	9.9	18.53		
40128	–0.446	0.051	–100.1	5.5	17.60		
14831	0.163	0.421	–103.6	1.4	14.98	0.300	AC735
40129	–0.291	0.345	–111.3	4.0	16.83	0.262	
40130	–0.341	0.295	–95.8	2.1	16.23	0.959	
40131	–0.202	–0.404	–108.9	3.7	16.98		
40132	–0.431	–0.135	–110.6	5.6	17.51		
14526	0.201	0.406	–107.3	2.0	15.12	0.431	AC733
14921	0.155	0.427	–119.1	3.8	16.29		
40133	–0.453	–0.025	–122.5	7.5	17.72		
40134	–0.330	–0.314	–117.1	2.4	16.30	0.407	
26173	0.449	–0.085	–107.4	1.6	15.08	0.915	AC571
40135	–0.152	0.431	–105.9	1.4	15.54	0.045	
40136	–0.447	0.094	–112.4	1.2	14.08	0.524	AC14
40137	0.449	0.090	–90.5	4.1	17.27		
40138	–0.288	0.356	–122.3	1.6	15.54	0.097	
40139	–0.457	0.026	–116.0	3.4	17.01		
26988	0.227	–0.400	–106.3	3.7	16.58		
27117	0.340	–0.311	–105.4	1.9	15.75	0.864	
15046	0.146	0.438	–124.9	7.6	17.33		
26616	0.437	–0.151	–122.0	7.4	17.38		
24821	–0.085	–0.455	–114.8	5.6	16.86		
40140	–0.463	–0.019	–107.0	1.2	14.24	0.772	AC523
40141	–0.250	0.391	–113.5	2.3	16.35	0.616	
26189	0.058	–0.463	–106.1	4.4	15.91		
26928	0.194	–0.425	–124.3	6.5	15.98		

TABLE 1—*Continued*

ID	RA	DEC	V(km s^{-1})	$\sigma_{\rm V}$	m_V	Prob	ID$_{\rm AC}$
12242	0.403	0.238	–109.8	6.9	17.62		
40142	–0.391	–0.257	–84.5	8.0	17.75		
27208	0.328	–0.335	–113.9	1.3	14.83	0.154	AC557
12862	0.362	0.297	–95.8	3.6	16.95	0.455	
40143	–0.466	–0.059	–92.9	4.0	17.54		
27054	0.225	–0.412	–110.6	2.5	16.33	0.218	
40144	–0.427	–0.196	–101.3	3.2	17.14	0.002	
26638	0.124	–0.456	–122.4	6.0	17.28		
27212	0.372	–0.293	–94.9	6.7	15.74		AC560
26129	0.470	–0.059	–103.1	6.1	17.31		
40145	–0.407	–0.241	–116.8	0.5	12.95	0.016	AC13
40146	–0.474	0.013	–98.0	4.2	17.14		
15170	0.142	0.454	–111.3	4.3	15.88		AC734
40147	–0.470	–0.075	–117.2	4.8	17.87		
11427	0.454	0.147	–114.8	8.0	17.70		
40148	0.465	0.108	–108.8	4.4	17.39		
40149	–0.110	–0.464	–106.8	4.1	17.95		
40150	–0.388	0.278	–99.2	7.5	18.04		
40151	–0.021	0.477	–115.0	1.6	15.52	0.745	AC801
27140	0.228	–0.422	–104.8	8.7	17.32		
20200	0.471	0.091	–124.1	8.3	16.56		
40152	–0.410	0.249	–110.6	2.6	16.80	0.926	
27330	0.336	–0.343	–90.4	1.8	15.30	0.226	
40153	–0.081	0.473	–106.6	4.1	16.90		
40154	–0.382	0.292	–92.1	4.8	18.08		
40155	0.482	–0.032	–118.8	4.6	17.23		
12598	0.392	0.286	–96.9	2.8	16.77	0.876	
40156	–0.092	0.478	–99.3	1.7	15.91	0.352	
40157	–0.391	–0.288	–107.8	1.3	14.73	0.989	AC503
40158	–0.109	0.474	–111.3	4.2	17.57		
40159	–0.195	0.447	–111.0	1.2	14.10	0.237	AC15
40160	–0.407	–0.267	–97.7	4.6	17.58		
27167	0.213	–0.440	–94.4	3.5	18.23		
14660	0.213	0.443	–108.0	2.2	14.72	0.002	AC731
40161	–0.139	0.471	–102.2	1.3	13.98	0.377	AC819
40162	–0.293	–0.394	–109.1	8.4	18.36		
12217	0.422	0.253	–117.3	9.0	18.96		
40163	–0.492	–0.016	–126.2	4.3	17.03		
19934	0.494	0.015	–97.5	2.3	16.23	0.957	
27416	0.293	–0.399	–98.5	4.1	17.16		
11776	0.450	0.208	–113.3	2.3	15.64	0.157	AC672
11195	0.479	0.127	–112.2	3.0	16.24	0.653	
27254	0.218	–0.447	–116.5	8.1	16.34		
26585	0.486	–0.101	–85.4	9.6	18.16		
40164	–0.437	–0.237	–100.0	6.0	17.94		
14291	0.259	0.425	–115.6	3.4	14.63		
16216	–0.002	0.498	–90.2	1.3	14.58	0.472	AC800
40165	–0.261	–0.424	–130.4	4.4	17.69		
40166	–0.349	0.355	–122.2	1.8	16.14	0.082	
40167	0.498	–0.048	–114.8	2.5	16.57		
40168	–0.317	–0.387	–92.6	0.5	12.86	0.913	AC463
40169	–0.334	0.373	–85.9	2.7	16.69	0.808	
40170	–0.475	0.154	–125.9	7.2	17.50		
27165	0.186	–0.465	–89.6	5.0	17.41	0.933	
27317	0.227	–0.447	–93.5	9.8	17.97		
40171	–0.175	–0.470	–99.7	2.3	16.89	0.049	AC429

Table 1—*Continued*

ID	RA	DEC	V(km s^{-1})	σ_V	m_V	Prob	ID_{AC}
40172	–0.486	0.123	–108.0	8.0	18.31		
27528	0.357	–0.353	–122.1	3.3	15.98		AC555
40173	–0.112	0.490	–135.9	6.6	17.43		
14036	0.291	0.411	–108.3	4.4	15.10		AC727
40174	–0.480	–0.150	–98.3	1.2	14.65	0.826	AC530
40175	–0.498	0.073	–101.2	7.5	17.89		
15664	0.095	0.495	–86.4	1.4	14.18	0.684	AC754
27518	0.302	–0.403	–112.3	3.2	16.13		
24813	–0.121	–0.490	–98.8	5.8	17.13		
40176	–0.346	–0.371	–94.8	8.3	17.89		
40177	–0.374	–0.342	–97.7	1.3	14.98	0.667	AC468
16335	–0.013	0.508	–104.7	2.1	15.72	0.437	
40178	–0.144	0.488	–96.9	1.2	14.73	0.278	AC820
40179	–0.478	–0.173	–110.8	3.8	17.61		
40180	–0.506	–0.057	–87.4	5.8	17.19	0.418	
26995	0.487	–0.152	–111.4	3.9	16.68		
20106	0.508	0.036	–85.1	6.6	16.91		
40181	–0.465	0.209	–104.8	7.6	17.80		
40182	–0.205	–0.469	–100.3	5.0	17.58		
40183	–0.501	–0.108	–95.4	0.7	13.48	0.858	AC529
27628	0.331	–0.392	–115.8	4.0	17.19		
40184	–0.048	0.510	–109.9	6.3	17.75		
40185	–0.214	–0.466	–107.0	2.6	16.81	0.956	AC431
40186	–0.090	0.506	–108.9	2.9	16.90	0.856	
27295	0.470	–0.209	–102.4	7.2	17.36		
19775	0.515	–0.036	–104.9	3.1	15.90		
40187	–0.311	–0.412	–93.3	4.3	17.70		
27028	0.131	–0.500	–102.9	1.5	15.30	0.141	
27582	0.275	–0.439	–120.5	1.6	15.25	0.924	
27237	0.482	–0.190	–113.4	7.2	17.82		
26472	0.038	–0.519	–103.5	4.8	16.70	0.456	
20465	0.509	0.104	–105.6	9.3	17.79		
27668	0.415	–0.318	–106.2	8.0	17.99		
40188	–0.416	0.318	–106.2	5.0	17.46		
40189	–0.084	0.517	–131.9	3.6	17.34		
40190	–0.354	–0.387	–96.7	6.3	17.85		
40191	–0.332	0.407	–117.7	5.3	17.51		
27620	0.263	–0.457	–118.2	4.1	17.24		
40192	–0.197	–0.489	–129.6	4.6	17.21	0.938	
40193	–0.265	0.457	–115.2	3.0	17.11		
26515	0.033	–0.529	–127.1	7.6	16.87		
40194	–0.215	0.484	–126.0	2.1	16.33	0.339	
40195	–0.509	0.147	–96.7	7.2	17.79		
27617	0.251	–0.468	–88.4	1.5	15.10	0.328	AC376
40196	–0.494	0.194	–112.1	3.3	16.59		
20236	0.531	0.037	–104.4	5.8	17.45		
13337	0.371	0.382	–103.2	1.5	15.35	0.327	
27375	0.497	–0.196	–93.2	5.5	16.61		
13564	0.354	0.401	–120.0	2.8	15.92	0.502	
12616	0.426	0.324	–105.1	2.2	15.54	0.793	
16578	–0.030	0.534	–108.7	1.2	14.22	0.843	AC803
40197	–0.163	–0.510	–106.0	5.4	18.07		
40198	–0.316	0.432	–81.1	7.5	18.18		
26576	0.035	–0.535	–109.0	3.6	16.87		
27853	0.370	–0.388	–102.7	1.5	15.34	0.627	
27633	0.470	–0.260	–107.4	1.8	15.27	0.592	

TABLE 1—*Continued*

ID	RA	DEC	V(km s^{-1})	σ_V	m_V	Prob	ID$_{AC}$
40199	–0.457	–0.285	–99.2	4.3	17.53		
40200	–0.527	0.112	–103.7	5.1	18.39		
40201	–0.079	0.534	–106.0	3.9	17.22	0.920	
40202	–0.408	0.355	–122.2	3.4	17.07		
40203	–0.435	–0.322	–113.4	1.5	15.97	0.886	
19705	0.537	–0.074	–98.4	3.5	19.84	0.797	
40204	–0.222	0.494	–114.7	2.3	15.64		AC825
40205	–0.518	0.159	–117.6	5.9	17.67		
40206	–0.535	0.090	–120.5	7.0	17.90		
40207	–0.542	–0.004	–97.4	9.8	17.84		
14905	0.226	0.494	–116.5	7.4	17.59		
26241	–0.017	–0.544	–110.2	1.0	13.82	0.674	AC407
40208	–0.505	0.203	–121.8	4.9	17.38	0.793	
27909	0.407	–0.364	–103.1	2.8	16.02	0.955	
27943	0.384	–0.391	–106.6	3.4	16.78		
27874	0.443	–0.322	–112.0	10.0	18.38		
20399	0.546	0.053	–115.1	0.7	13.40	0.567	AC11
40209	–0.547	–0.043	–95.5	4.2	17.44		
27077	0.096	–0.540	–96.1	4.2	15.74		
27488	0.513	–0.196	–117.7	1.6	15.03	0.026	
11548	0.504	0.219	–98.3	4.7	17.34		
27190	0.114	–0.539	–103.2	0.8	13.41	0.241	AC12
14287	0.298	0.464	–88.6	2.5	15.68		
27401	0.156	–0.529	–88.4	4.1	16.87		
13806	0.346	0.430	–95.2	1.9	15.95	0.349	
20544	0.546	0.083	–98.8	3.9	16.65		
40210	–0.106	0.542	–122.6	1.9	16.05	0.296	
27963	0.340	–0.436	–93.4	4.9	15.89		
40211	–0.553	–0.021	–117.5	1.3	14.95	0.172	AC544
19706	0.547	–0.085	–119.2	1.4	16.39	0.269	
27329	0.133	–0.539	–97.7	4.2	16.99		
24977	–0.148	–0.535	–107.0	2.2	15.73		
40212	–0.362	0.424	–114.1	1.5	15.23	0.530	
40213	–0.474	–0.293	–116.0	2.2	16.45	0.863	
20231	0.558	0.008	–119.1	0.7	13.25	0.000	AC650
27285	0.117	–0.548	–98.0	6.8	16.48		
11178	0.532	0.175	–99.4	2.5	16.41	0.404	
40214	–0.377	–0.414	–110.2	1.1	14.26	0.963	
40215	–0.438	0.350	–98.3	2.4	16.57	0.623	
27981	0.316	–0.463	–126.2	2.5	15.20	0.749	AC373
40216	–0.552	–0.098	–87.4	5.4	17.54		
40217	–0.545	–0.139	–117.6	2.7	16.33	0.659	
40218	–0.561	–0.028	–95.3	3.5	17.30		
40219	–0.562	0.026	–99.0	2.6	16.65	0.297	
25244	–0.132	–0.548	–95.9	0.5	13.00	0.872	
15806	0.124	0.550	–113.8	6.6	17.63		
20098	0.564	–0.023	–115.6	6.0	17.77		
24954	–0.158	–0.542	–94.5	5.5	17.35		
28056	0.440	–0.357	–124.2	8.9	17.73		
20621	0.561	0.085	–98.0	0.6	14.15	0.247	AC651
26790	0.026	–0.568	–107.1	2.5	16.35		
40220	–0.407	–0.399	–105.2	1.9	16.04	0.863	
40221	–0.553	0.143	–97.8	4.9	17.21		
27991	0.487	–0.300	–119.1	6.8	17.85		
20863	0.557	0.141	–121.7	7.8	18.03		
16590	0.010	0.576	–117.9	5.9	17.34		

TABLE 1—*Continued*

ID	RA	DEC	V(km s^{-1})	$\sigma_{\rm V}$	m_V	Prob	ID$_{\rm AC}$
15424	0.185	0.545	–124.7	5.9	17.39		
40222	–0.575	–0.035	–111.5	3.7	17.14	0.918	AC542
28104	0.474	–0.330	–116.1	0.5	13.11	0.548	
27382	0.562	–0.134	–91.0	3.8	16.23		
20268	0.578	–0.006	–108.9	4.7	17.23		
40223	–0.578	0.007	–113.6	1.4	15.51	0.190	AC546
26430	–0.030	–0.579	–103.0	10.0	18.00		
40224	–0.574	–0.090	–119.0	8.2	17.79		
40225	–0.385	0.436	–124.0	0.7	12.65	0.000	
26743	0.005	–0.583	–107.7	1.7	15.34	0.022	
27938	0.235	–0.534	–87.7	4.5	15.95		
28221	0.432	–0.392	–94.2	7.2	17.51		
27400	0.567	–0.132	–106.3	2.8	16.62		
25368	–0.138	–0.566	–85.7	3.3	17.03	0.445	
12032	0.500	0.302	–125.8	6.9	17.87		
20715	0.577	0.090	–103.1	5.2	17.55		
40226	–0.361	0.461	–108.8	2.0	16.07	0.323	
40227	–0.584	–0.023	–104.7	3.6	17.07		
19703	0.575	–0.113	–121.6	8.4	19.12		
40228	–0.361	–0.462	–105.3	2.0	16.40	0.472	
40229	–0.365	0.459	–118.9	4.9	17.33		
15366	0.203	0.551	–108.0	1.9	16.07	0.312	
13521	0.397	0.435	–100.9	5.8	17.49		
40230	–0.541	–0.232	–103.4	6.2	18.01		
40231	–0.394	–0.439	–120.1	1.6	15.80	0.343	
28119	0.519	–0.289	–118.0	2.8	15.79	0.010	
28309	0.366	–0.470	–125.2	3.2	16.48		
25443	–0.144	–0.579	–94.7	4.2	17.88		
40232	–0.549	0.236	–123.8	3.3	16.68		
40233	–0.598	0.029	–102.2	2.1	16.26	0.284	
20779	0.594	0.085	–107.3	6.7	18.43		
28321	0.343	–0.494	–93.8	4.6	17.17		
14146	0.349	0.490	–114.9	1.7	15.88	0.795	
16689	0.018	0.602	–107.9	4.4	17.22		
28327	0.482	–0.361	–100.3	2.7	16.82		
11736	0.532	0.281	–109.3	6.7	17.48		
16940	–0.033	0.601	–111.3	2.7	16.54	0.547	
40234	–0.435	–0.415	–87.2	2.7	16.81	0.638	
40235	–0.531	0.283	–112.0	0.5	12.73	0.011	
40236	–0.539	–0.267	–112.4	1.4	15.52	0.275	
40237	–0.541	0.264	–118.9	3.2	16.94		
40238	–0.288	0.530	–103.6	9.2	18.27		
40239	–0.373	–0.475	–104.0	6.2	18.16		
40240	–0.582	–0.164	–102.9	6.7	18.08		
27671	0.586	–0.155	–93.6	1.2	14.81	0.102	
27980	0.203	–0.571	–103.9	3.8	16.76	0.437	
15155	0.247	0.556	–95.2	9.3	17.51		
27931	0.571	–0.208	–113.1	4.8	17.42		
40241	–0.550	0.262	–115.7	5.2	17.17		
28113	0.233	–0.564	–119.0	2.1	16.13	0.632	
21208	0.579	0.193	–105.2	2.1	16.11	0.670	
17053	–0.049	0.609	–105.7	3.9	16.00		
40242	–0.607	0.065	–125.0	1.3	15.20	0.382	
26269	–0.078	–0.607	–106.5	1.4	14.70	0.871	
25917	–0.114	–0.602	–115.7	3.4	16.68		
20026	0.607	–0.082	–96.6	2.6	16.43	0.708	

TABLE 1—*Continued*

ID	RA	DEC	V(km s^{-1})	σ_V	m_V	Prob	ID_{AC}
40243	–0.215	0.574	–117.0	1.6	15.71	0.404	
40244	–0.596	–0.149	–104.0	2.7	16.79	0.832	
21000	0.603	0.120	–122.5	3.9	17.08		
12289	0.507	0.350	–113.2	4.0	17.17		
40245	–0.144	0.599	–126.5	1.7	16.22	0.065	
40246	–0.235	–0.570	–79.2	4.7	17.81		
40247	–0.382	0.483	–124.3	2.3	16.57		
40248	–0.591	–0.177	–95.4	3.3	16.68		
28146	0.565	–0.250	–78.8	6.0	16.93		
21082	0.602	0.141	–108.9	6.5	17.72		
40249	–0.414	0.458	–117.6	4.0	17.10		
20118	0.614	–0.072	–125.6	2.3	15.57		
26895	–0.012	–0.619	–110.3	4.7	17.18		
12911	0.467	0.408	–114.4	8.9	17.43		
40250	–0.380	–0.490	–108.9	9.2	18.57		
40251	–0.586	0.205	–114.1	1.4	15.70	0.554	
25749	–0.139	–0.607	–116.7	5.7	17.85		
40252	–0.609	–0.122	–100.0	1.1	14.50	0.382	AC535
28514	0.365	–0.505	–111.4	6.5	16.30		
26170	–0.102	–0.616	–93.4	8.3	16.06		
20097	0.623	–0.084	–106.6	2.2	15.58	0.016	
16991	–0.015	0.629	–85.3	4.1	16.73		
26205	–0.102	–0.621	–106.0	1.5	14.81	0.216	
40253	–0.609	–0.155	–107.5	9.6	18.24		
40254	–0.616	0.129	–102.9	7.6	16.90		
16629	0.055	0.627	–93.5	5.8	17.17		
40255	–0.196	0.599	–120.9	7.4	17.75		
40256	–0.249	0.581	–103.5	5.1	17.59		
40257	–0.562	0.290	–118.0	6.4	17.77		
40258	–0.622	0.124	–119.5	2.9	16.88	0.013	
40259	–0.445	0.453	–111.7	5.9	18.14		
28669	0.468	–0.430	–122.4	9.4	18.07		
19931	0.625	–0.120	–109.7	6.2	17.35		
28640	0.377	–0.513	–101.7	9.3	17.06		
40260	–0.369	–0.519	–114.8	9.0	18.15		
26978	–0.020	–0.638	–96.1	1.6	15.44	0.147	
40261	–0.637	–0.036	–101.2	1.4	15.01	0.937	
40262	0.591	0.242	–97.2	4.6	17.69		
40263	–0.500	0.400	–109.4	6.6	17.86		
40264	–0.512	0.388	–79.9	7.9	18.04		
26046	–0.130	–0.631	–103.1	3.6	15.76		
14495	0.345	0.545	–108.7	2.6	16.60	0.474	
11891	0.554	0.331	–106.4	4.2	17.09		
40265	–0.516	–0.387	–92.4	3.6	17.03		
40266	–0.604	–0.227	–108.2	1.2	14.55	0.995	AC539
15282	0.260	0.591	–96.5	3.4	15.89	0.425	
16665	0.065	0.645	–107.9	9.5	17.62		
28602	0.554	–0.337	–109.2	5.0	17.28		
28745	0.475	–0.443	–122.7	3.9	16.74		
28752	0.429	–0.488	–104.5	1.6	15.52	0.503	
40267	–0.521	–0.389	–102.8	2.8	16.51	0.009	
40268	–0.580	–0.295	–77.4	3.2	16.81		
40269	–0.651	–0.010	–120.1	8.6	17.69		
28413	0.595	–0.267	–98.4	3.0	16.69	0.467	
16865	0.033	0.652	–122.2	6.3	15.60		
20567	0.653	–0.022	–109.2	4.7	17.16		

TABLE 1—*Continued*

ID	RA	DEC	V(km s^{-1})	σ_V	m_V	Prob	ID_{AC}
40270	–0.629	0.182	–116.9	4.8	17.25		
28393	0.231	–0.614	–102.9	2.6	16.01	0.546	
27604	0.055	–0.656	–108.7	0.5	12.84	0.710	
40271	–0.256	–0.606	–105.9	4.9	17.62		
40272	–0.397	–0.526	–98.0	6.2	18.06		
28655	0.302	–0.588	–104.7	2.0	16.08	0.865	
11920	0.564	0.345	–111.5	2.5	16.15		
40273	–0.641	–0.158	–100.8	1.9	16.53	0.451	
16131	0.158	0.643	–113.9	7.3	17.30		
27928	0.110	–0.654	–87.9	2.8	15.56		
28245	0.182	–0.637	–79.9	10.0	17.56		
28634	0.585	–0.311	–104.5	2.2	15.70	0.876	
26525	–0.096	–0.656	–91.0	7.3	17.27		
26391	–0.111	–0.654	–98.6	3.3	15.78	0.935	
40274	–0.237	0.619	–102.3	0.6	13.11	0.682	AC808
40275	–0.428	–0.507	–103.7	4.1	16.75	0.673	
40276	–0.552	0.367	–94.0	5.8	17.61		
40277	–0.498	0.439	–110.6	1.6	15.99	0.334	
40278	–0.441	0.499	–113.2	1.7	16.15	0.766	
40279	–0.467	0.474	–106.9	0.6	13.16	0.032	
28807	0.381	–0.546	–92.4	2.8	16.49		
28849	0.417	–0.519	–123.2	6.7	17.55		
28590	0.599	–0.291	–110.1	1.4	14.00	0.672	
27047	–0.036	–0.665	–92.8	8.2	16.97		
21527	0.632	0.213	–117.6	3.0	16.72		
40280	–0.529	0.411	–116.0	9.7	18.35		
26932	–0.057	–0.669	–111.9	1.3	14.80	0.336	
40281	–0.351	0.571	–102.7	4.3	16.99		
40282	0.155	0.654	–83.8	10.1	18.51		
13529	0.455	0.494	–101.8	4.6	17.72		
28838	0.366	–0.566	–108.0	1.8	15.32	0.199	
40283	–0.485	0.468	–108.1	6.0	17.73		
28666	0.606	–0.297	–113.4	3.9	16.37		
40284	–0.571	–0.360	–120.4	3.7	17.50		
13878	0.427	0.524	–120.5	7.7	17.75		
21645	0.632	0.245	–115.4	2.1	16.28	0.458	
40285	–0.430	0.523	–117.6	1.8	15.94	0.180	
40286	–0.677	0.021	–114.4	3.7	17.26	0.837	
19878	0.659	–0.165	–112.3	1.5	15.19	0.843	
40287	–0.572	0.369	–129.9	3.8	17.30	0.257	
40288	–0.539	–0.418	–107.5	7.1	17.59		
40289	–0.619	–0.285	–97.7	8.7	18.19		
40290	–0.678	–0.074	–99.0	4.2	17.37		
17134	0.008	0.683	–102.8	0.6	14.22	0.597	
40291	–0.583	0.356	–123.6	8.4	18.02		
28739	0.609	–0.312	–93.1	1.2	14.32	0.727	
17007	0.036	0.684	–128.2	2.4	16.35	0.178	
28826	0.320	–0.607	–100.3	7.2	17.48		
14519	0.373	0.576	–114.0	2.1	16.04	0.713	
17599	–0.092	0.681	–106.9	7.1	18.03		
17485	–0.063	0.685	–100.0	4.3	15.92		
40292	–0.481	0.492	–100.7	2.7	16.57		
40293	–0.490	0.483	–131.6	6.4	17.91		
28763	0.289	–0.625	–116.8	2.3	15.95	0.063	
25166	–0.241	–0.645	–98.9	4.3	15.88		
13326	0.483	0.492	–114.4	2.9	15.73	0.388	

TABLE 1—*Continued*

ID	RA	DEC	V(km s^{-1})	σ_V	m_V	Prob	ID_{AC}
28937	0.367	–0.585	–110.3	0.5	13.38	0.000	
16371	0.146	0.676	–90.2	3.4	16.88	0.678	
40294	–0.593	–0.356	–117.1	1.4	15.47	0.297	
29055	0.481	–0.501	–102.4	6.3	17.80		
21039	0.694	0.036	–109.8	2.0	15.90	0.408	
14945	0.335	0.610	–120.6	7.8	17.72		
17918	–0.172	0.676	–109.8	6.6	18.11		
40295	–0.688	–0.113	–126.4	2.0	16.26	0.464	
11739	0.605	0.353	–112.5	5.1	15.97		
28625	0.216	–0.667	–101.3	3.2	16.70	0.289	
40296	–0.679	–0.173	–105.7	7.5	18.01		
28961	0.341	–0.614	–100.0	4.1	15.95		
28918	0.319	–0.627	–98.0	2.2	15.94	0.392	
40297	–0.435	–0.555	–110.9	1.4	15.75	0.448	
21552	0.686	0.165	–97.1	1.6	15.29	0.001	AC665
29149	0.475	–0.527	–78.1	3.5	15.97	0.024	
40298	–0.472	–0.529	–106.7	1.3	15.22	0.350	
20830	0.714	–0.027	–101.0	3.1	15.92		
40299	–0.684	–0.203	–112.9	1.8	16.11	0.937	
40300	–0.676	–0.232	–112.0	4.1	17.29		
40301	–0.410	–0.589	–89.6	5.4	16.62		
28277	0.112	–0.711	–93.8	1.5	15.37	0.397	
21338	0.715	0.081	–109.8	2.8	16.46	0.943	
27228	–0.065	–0.717	–117.6	2.0	15.99	0.689	
40302	–0.522	0.495	–107.7	4.1	16.88		
40303	–0.537	0.480	–117.0	1.9	15.95	0.504	
40304	–0.549	–0.468	–101.5	7.6	17.62		
40305	–0.522	–0.502	–94.1	1.7	15.74	0.533	
16895	0.096	0.720	–103.3	4.1	17.03	0.984	
15671	0.273	0.673	–104.5	1.7	15.79	0.260	
40306	–0.707	0.164	–116.5	4.4	17.45	0.285	
28054	0.056	–0.727	–98.9	1.3	14.29	0.976	
28812	0.228	–0.694	–107.2	1.3	15.09	0.965	
21501	0.721	0.118	–103.6	8.1	17.25		
40307	–0.698	0.211	–102.3	5.7	17.76		
20081	0.709	–0.175	–105.3	3.6	16.94	0.848	
11816	0.622	0.385	–98.4	3.9	16.90		
40308	–0.385	0.623	–99.1	6.2	17.53		
28942	0.269	–0.682	–92.6	3.9	16.87		
29280	0.462	–0.569	–96.6	6.7	17.47		
17757	–0.083	0.729	–93.9	3.0	15.88		
29297	0.512	–0.526	–93.2	3.7	16.93		
40309	–0.631	–0.374	–117.8	2.6	16.17		
40310	–0.734	0.032	–108.1	3.3	17.13	0.871	
14616	0.398	0.618	–85.6	3.7	16.97		
17820	–0.097	0.730	–123.5	5.9	17.14		
40311	–0.703	0.221	–101.3	3.4	16.99	0.306	
17906	–0.118	0.729	–123.9	2.9	16.29	0.662	
18013	–0.144	0.728	–88.9	1.5	14.87	0.530	
40312	–0.642	–0.373	–101.7	6.5	17.09		
40313	–0.717	–0.193	–99.6	2.8	16.50	0.670	
25827	–0.232	–0.708	–116.4	7.4	17.43		
16259	0.209	0.717	–113.0	2.9	16.61		
29233	0.370	–0.648	–114.3	5.1	17.60		
20690	0.742	–0.084	–102.6	4.9	17.17		
26933	–0.126	–0.736	–108.5	1.2	14.62	0.531	

Table 1—*Continued*

ID	RA	DEC	V(km s^{-1})	$\sigma_{\rm V}$	m$_V$	Prob	ID$_{\rm AC}$
40314	–0.518	0.538	–107.4	3.2	17.07		
40315	–0.740	0.096	–94.6	4.8	17.61	0.931	
40316	–0.698	–0.270	–96.8	4.3	17.39		
40317	–0.408	0.630	–107.8	1.2	14.43	0.507	
40318	–0.595	0.458	–129.1	3.8	17.16	0.445	
28430	0.104	–0.744	–106.3	3.2	15.89		
40319	–0.684	–0.311	–111.7	1.8	16.15	0.980	
40320	0.681	0.322	–107.8	3.3	16.81	0.837	
12658	0.580	0.483	–108.0	5.2	17.40		
20166	0.732	–0.183	–100.3	1.7	15.67	0.681	
21375	0.752	0.055	–108.6	5.2	17.29		
40321	–0.753	–0.032	–107.6	5.0	17.40	0.835	
40322	–0.310	0.691	–120.2	1.6	16.10	0.090	
40323	–0.417	–0.632	–106.5	3.3	17.10		
40324	–0.591	–0.474	–110.7	0.6	14.06	0.404	
40325	–0.512	–0.561	–97.9	1.2	14.23	0.723	
40326	–0.610	–0.453	–105.0	5.2	17.37		
17721	–0.040	0.763	–107.1	5.7	17.55		
16506	0.190	0.741	–115.3	1.3	14.51	0.738	
40327	–0.580	–0.499	–86.2	5.8	17.41		
11396	0.675	0.361	–116.0	2.3	16.23	0.168	
20757	0.760	–0.091	–108.7	8.7	17.42		
29447	0.611	–0.467	–94.3	8.6	17.64		
18130	–0.145	0.755	–119.3	4.8	17.11		
17028	0.109	0.762	–121.3	5.9	15.96		
40328	–0.585	0.503	–125.6	5.6	17.69		
40329	–0.673	–0.377	–103.5	2.9	17.07	0.513	
40330	–0.270	0.725	–121.3	1.7	16.24	0.061	
40331	–0.728	–0.261	–120.0	4.1	17.22	0.023	
28943	0.201	–0.747	–112.6	1.4	14.97	0.648	
13567	0.524	0.570	–110.7	5.1	17.25		
20213	0.749	–0.193	–107.7	2.6	15.88	0.746	
25460	–0.287	–0.720	–116.5	0.8	13.01	0.487	
40332	–0.352	0.690	–123.1	5.9	17.99		
29478	0.441	–0.639	–112.9	4.6	16.94	0.649	
29544	0.558	–0.539	–100.8	0.9	14.17	0.797	
29272	0.697	–0.341	–117.4	1.4	14.91	0.859	
21465	0.775	0.052	–100.8	5.7	18.07		
29539	0.492	–0.603	–94.3	1.7	15.46	0.692	
29573	0.544	–0.559	–104.4	4.1	16.94		
40333	–0.600	0.498	–119.7	5.2	17.57		
21653	0.774	0.101	–103.0	4.7	17.35		
40334	–0.678	0.393	–123.7	1.7	16.06	0.351	
20579	0.771	–0.140	–97.1	4.1	17.22		
40335	–0.580	–0.527	–126.5	9.5	17.87		
26650	–0.190	–0.762	–95.5	7.4	17.25		
40336	–0.394	0.681	–108.0	1.5	15.70	0.919	
40337	–0.436	0.654	–116.6	1.4	15.19	0.975	
21829	0.780	0.139	–105.1	5.9	17.51		
40338	–0.778	–0.149	–115.7	4.9	17.42		
28749	0.124	–0.783	–93.3	1.4	15.35	0.353	
18048	–0.093	0.788	–103.1	3.1	17.00	0.740	
26772	–0.187	–0.774	–113.0	1.6	15.32	0.675	
26651	–0.199	–0.771	–99.6	9.4	16.81		
12740	0.605	0.520	–118.2	4.0	17.08		
28127	–0.006	–0.798	–94.5	0.6	13.31	0.253	

TABLE 1—*Continued*

ID	RA	DEC	V(km s^{-1})	σ_V	m_V	Prob	ID_{AC}
40339	–0.411	0.688	–132.9	9.7	17.71		
40340	–0.584	0.548	–120.1	3.2	17.09		
40341	–0.793	–0.130	–115.2	6.1	17.89		
29679	0.627	–0.503	–103.0	1.9	16.12	0.718	
40342	–0.750	–0.292	–100.7	1.7	15.65	0.750	
29603	0.419	–0.688	–112.5	3.8	16.73		
28501	0.053	–0.805	–116.9	10.1	17.73		
26618	–0.211	–0.779	–94.7	1.9	15.57	0.546	
13249	0.573	0.570	–114.1	2.0	16.24	0.141	
29354	0.744	–0.315	–99.3	3.4	17.33	0.585	
40343	–0.705	0.397	–109.3	5.1	17.49	0.853	
40344	–0.504	0.635	–116.2	9.7	18.35		
28225	0.001	–0.811	–115.3	1.7	15.38	0.273	
12220	0.654	0.484	–106.3	3.3	16.75		
22367	0.743	0.330	–109.8	1.7	16.04	0.837	
40345	–0.511	–0.634	–108.2	6.5	18.03		
15811	0.325	0.751	–97.6	1.7	15.58	0.507	
22010	0.801	0.166	–115.7	7.4	17.91		
40346	–0.679	–0.457	–116.7	3.1	16.98		
40347	–0.747	–0.335	–99.0	5.6	17.96		
29666	0.411	–0.710	–109.2	1.2	14.33	0.633	
40348	–0.329	0.751	–117.4	8.1	18.12		
29269	0.233	–0.789	–106.4	1.5	14.83	0.919	
29815	0.531	–0.628	–113.7	1.9	15.80	0.981	
40349	–0.749	0.337	–121.0	4.4	17.42		
11690	0.698	0.436	–111.9	2.5	16.41	0.894	
40350	–0.786	0.244	–99.4	1.2	14.05	0.758	
28679	0.067	–0.821	–114.3	1.5	15.31	0.720	
40351	–0.492	0.662	–116.8	4.7	17.38		
21917	0.818	0.123	–112.4	5.6	17.17		
29320	0.242	–0.792	–109.5	6.6	17.44		
26200	–0.269	–0.783	–120.5	5.0	16.95		
21686	0.827	0.055	–119.2	5.8	17.69		
40352	–0.426	0.711	–104.9	2.2	16.40	0.298	
27656	–0.107	–0.823	–99.3	1.7	15.69	0.730	
40353	–0.800	0.224	–111.2	1.1	13.59	0.004	
15692	0.351	0.754	–118.8	4.9	17.04		
29133	0.173	–0.816	–107.2	6.0	17.31		
18340	–0.131	0.824	–130.2	5.5	15.95		
25536	–0.328	–0.770	–100.6	6.4	17.14		
29663	0.363	–0.756	–102.2	1.3	14.69	0.494	
40354	–0.822	0.183	–105.0	4.1	17.34		
28516	0.017	–0.843	–104.1	1.9	15.79	0.635	
22135	0.826	0.175	–105.5	5.3	17.23		
18745	–0.270	0.799	–130.2	1.6	15.07	0.086	
29613	0.328	–0.778	–118.6	6.5	16.82		
29939	0.558	–0.636	–102.0	2.8	15.83	0.003	
40355	–0.820	0.214	–94.9	7.5	17.50		
29096	0.142	–0.837	–119.6	1.2	14.21	0.463	
21227	0.849	–0.079	–94.6	4.7	17.11		
25684	–0.329	–0.787	–91.0	4.2	16.90		
22478	0.792	0.319	–92.6	3.9	15.88		
29428	0.238	–0.821	–103.6	0.5	12.88	0.186	
29325	0.202	–0.832	–108.0	1.6	15.71	0.277	
40356	–0.404	–0.754	–111.6	8.7	18.38		
26379	–0.274	–0.812	–120.1	4.5	15.86		

TABLE 1—*Continued*

ID	RA	DEC	V(km s^{-1})	σ_V	m_V	Prob	ID_{AC}
18581	–0.182	0.840	–118.1	5.1	17.12		
22277	0.835	0.207	–120.0	5.5	17.89		
21328	0.859	–0.068	–117.3	1.2	14.89	0.823	
29692	0.325	–0.800	–109.8	1.3	15.00	0.390	
15371	0.413	0.761	–123.6	4.1	16.96	0.252	
18161	–0.043	0.866	–102.7	2.9	15.94	0.989	
29113	0.122	–0.859	–120.1	10.1	17.75		
14520	0.503	0.707	–119.6	1.9	16.02	0.603	
22556	0.803	0.336	–117.6	1.7	15.64	0.270	
20653	0.847	–0.199	–113.8	1.1	14.54	0.825	
27894	–0.110	–0.863	–95.7	7.4	17.55		
40357	–0.795	0.355	–94.6	8.7	16.96		
22128	0.860	0.137	–109.5	1.2	14.48	0.081	
15484	0.404	0.772	–111.3	3.2	16.72	0.766	
40358	–0.864	0.128	–122.8	7.0	17.42		
16705	0.253	0.840	–106.5	8.7	16.47		
22510	0.827	0.293	–111.3	1.3	14.94	0.335	
40359	–0.863	–0.164	–116.7	5.4	17.88		
17463	0.126	0.871	–96.1	2.1	16.09	0.580	
40360	–0.880	–0.053	–108.5	3.3	17.33	0.589	
17167	0.181	0.863	–109.2	2.6	16.67	0.566	
40361	–0.528	–0.708	–105.4	1.2	14.68	0.331	
30082	0.519	–0.718	–109.6	1.7	15.75	0.038	
40362	–0.676	–0.575	–109.0	9.1	18.11		
13076	0.644	0.614	–103.0	1.3	13.97	0.508	
40363	–0.661	–0.596	–110.1	3.6	17.08	0.546	
40364	–0.396	0.799	–99.5	5.4	17.91		
40365	–0.446	0.773	–137.6	5.4	17.20		
40366	–0.491	–0.745	–100.4	4.0	17.16		
18856	–0.247	0.859	–112.7	3.3	15.86		
40367	–0.895	0.019	–98.5	1.9	16.07	0.588	
40368	–0.769	0.463	–114.1	5.3	17.40	0.673	
40369	–0.623	0.649	–110.2	5.1	17.42		
28145	–0.107	–0.900	–101.6	3.3	16.82		
25941	–0.351	–0.836	–98.9	1.2	13.69	0.474	
40370	–0.461	–0.781	–98.8	3.3	17.00	0.305	
16361	0.320	0.848	–120.8	3.4	16.61		
17779	0.086	0.903	–104.7	3.4	15.86		
40371	–0.741	0.529	–117.3	1.5	14.54	0.192	
40372	–0.895	–0.169	–102.5	1.6	15.85	0.574	
30150	0.763	–0.499	–112.6	7.5	17.70		
30014	0.383	–0.829	–81.3	4.4	16.90		
15265	0.462	0.788	–119.0	1.6	15.07	0.677	
28727	–0.014	–0.913	–86.7	8.4	17.55		
40373	–0.789	–0.459	–118.2	1.1	14.22	0.639	
29627	0.216	–0.890	–123.0	3.6	16.84		
40374	–0.524	–0.750	–104.0	8.0	18.21		
16074	0.366	0.839	–89.4	6.5	17.35		
26309	–0.329	–0.856	–116.0	3.6	16.85	0.818	
30280	0.611	–0.685	–118.4	7.7	17.72		
18203	0.003	0.923	–120.3	5.6	16.04		
15344	0.458	0.801	–98.2	2.0	15.16	0.702	
28593	–0.051	–0.921	–98.8	2.3	16.15	0.819	
15797	0.407	0.830	–119.5	5.5	17.07		
40375	–0.475	0.792	–108.1	2.3	16.74	0.666	
40376	–0.638	0.668	–111.5	2.2	16.04	0.816	

TABLE 1—*Continued*

ID	RA	DEC	V(km s^{-1})	σ_V	m_V	Prob	ID$_{AC}$
18025	0.050	0.924	–120.2	1.5	14.51	0.909	
14550	0.544	0.752	–112.1	6.0	17.01		
40377	–0.871	0.325	–99.4	6.7	17.58		
40378	–0.922	0.110	–112.2	8.0	18.09		
40379	–0.479	–0.798	–88.0	3.9	17.38	0.271	
30198	0.453	–0.813	–98.8	1.7	15.58	0.890	
40380	–0.638	–0.679	–101.1	4.5	17.33		
22061	0.931	0.046	–154.4	2.9	15.47		
40381	–0.551	–0.754	–107.4	4.6	17.17		
13767	0.622	0.699	–123.0	3.4	15.81		
30359	0.638	–0.688	–103.9	4.0	17.03		
40382	–0.559	–0.753	–104.7	6.0	17.44		
17402	0.188	0.920	–124.5	8.9	17.50		
15261	0.482	0.807	–131.3	7.8	19.26		
14676	0.539	0.771	–93.4	9.9	16.78		
29885	0.268	–0.904	–95.2	9.5	16.17		
22883	0.855	0.400	–111.0	3.5	16.01		
28163	–0.139	–0.934	–87.0	3.3	16.90		
11542	0.798	0.509	–110.8	1.5	14.90	0.889	
40383	–0.464	–0.825	–101.4	2.5	16.72	0.891	
40384	–0.942	0.087	–97.8	4.4	17.61		
27484	–0.232	–0.918	–102.4	1.3	13.71	0.233	
30253	0.443	–0.839	–97.1	6.9	16.81		
17270	0.222	0.926	–115.1	2.7	16.38	0.877	
27839	–0.194	–0.933	–107.9	3.7	16.91		
40385	–0.908	0.292	–112.1	4.1	17.27		
40386	–0.703	0.647	–114.3	3.8	17.39		
40387	–0.945	0.166	–118.3	5.0	16.51		
21187	0.942	–0.181	–106.9	3.4	16.90		
16905	0.290	0.917	–107.2	3.9	15.83		
40388	–0.929	0.253	–117.7	1.5	14.91	0.476	
40389	–0.682	–0.682	–108.7	3.3	17.12		
30342	0.472	–0.842	–94.5	1.5	15.05	0.647	
17823	0.129	0.957	–114.3	9.7	17.17		
16804	0.309	0.915	–112.6	2.8	16.04	0.132	
30433	0.590	–0.764	–95.0	0.9	13.58	0.164	
15359	0.489	0.835	–116.1	0.5	13.14	0.596	
20961	0.940	–0.229	–110.4	2.4	16.44	0.102	
22550	0.951	0.182	–114.9	4.1	17.19		
14193	0.609	0.756	–127.3	1.4	14.67	0.866	
22270	0.969	0.069	–92.4	2.8	15.80	0.200	
18819	–0.129	0.965	–109.2	4.2	16.89		
18971	–0.177	0.958	–115.1	7.5	17.39		
29610	0.130	–0.970	–105.1	4.1	15.97		
21628	0.972	–0.106	–120.9	5.2	17.48		
20126	0.907	–0.369	–98.8	4.5	17.36		
29140	0.005	–0.980	–97.9	1.2	13.91	0.361	
20242	0.918	–0.357	–112.8	3.3	16.88	0.684	
20350	0.924	–0.341	–88.8	7.7	16.94		
21159	0.964	–0.209	–100.4	4.3	17.23		
40390	–0.433	–0.886	–107.7	1.8	14.70		
18187	0.070	0.986	–123.0	2.9	16.23	0.487	
30506	0.588	–0.794	–118.9	6.5	17.92		
40391	–0.772	–0.621	–98.5	3.1	17.07		
30536	0.608	–0.784	–110.3	2.7	16.37	0.048	
13957	0.645	0.753	–125.6	8.0	17.56		

Table 1—*Continued*

ID	RA	DEC	V(km s^{-1})	$\sigma_{\rm V}$	m$_V$	Prob	ID$_{\rm AC}$
11439	0.839	0.531	–119.1	1.9	15.76	0.533	
18612	–0.042	0.992	–106.5	4.1	17.06		
30574	0.699	–0.708	–98.0	8.3	17.86		
14387	0.609	0.790	–105.4	8.5	17.83		
18534	–0.010		–118.5	3.4	16.63	0.841	
40392	–0.624	–0.784	–105.6	8.0	18.42		
40393	–0.672	0.743	–119.3	0.5	12.83	0.000	
30489	0.514	–0.862	–121.8	1.6	15.06	0.168	
12042	0.801	0.603	–91.7	4.7	15.97		
30571	0.587	–0.816	–98.9	5.9	16.16		
40394	–0.509	–0.871	–101.7	2.9	16.80	0.019	
40395	–0.501	–0.877	–89.9	4.3	17.45		
28561	–0.139	–1.002	–107.1	3.1	15.95		
40396	–0.695	–0.736	–103.9	1.5	14.99	0.777	
40397	–0.632	0.794	–100.7	2.7	16.54		
40398	–0.525	–0.875	–105.8	8.4	17.93		
40399	–0.837	0.583	–109.5	6.1	17.37		
14727	0.590	0.833	–95.3	1.9	15.79	0.760	
23115	0.929	0.423	–105.2	3.8	16.03	0.923	
30079	0.230	–0.997	–108.5	3.0	16.64	0.697	
40400	–0.996	0.235	–108.3	6.6	17.36		
30648	0.830	–0.608	–103.8	2.2	16.12	0.709	
19515	–0.346	0.969	–120.2	3.9	16.18		
16774	0.364	0.964	–112.7	1.9	15.43		
30620	0.545	–0.875	–110.6	6.5	17.41		
40401	–0.580	–0.853	–104.9	6.5	17.92		
40402	–0.800	0.655	–111.3	8.3	17.85		
40403	–1.014	–0.205	–107.3	7.9	17.88		
30607	0.881	–0.547	–105.4	3.7	16.92		
16383	0.419	0.951	–108.0	7.3	17.60		
18610	0.008	1.040	–108.8	2.7	16.58		
21535	1.023	–0.182	–111.7	9.6	17.77		
21659	1.029	–0.157	–113.4	4.7	17.13		
40404	–1.031	–0.153	–115.9	8.8	18.57		
40405	–0.975	0.371	–103.7	1.9	16.35	0.295	
16939	0.352	0.986	–105.3	0.7	13.13	0.042	
28806	–0.128	–1.040	–105.1	4.3	15.97		
15357	0.552	0.897	–107.3	5.8	17.27		
40406	–1.048	0.115	–101.5	1.6	15.64	0.648	
29393	–0.011	–1.055	–119.2	1.5	14.92	0.357	
20734	1.001	–0.338	–107.4	3.3	15.83		
22376	1.056	0.016	–111.1	2.1	16.09	0.919	
29302	–0.033	–1.055	–107.6	3.2	16.63	0.150	
40407	–1.000	0.347	–109.3	9.2	18.13		
40408	–0.838	–0.649	–93.9	5.7	17.36		
17198	0.322	1.011	–118.7	8.5	17.42		
40409	–0.293	–1.021	–100.6	1.7	15.95	0.662	
40410	–0.702	–0.797	–105.5	2.0	16.38	0.949	
30772	0.592	–0.883	–103.3	2.8	16.59	0.831	
23374	0.943	0.501	–109.7	4.8	17.33		
40411	–0.525	0.931	–110.9	3.4	16.35		
40412	–0.999	–0.380	–102.6	1.5	15.55	0.702	
30279	0.242	–1.042	–98.7	1.5	14.86	0.410	
19898	0.962	–0.468	–91.3	4.0	15.96		
20982	1.026	–0.312	–89.5	7.0	17.65		
30771	0.547	–0.926	–106.3	6.6	16.03		

TABLE 1—*Continued*

ID	RA	DEC	V(km s^{-1})	σ_V	m_V	Prob	ID_{AC}
19686	–0.364	1.014	–99.9	7.7	17.58		
21515	1.057	–0.221	–101.9	2.8	16.49	0.363	
15734	0.530	0.941	–120.8	1.6	15.19	0.259	
11527	0.896	0.604	–100.3	2.2	15.50	0.634	
30642	0.433	–0.991	–102.9	1.8	15.24	0.252	
29897	0.090	–1.079	–111.2	0.7	13.39	0.936	
40413	–0.740	–0.789	–108.5	1.4	14.42	0.995	
22190	1.084	–0.071	–107.1	3.3	15.87		
17939	0.213	1.067	–101.9	3.4	16.46		
21562	1.066	–0.218	–106.8	5.1	17.20		
40414	–1.027	–0.365	–111.2	2.2	16.80	0.744	
40415	–1.015	0.399	–109.0	4.9	17.21		
28801	–0.169	–1.079	–112.9	1.9	15.85	0.848	
30899	0.649	–0.879	–105.8	2.2	16.03	0.544	
40416	–0.982	–0.479	–96.4	6.4	17.62		
23373	1.002	0.440	–104.7	3.2	16.61		
40417	–0.752	–0.796	–122.5	2.1	16.19	0.151	
30641	0.393	–1.029	–103.6	3.7	16.55		
40418	0.933	0.588	–85.4	3.9	16.51		
40419	–0.653	–0.888	–113.3	1.8	15.97	0.582	
21378	1.076	–0.273	–147.3	5.9	15.85		
40420	–1.061	0.333	–103.1	7.1	17.71		
40421	–1.028	–0.430	–108.4	2.0	16.15	0.818	
40422	–0.289	–1.077	–99.1	2.2	16.56	0.345	
20249	1.018	–0.456	–111.4	3.7	16.84		
22836	1.111	0.122	–107.6	0.6	14.09	0.328	
19028	–0.031	1.119	–113.6	3.7	16.70		
40423	–1.118	0.034	–111.5	1.4	15.08	0.960	
20202	1.019	–0.466	–106.6	4.6	17.05		
29322	–0.094	–1.119	–108.6	4.2	15.83		
40424	–0.371	–1.060	–102.7	1.8	15.74	0.686	
40425	–0.487	–1.014	–121.7	5.6	17.92		
40426	–0.664	–0.907	–95.8	0.8	14.42	0.863	
40427	–0.790	0.799	–107.8	2.8	16.33		
22893	1.117	0.139	–116.5	3.4	16.08		
40428	–1.043	–0.423	–105.1	4.0	16.40		
40429	–1.044	–0.423	–105.9	2.3	16.33		
40430	–0.445	1.036	–106.5	2.3	16.34		
19224	–0.095	1.124	–118.1	3.9	15.87	0.495	
40431	–1.097	0.260	–115.8	3.0	17.02		
14503	0.693	0.894	–107.3	4.9	17.08		
19518	–0.205	1.112	–114.1	2.1	15.68		
23288	1.088	0.323	–114.0	8.7	18.02		
40432	–1.033	–0.475	–106.9	5.7	17.64		
31072	0.722	–0.881	–109.6	3.7	16.81		
30752	0.388	–1.074	–109.9	3.3	16.95		
20453	1.054	–0.453	–107.6	6.1	17.45		
40433	–0.465	1.052	–112.4	7.5	17.75		
22750	1.153	0.050	–109.9	6.0	16.43		
40434	–0.603	–0.984	–92.5	6.8	18.01		
40435	–0.850	–0.782	–89.8	5.9	17.54		
14789	0.684	0.935	–114.8	1.9	15.23		
15130	0.653	0.958	–108.2	2.6	16.19		
30924	0.466	–1.062	–101.9	1.6	15.15	0.740	
40436	–1.116	0.318	–105.6	0.6	13.64	0.586	
31162	0.766	–0.873	–108.4	2.6	16.47	0.831	

TABLE 1—*Continued*

ID	RA	DEC	V(km s^{-1})	σ_V	m_V	Prob	ID_{AC}
29206	–0.153	–1.151	–97.7	1.7	15.77	0.382	
17520	0.353	1.109	–117.7	2.4	15.88		
40437	0.979	0.630	–116.0	9.0	18.48		
40438	1.019	–0.570	–113.3	8.8	17.98		
29653	–0.063	–1.167	–92.3	3.3	16.61		
40439	–0.305	–1.128	–104.9	0.6	13.39	0.201	
22666	1.170	0.000	–109.0	6.2	16.19		
40440	–1.152	0.205	–107.8	5.5	17.19		
40441	–1.134	–0.298	–100.4	1.3	14.86	0.725	
40442	–1.171	0.024	–106.9	2.3	16.45	0.437	
18393	0.187	1.158	–88.1	6.5	16.00		
23592	1.077	0.466	–93.4	1.7	14.50		
23647	1.058	0.512	–107.7	3.5	15.67		
30994	0.490	–1.071	–95.6	4.6	16.99		
30377	0.147	–1.171	–130.4	8.0	17.54		
23417	1.136	0.323	–113.3	6.1	17.23		
19567	–0.162	1.170	–127.5	9.1	17.53		
40443	–1.121	–0.373	–111.8	1.5	15.99	0.426	
40444	1.036	–0.574	–117.2	2.4	16.31	0.333	
21551	1.146	–0.302	–110.2	7.3	17.87		
22898	1.184	0.076	–118.9	1.7	14.91	0.034	
12528	0.897	0.779	–83.7	5.4	17.46		
40445	–0.368	–1.129	–109.7	4.4	17.42		
40446	–1.107	–0.429	–95.4	2.0	16.22	0.047	
31229	0.908	–0.769	–112.5	5.4	15.93		
40447	–1.099	–0.458	–116.4	0.7	13.28	0.877	
31143	0.589	–1.035	–103.3	6.5	17.46		
40448	–0.937	–0.735	–98.9	9.1	18.28		
40449	–1.079	–0.504	–112.2	1.4	15.04	0.536	
31069	0.525	–1.070	–100.1	4.2	16.93		
40450	–1.082	–0.504	–112.2	3.1	15.50		
20486	1.091	–0.483	–151.5	4.1	15.91		
22220	1.184	–0.161	–95.9	9.3	17.66		
29899	–0.029	–1.194	–95.9	8.8	16.86		
40451	–1.035	0.596	–108.4	4.6	17.42		
40452	–0.413	1.122	–87.2	2.6	16.30		
20087	1.070	–0.538	–98.7	3.1	16.51	0.260	
22844	1.203	0.033	–120.1	10.0	17.56		
40453	–1.194	–0.153	–95.9	7.0	18.09		
19394	–0.073	1.205	–109.3	4.8	16.99		
23164	1.198	0.165	–114.9	1.7	15.36	0.524	
23833	1.048	0.604	–111.0	3.4	16.61		
40454	–0.290	–1.176	–106.4	3.4	16.77		
23526	1.162	0.349	–107.7	0.9	14.73	0.922	
23746	1.107	0.499	–104.9	6.9	16.97		
31318	0.773	–0.938	–106.1	1.9	15.85	0.561	
17724	0.361	1.164	–108.2	0.6	13.93	0.856	
31328	0.929	–0.790	–102.8	1.9	15.69	0.701	
31341	0.845	–0.881	–99.5	1.5	14.50	0.256	
40455	–1.212	0.148	–99.1	3.2	17.12		
31329	0.957	–0.764	–98.3	7.8	17.62		
40456	–1.217	0.136	–86.7	4.1	17.18		
31343	0.955	–0.775	–109.1	6.8	17.36		
31273	0.626	–1.061	–114.1	0.5	12.94	0.001	
40457	–1.132	0.486	–114.0	1.8	15.21		
40458	–1.232	–0.010	–100.4	7.2	17.88		

TABLE 1—*Continued*

ID	RA	DEC	V(km s^{-1})	$\sigma_{\rm V}$	m$_V$	Prob	ID$_{\rm AC}$
18707	0.163	1.223	–104.3	7.2	17.59		
40459	–0.565	–1.097	–107.3	6.7	18.31		
31370	0.753	–0.982	–100.4	4.3	15.98	0.850	
23941	1.078	0.619	–113.6	1.9	15.04		
23956	1.069	0.636	–113.8	9.3	17.36		
40460	–0.788	–0.964	–103.9	6.2	18.09		
19010	0.096	1.242	–113.0	4.1	16.58		
23932	1.094	0.599	–122.2	5.5	17.64		
40461	–0.876	0.890	–110.1	9.6	18.25		
31432	0.815	–0.948	–92.5	3.6	16.67		
31442	0.862	–0.908	–107.4	2.9	15.84	0.903	
22945	1.251	0.028	–98.0	7.6	17.11		
16979	0.507	1.149	–134.4	1.9	15.29		
23014	1.256	0.053	–120.0	0.7	14.19	0.146	
40462	–1.235	–0.267	–112.5	2.3	16.49	0.248	
18873	0.149	1.261	–102.6	3.1	15.72		
20119	1.126	–0.589	–109.8	5.3	17.37		
40463	–0.711	1.053	–98.1	0.7	12.73	0.000	
23140	1.269	0.087	–109.6	3.8	15.73		
40464	–0.667	1.086	–107.4	4.5	17.11		
40465	–0.925	–0.877	–113.3	1.7	15.72	0.523	
40466	–0.333	1.233	–106.8	3.0	16.89		
31503	0.780	–1.014	–120.8	2.8	16.37		
21598	1.226	–0.372	–107.1	9.9	17.88		
40467	–1.039	–0.757	–117.3	1.4	14.95	0.436	
40468	–1.275	0.174	–105.0	4.2	17.55	0.288	
31539	0.874	–0.946	–148.9	2.8	16.03		
11175	1.075	0.717	–107.8	0.6	12.79	0.242	
40469	–0.929	–0.901	–108.3	2.1	15.61	0.486	
23797	1.234	0.396	–116.8	7.6	17.33		
40470	–1.270	–0.260	–111.4	2.4	16.43	0.754	
31549	0.998	–0.831	–114.4	3.4	17.12	0.333	
23464	1.285	0.193	–121.2	3.3	16.60	0.081	
40471	–0.830	–1.000	–105.2	4.8	17.33	0.778	
40472	–1.292	–0.138	–115.8	2.2	16.61	0.547	
40473	–0.727	1.079	–126.5	2.0	15.30		
18465	0.285	1.275	–121.7	2.2	15.51		
40474	–1.227	–0.455	–99.4	0.8	13.97	0.055	
11346	1.074	0.750	–107.8	6.5	17.38		
40475	–1.127	–0.670	–110.8	2.8	16.51	0.002	
40476	–1.197	–0.535	–109.4	7.8	18.13		
40477	–0.330	–1.269	–109.4	1.1	14.36	0.391	
40478	–1.024	0.821	–103.0	1.8	14.96		
31434	0.574	–1.182	–102.0	2.1	15.89	0.407	
40479	–1.098	0.722	–110.2	5.8	17.12		
40480	–1.327	0.013	–106.3	2.9	17.02		
31619	0.972	–0.907	–109.1	2.1	15.79	0.936	
40481	–0.424	–1.261	–122.2	3.2	16.98		
15103	0.782	1.081	–98.3	2.6	15.52		
31622	0.850	–1.029	–108.7	7.6	17.00		
40482	–1.190	0.606	–118.1	4.3	17.20		
40483	–0.061	–1.339	–116.9	7.1	18.21		
40484	–0.401	–1.281	–108.5	1.6	15.58	0.749	
40485	–1.136	–0.715	–112.3	1.5	14.91	0.459	
40486	–0.696	–1.148	–114.6	4.6	17.64		
40487	–1.181	0.642	–111.8	3.7	17.09		

TABLE 1—*Continued*

ID	RA	DEC	V(km s^{-1})	σ_V	m_V	Prob	ID$_{AC}$
20483	1.207	–0.600	–111.7	4.7	16.01		
40488	–0.874	–1.032	–102.9	0.6	13.61	0.080	
40489	–1.057	–0.843	–92.9	6.1	17.89		
40490	0.015	–1.357	–96.1	0.9	13.84	0.590	
40491	–1.017	–0.898	–102.8	3.6	17.15	0.386	
21485	1.280	–0.453	–111.6	4.5	16.60		
40492	–0.309	1.323	–111.0	8.2	18.20		
40493	–1.023	0.895	–98.6	0.9	15.44	0.038	
31674	1.038	–0.879	–103.7	6.4	15.69		
24042	1.277	0.470	–116.2	6.4	17.29		
40494	–1.154	–0.723	–107.0	1.9	15.98	0.382	
31689	0.884	–1.036	–106.6	2.7	14.95	0.093	
40495	–0.948	–0.979	–107.9	9.4	17.93		
40496	–1.231	0.595	–96.5	8.3	18.09		
22458	1.347	–0.248	–122.7	8.3	17.30		
40497	–0.575	–1.242	–113.8	2.8	16.73	0.479	
40498	–1.021	–0.913	–110.0	5.0	17.49		
23272	1.372	0.029	–115.3	6.6	17.09		
31696	0.799	–1.122	–105.0	2.0	15.23	0.265	
40499	–1.019	–0.933	–104.9	1.8	15.92	0.912	
17677	0.500	1.291	–113.4	5.0	17.07		
40500	–1.216	0.663	–124.4	3.1	16.80		
31163	0.244	–1.377	–97.9	3.6	14.83		
40501	–0.971	1.009	–87.9	2.7	16.31		
18151	0.430	1.335	–124.9	7.8	17.64		
23680	1.389	0.189	–119.0	6.4	16.71		
40502	–0.961	1.023	–104.6	1.0	13.38	0.740	
19549	0.079	1.405	–106.7	3.1	15.71		
23908	1.375	0.307	–118.2	3.4	15.54		
23996	1.367	0.355	–122.9	6.4	17.12		
40503	–1.343	–0.438	–101.2	7.0	17.91		
40504	–0.403	–1.356	–111.5	4.3	16.92		
40505	–1.192	–0.770	–99.7	7.7	17.63		
19122	0.225	1.404	–129.2	6.3	15.92		
40506	–0.171	1.412	–114.4	4.3	17.19		
40507	–1.373	0.371	–110.4	7.9	17.97		
40508	–1.404	–0.257	–108.1	1.8	14.93		
40509	–1.427	–0.024	–102.1	7.8	17.89		
40510	–0.939	–1.076	–89.3	5.1	16.85		
40511	–1.252	0.687	–109.0	3.1	16.59		
24237	1.325	0.535	–131.5	4.9	17.42		
40512	–1.403	–0.268	–106.1	3.2	16.77		
40513	–1.236	0.721	–116.2	2.4	15.98		
40514	–1.157	–0.844	–106.6	0.7	13.41	0.502	
40515	–1.432	–0.050	–117.3	4.1	17.32		
40516	–0.877	–1.146	–106.2	9.9	18.04		
31323	0.273	–1.421	–116.0	0.6	13.44	0.950	
24053	1.419	0.333	–131.3	4.6	17.03		
40517	–1.265	–0.733	–112.3	2.9	16.46		
40518	–1.455	–0.153	–124.4	3.8	16.72		
31763	0.645	–1.314	–101.7	6.4	15.17		
31862	1.189	–0.854	–119.9	3.9	16.43		
40519	–1.277	–0.720	–108.5	7.8	17.87		
31920	1.072	–1.006	–120.4	3.4	15.28		
40520	–1.332	–0.623	–111.5	6.8	17.63		
40521	–1.392	–0.490	–102.2	4.4	17.16		

TABLE 1—*Continued*

ID	RA	DEC	V(km s^{-1})	σ_V	m_V	Prob	ID_{AC}
40522	0.109	–1.474	–98.2	0.7	13.99	0.577	
40523	–0.610	1.351	–122.8	5.1	17.18		
40524	–0.997	–1.114	–104.9	1.7	15.19	0.542	
40525	–1.252	–0.836	–113.1	3.7	16.88		
40526	–1.234	–0.871	–123.5	8.3	16.75		
40527	–1.235	–0.871	–112.6	3.1	16.67		
40528	–0.887	–1.262	–114.7	2.5	16.56	0.682	
40529	–1.009	1.167	–132.5	7.2	17.83		
40530	–1.122	1.061	–116.7	4.8	17.33		
40531	–0.628	1.414	–128.5	5.6	17.85		
40532	–1.402	0.711	–102.0	0.6	13.17	0.395	
40533	–1.284	–0.970	–122.3	3.1	16.24		
40534	–1.073	–1.204	–105.3	4.7	16.27		
24566	1.534	0.531	–105.3	0.6	13.95	0.559	
40535	–1.276	1.018	–108.2	0.8	13.25	0.804	
22417	1.563	–0.483	–104.2	0.7	14.10		
40536	0.943	1.356	–99.4	0.6	12.80	0.388	
23995	1.663	0.055	–112.3	1.1	14.28		
40537	–0.650	1.542	–96.8	0.7	13.20	0.845	
40538	–0.300	–1.648	–103.3	0.9	14.77		
18728	0.536	1.600	–112.7	1.4	14.26		
40539	–1.372	1.007	–104.7	0.8	12.89	0.656	
40540	–1.484	0.835	–106.8	0.8	13.32	0.911	
40541	1.450	0.936	–111.9	0.8	13.60		
40542	1.455	0.938	–111.4	1.2	13.50		
40543	1.393	–1.035	–107.6	0.7	14.89		
40544	–0.793	1.553	–98.6	1.6	14.42		
40545	1.071	1.461	–105.6	1.0	15.55		
40546	1.799	0.268	–111.4	1.2	14.09		
40547	0.002	–1.859	–99.1	0.6	14.51	0.560	
40548	–0.748	1.702	–106.7	0.8	15.62		
40549	–1.825	–0.363	–92.5	1.2	15.10		
40550	–0.784	1.701	–123.2	1.7	14.50		
40551	0.077	–1.877	–99.0	0.7	14.48	0.324	
40552	1.541	–1.101	–108.7	1.0	14.55		
40553	–0.150	1.898	–109.6	0.9	15.12		
40554	1.553	1.110	–112.9	0.8	14.23		
40555	1.528	1.165	–107.2	0.8	14.09		
40556	–0.910	1.740	–124.8	0.8	14.29		
40557	–0.517	1.930	–95.4	0.9	15.18		
40558	–1.695	–1.082	–110.6	0.8	14.93		
40559	1.727	1.080	–117.2	0.8	14.54		
40560	1.767	–1.071	–103.4	0.9	14.24	0.149	
40561	1.992	–0.635	–98.9	0.8	15.42		
40562	1.449	–1.539	–100.7	0.7	14.38	0.398	
40563	–0.720	–2.022	–99.9	1.0	15.66		
40564	–2.120	–0.450	–109.4	0.8	14.92		
40565	–1.960	–0.982	–111.1	0.7	14.16	0.124	
40566	2.088	–0.730	–106.4	1.1	15.25		
40567	2.198	–0.359	–110.5	0.6	13.73	0.577	
40568	2.209	0.562	–114.3	0.6	13.92	0.207	
40569	–1.732	–1.503	–114.8	1.3	14.74		
40570	–2.233	–0.615	–103.2	0.8	14.98		
40571	2.165	0.842	–109.9	0.8	15.15		
40572	–2.097	1.067	–110.1	0.5	13.05	0.257	
40573	–1.847	1.473	–112.8	1.1	13.35		

TABLE 1—*Continued*

ID	RA	DEC	V(km s^{-1})	σ_V	m_V	Prob	ID_{AC}
40574	0.627	2.283	–99.6	0.8	15.46		
40575	1.561	1.786	–101.7	0.8	14.44	0.656	
40576	0.519	–2.403	–99.9	0.6	13.53	0.158	
40577	–2.447	0.415	–104.5	0.8	15.17		
40578	–1.667	–1.851	–107.0	0.8	14.54	0.966	
40579	0.312	2.477	–112.1	0.8	15.32		
40580	–1.548	–2.028	–110.6	0.8	15.03		
40581	–2.378	–0.943	–109.2	0.9	14.85		
40582	–0.548	2.545	–107.2	0.6	13.02	0.928	
40583	0.750	2.497	–104.5	0.8	14.71		
40584	–1.773	1.957	–111.5	0.8	15.61		
40585	–1.747	2.067	–104.2	1.0	15.23		
40586	1.505	–2.330	–105.9	0.9	15.25		
40587	–0.692	2.686	–112.0	0.8	13.36	0.406	
40588	–2.036	–1.939	–100.6	0.6	13.49	0.929	
40589	–1.297	2.497	–101.4	0.7	13.66	0.433	
40590	0.620	–2.753	–103.4	1.1	15.59		
40591	2.578	–1.185	–114.9	0.8	14.78		
40592	–2.550	–1.278	–112.8	0.6	13.82	0.994	
40593	2.249	–1.760	–112.2	0.6	13.79	0.596	
40594	1.367	–2.555	–105.6	0.8	15.19		
40595	2.813	0.890	–110.8	0.6	14.40	0.584	
40596	–2.390	1.734	–102.2	0.7	14.22	0.033	
40597	–2.812	–0.928	–112.6	1.0	15.37		
40598	2.966	0.121	–99.8	0.6	13.32	0.182	
40599	–2.125	–2.135	–93.9	0.9	15.08		
40600	2.124	–2.211	–111.6	0.8	14.13	0.175	
40601	–0.477	3.172	–108.9	0.7	14.67		
40602	1.033	–3.073	–104.7	0.7	14.06		
40603	1.161	–3.054	–105.9	1.2	13.91		
40604	–2.922	–1.562	–109.6	1.2	14.87		
40605	–3.055	–1.280	–108.6	0.6	13.72	0.750	
40606	–2.210	2.493	–109.3	0.9	15.39		
40607	–3.004	1.488	–109.8	0.7	14.44	0.910	
40608	1.735	–2.917	–110.3	0.8	15.40		
40609	–1.548	–3.030	–110.2	1.2	15.55		
40610	–2.940	1.745	–107.5	1.0	15.17		
40611	3.195	–1.291	–106.8	0.7	14.11	0.764	
40612	2.950	1.810	–113.5	0.9	15.12		
40613	–0.864	3.355	–110.8	0.8	12.79	0.400	
40614	0.338	–3.562	–103.3	0.8	15.09		
40615	1.992	–3.007	–110.6	0.6	13.35	0.888	
40616	–3.622	0.010	–105.4	0.6	14.37	0.176	
40617	1.152	3.479	–110.5	0.6	13.98	0.825	
40618	0.350	3.657	–109.3	0.7	14.65		
40619	1.639	3.345	–117.5	0.7	14.25	0.095	
40620	2.345	2.918	–113.6	0.7	14.13	0.954	
40621	–1.685	–3.358	–98.8	0.9	15.20		
40622	–3.544	–1.486	–102.6	0.7	14.40	0.187	
40623	–3.918	–0.113	–108.7	0.8	15.25		
40624	–2.115	–3.327	–100.7	1.0	15.26		
40625	3.908	–0.610	–102.2	0.8	14.61		
40626	2.776	2.927	–100.1	0.6	14.06	0.130	
40627	4.051	0.378	–119.7	1.5	14.12		
40628	–2.517	–3.273	–94.9	1.4	16.50		
40629	–2.935	2.955	–106.1	0.8	16.11		

TABLE 1—*Continued*

ID	RA	DEC	V(km s^{-1})	$\sigma_{\rm V}$	m$_V$	Prob	ID$_{\rm AC}$
40630	–3.323	–2.525	–103.7	0.6	13.73	0.843	
40631	–2.477	–3.365	–105.2	0.8	15.97		
40632	–2.695	–3.270	–105.8	0.8	15.90		
40633	4.028	–1.600	–103.3	0.8	15.36		
40634	0.410	4.412	–105.1	0.8	15.23		
40635	–0.155	4.432	–109.8	0.7	14.96		
40636	4.150	1.573	–107.0	0.7	15.26		
40637	–1.447	4.262	–112.5	0.8	16.54		
40638	4.248	–1.589	–105.5	0.6	14.03	0.470	
40639	4.020	2.180	–108.2	0.8	15.59		
40640	4.512	–0.853	–110.0	1.1	16.48		
40641	–0.482	4.588	–105.3	1.0	16.18		
40642	2.744	3.723	–102.2	0.6	13.44	0.534	
40643	–2.172	4.110	–109.8	0.8	15.53		
40644	–4.015	–2.550	–101.7	0.9	16.56		
40645	–1.697	4.465	–108.3	0.8	15.74		
40646	–0.562	4.748	–106.3	1.0	16.35		
40647	–4.610	–1.617	–103.3	0.8	16.04		
40648	–3.415	–3.500	–102.9	0.8	15.71		
40649	4.878	–0.752	–106.8	0.8	15.62		
40650	–2.672	–4.202	–112.4	0.8	16.37		
40651	–4.340	–2.682	–109.1	0.8	15.30		
40652	2.987	4.185	–108.9	0.8	15.44		
40653	–0.820	5.082	–112.5	0.8	15.67		
40654	3.250	4.092	–108.0	0.8	15.64		
40655	–3.710	–3.747	–104.3	0.8	16.52		
40656	3.150	4.330	–110.5	1.2	15.84		
40657	–0.083	–5.455	–103.5	0.9	16.41		
40658	–4.815	2.640	–105.9	0.8	16.44		
40659	–5.157	1.965	–103.6	0.7	15.23		
40660	–1.490	–5.340	–108.7	0.8	15.60		
40661	4.360	3.567	–104.2	0.7	14.51		
40662	–0.373	–5.637	–106.9	0.8	15.49		
40663	5.435	1.555	–105.7	0.9	16.53		
40664	–5.363	–1.853	–105.3	0.8	16.36		
40665	2.730	–5.052	–108.3	0.8	16.31		
40666	–1.332	–5.663	–103.1	0.9	16.34		
40667	–5.690	–1.548	–105.2	0.7	15.32		
40668	–3.485	–4.877	–110.6	1.0	16.44		
40669	–2.132	5.702	–105.4	0.9	16.57		
40670	4.675	–3.935	–108.1	0.8	16.20		
40671	–0.837	6.127	–103.8	0.8	16.41		
40672	2.408	–5.868	–107.5	0.9	16.41		
40673	5.600	3.008	–109.1	0.7	15.50		
40674	4.235	–4.817	–107.0	0.8	15.48		
40675	–5.375	3.672	–107.1	1.2	16.48		
40676	3.350	–5.622	–105.0	0.9	16.08		
40677	–4.620	–4.690	–102.9	0.9	16.18		
40678	2.970	5.897	–114.5	0.8	16.26		
40679	–3.760	5.783	–108.3	0.7	14.36		
40680	1.217	–6.798	–103.5	0.7	14.20		
40681	–2.965	6.290	–113.5	0.9	16.56		
40682	–6.375	2.843	–111.6	0.8	15.02		
40683	–6.985	0.617	–109.2	0.8	16.08		
40684	–5.887	–3.945	–106.4	0.8	15.21		
40685	–5.830	4.132	–109.0	0.7	14.21		

TABLE 1—*Continued*

ID	RA	DEC	V(km s^{-1})	$\sigma_{\rm V}$	m$_V$	Prob	ID$_{\rm AC}$
40686	–0.897	–7.197	–106.9	0.7	14.86		
40687	–2.983	–6.660	–106.2	0.7	15.28		
40688	5.972	4.370	–108.9	0.7	15.56		
40689	–4.645	5.995	–104.2	0.7	15.49		
40690	7.043	–2.937	–104.3	0.9	16.22		
40691	–4.225	–6.387	–108.5	0.8	15.64		
40692	–6.965	–3.462	–106.6	0.7	15.11		
40693	–6.275	–5.083	–100.9	0.7	14.51		
40694	4.287	6.990	–105.9	0.7	15.45		
40695	–5.537	–6.093	–105.8	0.8	15.63		
40696	8.288	–1.088	–104.6	0.7	14.85		
40697	–2.178	8.198	–110.1	0.7	15.53		
40698	8.470	–2.103	–106.0	0.8	15.97		
40699	3.168	–8.195	–106.1	0.7	14.65		
40700	–0.983	–8.905	–106.3	0.8	16.42		
40701	1.805	–8.798	–109.0	0.7	13.87		
40702	–6.000	–6.683	–103.5	0.7	15.06		
40703	–4.802	8.343	–111.2	0.7	15.83		
40704	6.738	7.083	–109.3	0.8	15.84		
40705	–1.582	9.657	–108.7	0.7	15.51		
40706	–9.417	3.350	–101.4	0.8	15.57		
40707	6.020	7.990	–106.5	0.8	14.70		
40708	–9.640	3.993	–105.5	0.9	16.57		
40709	–2.030	10.298	–110.4	0.8	14.91		
40710	4.148	9.765	–103.7	0.8	15.64		
40711	–2.525	10.325	–110.7	0.8	16.18		
40712	11.375	1.375	–104.3	0.7	13.75		
40713	–11.395	1.245	–100.9	0.7	14.68		
40714	–11.570	0.827	–112.6	0.7	13.62		
40715	–6.133	–10.360	–109.2	0.7	16.07		
40716	–10.310	6.603	–106.8	0.7	14.79		
40717	0.507	12.537	–114.9	0.8	16.49		
40718	–12.550	–0.807	–108.5	0.7	13.57		
40719	7.760	10.180	–106.0	0.7	13.96		
40720	12.665	–2.482	–109.4	0.7	15.11		
40721	1.000	–13.162	–111.1	0.8	16.49		
40722	–1.803	–13.172	–105.8	0.7	15.81		
40723	1.908	–13.220	–109.4	0.8	15.71		
40724	–11.975	6.612	–105.8	0.8	16.44		
40725	13.948	–2.825	–103.6	0.8	16.49		
40726	–13.370	–10.338	–102.9	0.7	14.90		

arXiv:astro-ph/9912172v1 8 Dec 1999

TABLE 2

M15 MULTIPLE VELOCITY MEASUREMENTS

ID	V_{FP95}	V_{FP94}	V_{FP92}	V_{FP91}	V_{PSC}	V_{FP98}	V_{Druk}	V_{Dub}
30	–114.1 0.9		–126.7 1.5					
36	–122.1 0.9	–122.4 1.4						
332	–110.5 0.7		–112.3 1.6	–108.3 2.3	–109.3 0.6		–109.1 0.8	
405	–117.3 1.2		–111.6 3.3	–117.1 4.6				
716	–118.6 1.3	–122.7 2.1						
1084	–107.5 0.8	–108.5 1.5	–108.0 2.7	–107.0 2.1				
1222	–126.5 1.1		–118.4 2.3	–125.9 2.9				
1254			–115.9 1.2	–95.3 1.4				
1422	–99.8 0.7	–100.0 1.1	–101.9 1.7	–104.1 3.4	–100.1 0.7			
1685	–124.4 0.9		–122.5 2.1	–120.6 3.6	–124.2 2.5			
1740	–99.6 1.3			–125.9 2.9				
1761	–114.6 0.9		–116.5 2.0	–113.4 2.8	–114.2 0.9			
2073	–92.8 4.2					–130.2 14.3		
2103	–121.6 2.2	–120.2 1.5	–119.3 3.3	–115.6 3.4				
2357	–102.5 1.5		–102.2 2.1			–104.8 4.8		
2515	–116.8 0.8	–126.2 1.8	–115.4 2.4	–116.0 4.9	–115.3 1.7			
2560	–121.7 1.9		–108.6 4.8					
2687	–92.8 0.9					–85.9 6.7		
2703	–87.4 0.9		–95.8 2.2	–89.0 3.1	–92.3 1.0	–86.8 2.2		
2883	–105.0 1.5					–100.1 6.0		
2976	–110.0 1.4					–117.4 5.3		
3084	–93.3 1.4	–109.0 2.9						
3129	–113.3 0.8	–116.7 0.7	–120.5 1.5	–114.5 2.8	–115.9 0.9			
3172	–79.2 0.8		–81.7 2.5		–83.8 1.3			
3199	–114.1 1.9					–125.7 4.5		
3200	–125.8 2.1					–151.0 6.4		
3316	–113.9 2.8					–127.0 5.1		
3592	–111.5 1.2					–113.1 4.4		
3593	–102.2 5.5					–106.6 8.3		
3809	–94.0 1.1		–99.6 2.4			–90.8 3.8		
3891	–123.7 1.1		–121.6 2.4	–132.2 3.0	–123.2 1.2	–131.9 2.0		
3911	–97.2 1.4					–106.0 4.2		
3982	–92.1 1.3					–92.4 3.1		
4113	–94.4 0.8		–99.9 3.3	–98.0 3.1	–97.2 0.9	–91.3 1.4		
4176	–93.1 0.7	–100.1 1.0			–97.6 0.8			
4328	–104.1 4.0					–118.4 4.6		
4341	–111.0 1.3					–119.6 4.9		
4456	–99.4 1.1					–104.0 3.5		
4626	–109.0 2.3					–127.1 8.7		
4658	–102.8 1.3					–102.6 2.5		
4756	–95.2 0.6	–88.5 0.9	–90.2 1.7		–86.7 1.3			
4843	–106.3 0.8		–111.8 3.3	–111.8 2.5				
4951	–108.1 2.7					–97.1 3.7		
5002	–95.2 1.3					–84.3 3.1		
5069	–106.9 0.9	–114.4 2.7						
5089	–102.7 0.8	–99.4 1.8	–105.7 1.6					
5166	–117.8 0.8	–126.4 0.6	–120.5 2.8	–117.6 2.8	–117.2 0.9	–118.9 4.2	–115.0 0.8	
5241	–109.0 0.8	–118.2 1.2	–123.8 1.4					
5364	–98.7 2.6					–110.3 4.8		
5407	–94.8 1.0		–103.8 2.7			–81.1 3.8		
5469	–122.0 0.9		–126.6 3.3		–123.9 1.2	–123.7 1.2		–122.2 1.1
5497	–119.9 3.4					–128.3 5.1		
5608	–108.8 1.5					–106.9 4.2		
5642	–102.0 4.0					–113.7 6.5		
5719	–104.6 3.3					–106.9 4.6		
5768	–114.2 6.6					–106.4 2.2		

TABLE 2—*Continued*

ID	V_{FP95}	V_{FP94}	V_{FP92}	V_{FP91}	V_{PSC}	V_{FP98}	V_{Druk}	V_{Dub}
5819	–88.7 4.1					–56.7 5.8		
5831	–112.2 6.4					–118.1 2.5		
5836	–96.2 1.4		–104.8 2.0			–95.6 3.5		
5933	–86.6 1.3					–75.0 2.2		–77.0 1.3
5956	–122.0 1.2			–116.9 4.1				
6041	–101.4 0.7		–99.0 1.5	–96.9 2.7	–96.9 1.3	–93.7 1.0		
6058	–104.3 1.4					–96.7 5.4		
6183	–94.1 2.8					–103.2 5.7		
6290	–102.8 0.8					–100.5 1.2		–104.3 1.2
6313	–99.9 1.0					–100.5 3.2		
6358	–108.8 2.4					–108.5 4.6		
6474	–123.9 3.4					–133.2 4.8		
6772	–115.2 3.3					–102.9 2.4		
6898	–108.5 2.0					–105.1 5.2		
6928	–108.4 0.9	–113.0 1.4				–106.1 1.2		–106.0 1.2
6947	–78.4 0.8	–72.9 0.6			–75.4 1.9	–68.5 1.4		–75.0 1.2
6954	–119.5 3.3					–114.2 5.0		
6962	–98.7 2.4					–121.3 9.0		
7001	–116.4 1.8					–108.0 22.8		
7165	–115.1 2.6					–125.3 6.7		
7384	–105.3 1.8					–102.0 3.3		
7610	–104.7 3.9					–120.9 3.5		
7718	–94.3 0.9		–98.6 3.3			–87.1 1.8		
7783	–102.6 1.2					–87.2 2.5		
8107	–115.2 2.8					–33.4 13.1		
8151	–97.6 0.9					–94.5 1.7		
8306	–115.1 4.0					–147.3 7.5		
8321	–103.3 1.2					–99.8 2.8		
8355	–99.3 0.9		–102.8 4.2			–97.0 1.7		
8369	–110.6 1.5					–110.5 2.3		
8408	–115.5 0.8	–119.9 0.9				–116.7 1.5		
8409	–93.0 1.4			–108.9 4.3				
8496	–91.8 3.0					–94.4 9.8		
8728	–107.8 1.8		–109.5 2.4		–107.2 2.2			
8754	–90.2 1.4	–80.1 5.8						
8777	–115.7 1.3					–115.0 1.7		
8944	–105.6 1.2					–105.0 3.7		
8977	–117.1 3.7					–92.2 14.9		
8991	–111.4 2.0					–117.0 4.2		
8998	–92.6 0.9					–92.1 2.9		
9158	–109.0 1.3	–121.0 3.5						
9234	–117.0 4.4					–114.7 5.2		
9281	–97.6 1.4					–104.4 3.6		
9936	–108.6 0.7	–116.8 1.0	–107.9 3.9	–113.1 3.2	–108.9 0.8	–113.9 2.9		
10012	–79.8 0.7		–85.5 1.6	–84.3 1.9	–85.0 0.6		–86.1 0.8	
10026	–124.6 0.8	–127.2 0.6	–128.8 1.5	–123.5 2.4	–125.0 0.7			
10077	–101.2 1.7					–101.3 12.0		
10399	–96.4 0.7		–95.4 2.0		–95.6 0.7	–93.1 3.4		
10464	–95.1 0.6		–99.4 1.5		–96.7 0.7			
10515	–97.8 1.1			–103.7 4.3				
11081	–109.9 0.9	–114.1 0.9	–112.7 1.6	–111.8 2.4	–110.8 1.2			
11087	–125.9 1.2	–129.7 0.9	–124.3 2.8	–122.5 2.5				
11175	–105.3 0.7				–107.8 0.8		–108.3 0.2	
11178	–100.4 2.3	–95.0 5.6						
11195	–111.6 2.8	–115.6 7.9						
11396	–118.0 2.5	–123.0 7.0	–110.0 3.8					

TABLE 2—*Continued*

ID	$V_{\rm FP95}$	$V_{\rm FP94}$	$V_{\rm FP92}$	$V_{\rm FP91}$	$V_{\rm PSC}$	$V_{\rm FP98}$	$V_{\rm Druk}$	$V_{\rm Dub}$
11439	–119.7 1.5	–116.6 4.0						
11527	–99.9 1.8	–102.6 4.8						
11529	–122.5 1.7	–120.8 5.0						
11542	–110.9 1.0	–110.4 1.8						
11609	–114.7 1.7	–116.3 2.7						
11690	–112.1 2.3	–111.3 4.9						
11776	–115.5 2.3	–108.6 3.5						
11977	–123.8 1.0	–123.3 1.5	–129.6 3.6					
12109	–100.7 1.1	–101.6 3.0						
12598	–96.8 2.5	–98.3 9.0						
12616	–105.4 1.9	–104.0 4.4						
12862	–94.6 3.7	–101.9 8.7						
13076	–102.4 0.7	–104.2 1.0						
13249	–116.8 1.9	–108.3 6.9	–107.9 4.0					
13314	–97.9 4.2	–108.7 5.2						
13326	–115.5 2.8	–108.5 7.1						
13337	–102.0 1.2	–102.8 2.3	–108.3 3.4					
13340	–101.8 4.4	–85.6 8.4						
13449	–116.3 4.3	–108.3 6.9	–112.8 4.6					
13564	–120.6 2.5	–113.8 9.4						
13806	–96.7 1.7	–88.4 5.3	–93.3 4.0					
14001	–112.6 1.5	–106.5 3.1						
14013	–114.6 0.8	–112.8 1.0	–118.1 1.8	–113.5 3.0				
14146	–115.2 1.5	–116.1 3.3	–112.4 3.9					
14193	–127.1 0.9	–127.7 1.5						
14225	–102.7 1.4		–106.6 3.1					
14495	–107.8 2.5	–112.3 5.3						
14519	–114.4 2.0	–112.6 3.8						
14520	–120.1 1.5	–117.5 4.0						
14526	–108.2 1.7		–104.5 3.8					
14660	–101.5 2.6		–114.9 2.7					
14667	–94.5 0.9	–91.8 1.9	–96.1 2.3					
14727	–95.0 1.4	–96.9 5.3						
14831	–103.9 1.2	–100.7 1.8	–107.4 3.1					
15012	–108.9 1.8	–112.3 3.5	–107.9 3.2					
15265	–118.6 1.2	–120.1 2.2						
15282	–97.8 3.5	–90.7 7.7						
15344	–98.6 1.6	–96.8 3.8						
15359	–116.0 0.7	–115.9 0.8			–117.1 0.6		–115.5 0.2	
15366	–110.1 1.8	–103.8 5.4	–104.1 3.6					
15371	–121.3 4.3	–133.0 9.0						
15484	–110.9 3.1	–113.6 7.9						
15664	–86.0 0.9	–88.9 2.5	–85.3 3.0					
15671	–102.8 1.4	–105.8 3.9	–110.0 3.7					
15734	–119.8 1.0	–123.8 2.4						
15811	–98.2 1.2	–95.7 2.7						
16216	–89.3 1.0	–90.1 1.4	–94.0 3.1					
16335	–103.7 1.9	–107.6 3.8						
16371	–91.0 3.6	–87.4 7.2						
16506	–115.1 0.9	–116.9 1.8	–114.0 2.2					
16578	–108.7 0.9	–107.8 1.3	–109.8 2.0					
16804	–110.7 2.7	–121.9 6.5						
16895	–103.3 4.7	–103.5 7.3						
16939	–106.8 0.6	–103.5 0.8			–107.4 0.9		–103.3 0.8	
16940	–111.8 2.4	–105.8 9.3						
17007	–129.4 2.0	–119.5 6.6						

TABLE 2—*Continued*

ID	V_{FP95}	V_{FP94}	V_{FP92}	V_{FP91}	V_{PSC}	V_{FP98}	V_{Druk}	V_{Dub}
17134	–104.9 0.8	–103.0 1.1	–104.5 1.9		–102.9 1.6		–102.0 0.5	
17167	–108.3 2.7	–111.6 4.5						
17270	–115.4 2.7	–114.3 5.6						
17463	–95.7 1.6	–99.3 5.9						
17724	–108.9 0.7				–107.8 1.0		–108.3 0.3	
17906	–124.5 2.8	–121.3 6.2						
18013	–89.5 1.0	–87.4 2.2						
18025	–120.1 1.0	–120.5 1.9						
18048	–103.5 2.9	–100.2 9.0						
18161	–102.7 3.0	–102.6 5.4						
18187	–121.9 2.9	–126.5 5.3						
18534	–118.2 3.4	–119.9 7.7						
18745	–132.0 1.2		–125.8 2.6					
19224	–115.8 4.9	–121.2 5.6						
19705	–98.0 3.6	–100.3 7.8						
19706	–120.1 1.4	–120.6 2.6	–113.3 3.0	–121.7 3.6				
19878	–112.3 1.2	–111.2 2.4		–114.0 3.3				
19934	–97.6 2.1	–97.3 4.8						
20026	–97.1 2.4	–94.5 6.0						
20081	–105.7 3.8	–104.1 7.0						
20087	–96.6 3.3	–104.5 5.7						
20097	–101.4 2.7	–112.2 2.5						
20166	–100.7 1.2	–99.0 2.8						
20213	–108.4 3.0	–101.7 8.1	–108.3 4.4					
20231	–133.2 0.7	–118.4 0.7	–114.8 1.7	–118.3 2.2	–114.2 1.1		–117.6 0.9	
20242	–113.5 3.4	–110.2 7.0						
20399	–112.2 0.9	–114.9 1.0	–114.5 1.4	–116.1 2.2	–116.3 1.2		–115.5 0.8	
20621	–96.4 0.8	–94.2 1.2	–96.7 1.7	–96.2 4.8			–98.9 0.3	
20653	–113.5 0.8	–113.1 1.4	–115.5 1.6	–111.9 4.0				
20961	–112.1 2.1	–101.2 5.8						
21039	–109.0 1.7	–113.1 3.9						
21208	–105.6 1.7	–103.0 5.2						
21328	–116.3 1.0	–117.0 1.8	–119.1 2.1	–118.7 4.8				
21338	–109.7 3.0		–110.1 4.6					
21515	–102.6 2.5	–93.2 9.8						
21552	–89.7 2.3	–106.1 2.8	–98.2 2.1					
21645	–114.5 1.9	–118.0 3.5						
22128	–107.2 0.8	–110.0 1.2	–114.2 2.2					
22270	–90.3 2.9	–98.4 5.1						
22367	–109.0 1.6	–109.5 5.1	–111.2 2.6					
22376	–111.3 1.8	–110.8 3.6						
22510	–110.5 0.9	–109.6 1.7	–114.7 2.2					
22556	–116.6 1.2	–121.4 3.3						
22836	–108.2 1.1	–109.2 1.6			–110.1 1.6		–106.8 0.3	
22898	–116.2 1.5	–123.9 2.1						
23014	–116.8 1.0	–120.6 1.7					–120.6 0.4	
23115	–105.3 3.9	–104.4 9.0						
23164	–115.4 1.1	–112.2 4.2						
23464	–118.0 3.5	–131.6 6.5						
23526	–107.5 1.5	–109.7 4.8					–107.7 0.6	
24566					–105.9 1.1		–105.1 0.2	
24834	–104.2 1.0		–100.5 3.5	–105.3 2.6				
24857	–112.1 1.3	–116.6 3.6						
25096	–115.7 1.6	–112.7 3.5						
25101	–102.3 2.0	–106.7 9.8						
25124	–104.5 3.3	–110.3 8.2						

TABLE 2—*Continued*

ID	V_{FP95}	V_{FP94}	V_{FP92}	V_{FP91}	V_{PSC}	V_{FP98}	V_{Druk}	V_{Dub}
25188	–115.7 2.9	–119.4 6.5						
25244	–95.5 0.8	–93.5 0.7	–97.0 1.8	–95.5 2.4	–96.5 0.9		–95.9 0.1	
25313	–98.5 1.6	–98.1 3.6						
25354	–125.1 3.9	–123.8 8.5						
25368	–82.0 5.8	–87.5 3.5						
25376	–90.7 2.1	–82.3 6.5						
25419	–118.7 3.7	–121.5 6.1						
25460	–115.3 0.6	–115.7 0.7	–115.2 1.4		–118.1 1.1			
25505	–114.9 2.2	–113.7 5.6						
25508	–114.6 1.0	–112.6 2.4						
25518	–101.0 3.2	–109.5 9.4						
25544	–97.4 3.7	–108.6 9.5						
25703	–101.4 1.7	–95.0 4.3		–127.2 2.3				
25783	–120.0 0.8	–123.8 0.9	–119.6 2.3	–120.4 3.0				
25941	–98.7 0.9	–97.5 1.0	–101.7 2.3					
26029	–117.2 1.2	–120.6 1.9						
26173	–107.4 1.5	–108.3 2.2	–106.2 3.6					
26205	–104.8 0.9	–108.8 1.9						
26241	–110.6 0.8	–110.2 1.1	–108.3 1.5	–115.6 4.1	–110.2 1.7			
26245	–111.2 2.1	–113.7 5.2						
26269	–106.4 1.0	–105.9 1.8	–108.1 3.0					
26309	–115.6 3.7	–117.8 8.3						
26391	–98.4 3.9	–99.0 5.1						
26422	–119.5 1.8	–123.3 3.7						
26425	–111.2 3.8	–118.0 8.1						
26453	–92.5 1.6	–104.2 2.4		–83.6 3.3				
26472	–101.5 5.3	–109.8 9.4						
26549	–102.3 1.0	–106.6 2.3		–102.1 4.4				
26586	–102.2 3.0	–103.2 8.5						
26618	–95.2 1.5	–92.2 4.0						
26735	–121.7 1.2	–117.3 2.5	–113.2 4.1	–109.8 4.7				
26743	–105.4 1.3	–114.6 2.9						
26772	–112.6 1.1	–114.1 2.3						
26796	–103.5 1.0	–104.3 1.9						
26860	–132.4 2.8	–137.1 4.9						
26932	–113.2 0.9	–108.6 1.7	–112.7 2.2					
26933	–109.4 0.9	–109.3 1.3	–106.3 1.7					
26978	–94.1 1.3	–96.3 3.1	–102.3 3.4					
27028	–101.8 1.2	–100.8 2.5	–109.4 3.3					
27054	–112.9 2.8	–106.4 3.8						
27117	–105.3 1.5	–106.1 4.0						
27165	–89.4 5.7	–90.3 9.5						
27190	–100.6 0.7	–105.0 0.8	–102.0 1.9	–100.4 3.2	–104.6 0.9			
27208	–114.9 1.0	–115.6 1.6	–108.2 2.9					
27228	–118.1 1.7	–116.1 3.7						
27330	–92.0 1.7	–87.3 2.5						
27484	–101.2 0.7	–104.5 0.9						
27488	–120.7 1.7	–119.8 2.8	–110.7 2.6					
27582	–120.6 1.2	–120.2 2.5						
27604	–108.0 0.9	–109.2 0.6	–110.8 1.4	–108.8 2.0	–110.0 1.1		–108.1 0.1	
27617	–87.4 1.1	–90.6 1.9						
27633	–106.9 1.3	–109.2 3.2						
27656	–99.0 1.3	–100.3 2.5						
27671	–92.1 0.9	–92.4 1.7	–94.4 2.3	–103.3 4.0				
27853	–103.5 1.4	–100.1 2.4	–103.5 2.6					
27909	–103.2 2.6	–102.8 6.9						

TABLE 2—*Continued*

ID	V_{FP95}	V_{FP94}	V_{FP92}	V_{FP91}	V_{PSC}	V_{FP98}	V_{Druk}	V_{Dub}
27980	–102.6 3.8	–110.7 9.3						
27981	–125.9 2.2	–128.5 7.3						
28054	–98.7 1.0	–98.9 1.2	–99.5 2.8					
28104	–114.0 0.7	–115.8 0.8	–114.0 1.3	–118.3 1.6	–116.5 0.8		–116.3 0.1	
28113	–118.6 1.7	–121.5 5.3						
28119	–124.8 3.5		–110.4 3.7					
28127	–91.4 0.7	–94.7 0.8	–95.9 1.6		–96.7 1.7		–94.6 0.1	
28225	–114.1 1.4	–117.9 2.1						
28277	–92.6 1.3	–93.5 2.3	–98.2 3.4					
28393	–102.0 2.5	–105.7 5.0						
28413	–99.3 2.9	–93.1 7.7						
28516	–103.7 1.4	–106.1 4.2						
28590	–109.9 1.0	–108.9 1.7	–112.8 3.2					
28593	–98.6 1.9	–100.2 6.2						
28625	–99.7 3.2	–108.3 7.0						
28634	–104.7 2.1	–103.9 3.8						
28655	–105.1 2.3	–107.1 6.4	–103.4 3.1					
28679	–113.8 1.3	–113.8 2.0	–117.0 3.3					
28739	–91.9 0.8	–93.4 1.3	–95.6 3.2	–95.5 4.2				
28749	–91.8 1.1	–97.4 2.9	–93.9 2.0					
28752	–103.6 1.4	–103.4 2.7	–108.3 3.4					
28763	–115.3 1.9	–129.6 7.0						
28801	–112.7 1.5	–113.7 4.1						
28812	–107.5 1.0	–107.4 2.1	–106.7 1.9					
28838	–109.5 1.6	–104.2 2.8						
28918	–98.6 1.7	–91.7 7.4						
28937	–109.8 1.0	–118.5 0.8	–112.7 1.4	–111.6 1.9	–98.3 1.2		–112.2 0.1	
28943	–111.6 1.0	–112.9 2.0	–114.9 2.7					
29096	–118.3 0.8	–122.0 1.3	–119.8 1.9					
29140	–96.2 0.8	–99.2 0.9			–99.9 2.3			
29149	–83.3 3.9	–66.1 6.0						
29206	–98.7 1.4	–95.2 2.7						
29269	–106.5 0.9	–106.1 2.4						
29272	–117.1 0.9	–117.1 2.1	–119.7 4.1					
29302	–109.2 3.0	–94.8 9.2						
29325	–107.0 1.4	–104.1 4.3	–112.0 2.7					
29354	–100.1 3.4	–95.0 8.4						
29393	–118.3 1.0	–121.3 1.9						
29428	–101.6 0.7	–107.7 0.6	–104.6 1.4		–104.0 0.7		–103.2 0.1	
29478	–114.0 5.0	–109.0 9.6						
29539	–93.8 1.3	–95.3 2.5						
29544	–100.8 0.7	–98.7 1.1	–101.0 1.8	–99.5 3.0	–102.1 1.4			
29663	–101.6 0.9	–101.0 1.5	–105.0 2.2					
29666	–108.6 0.8	–108.3 1.3	–111.2 1.9					
29679	–103.6 1.9	–105.9 5.5	–101.0 3.1					
29692	–108.4 1.0	–109.3 1.9	–112.7 2.0					
29815	–113.5 2.3	–113.6 3.2	–114.3 3.4					
29897	–111.3 0.9	–112.3 0.9			–111.3 1.1		–110.8 0.8	
29939	–93.6 3.7		–110.2 3.6					
30079	–108.1 2.8	–111.6 8.2						
30082	–106.0 1.7	–112.4 3.9	–116.4 3.2					
30198	–98.7 1.1	–99.3 3.6						
30279	–99.5 1.1	–96.9 1.6						
30342	–94.9 1.0	–93.4 2.2						
30433	–97.3 0.7	–96.0 0.8			–93.5 1.0			
30489	–120.6 1.1	–125.8 2.6						

TABLE 2—*Continued*

ID	V_{FP95}	V_{FP94}	V_{FP92}	V_{FP91}	V_{PSC}	V_{FP98}	V_{Druk}	V_{Dub}
30536	–107.9 2.6	–122.4 6.4						
30642	–101.8 1.4	–106.4 2.9						
30648	–103.4 1.9	–105.6 5.0						
30772	–103.5 2.5	–101.6 8.2						
30899	–105.3 1.8	–109.6 6.3						
30924	–101.5 1.1	–102.8 2.4						
31162	–108.2 2.3	–110.2 8.7						
31273	–117.4 0.7	–120.0 0.7			–114.7 0.9		–112.6 0.1	
31318	–106.7 1.5	–104.0 3.6						
31323					–116.0 1.0		–115.9 0.2	
31328	–102.4 1.4	–104.3 4.0						
31341	–98.4 0.9	–102.1 1.7						
31370	–101.0 5.1	–99.2 7.2						
31434	–101.2 1.8	–105.7 4.5						
31442	–107.5 2.8	–106.6 6.5						
31549	–112.9 3.4	–121.7 8.0						
31619	–109.2 1.9	–108.7 4.3						
31689	–102.7 3.2	–111.8 3.5						
31696	–103.5 1.8	–108.2 2.9						
40002	–81.2 1.0	–82.7 2.4						
40004	–90.6 1.2	–93.7 3.3						
40016	–117.2 1.0	–120.5 1.1						
40021	–118.2 1.9	–110.9 5.2						
40022	–92.9 3.3	–87.4 9.2						
40025	–94.1 1.0	–91.8 1.5	–107.1 3.8					
40026	–113.6 1.7	–122.6 4.1						
40032	–103.2 0.8	–103.9 1.4	–96.4 3.0					
40036	–101.3 1.1	–98.7 2.2						
40037	–115.3 1.4	–111.8 2.2	–121.8 2.4					
40039	–113.2 3.9	–104.3 7.5						
40040	–108.8 0.7	–111.1 0.7	–112.9 1.7		–109.3 1.0			
40042	–113.7 1.0	–113.6 0.8	–116.2 1.3	–116.7 1.8	–114.2 0.6			
40044	–125.0 1.4	–127.1 2.2		–120.6 4.4				
40046	–123.8 0.7	–126.8 0.8	–124.6 2.0	–124.2 2.6	–123.4 0.7			
40047		–128.2 0.7	–130.0 2.0	–122.5 1.6	–123.1 0.9			
40050	–105.7 1.7	–98.7 4.4						
40051	–113.3 1.4	–127.8 2.1	–118.6 2.4					
40052	–100.7 0.8	–101.8 1.2	–98.2 2.1					
40056	–117.4 3.4	–119.0 7.0						
40057	–135.4 2.2	–136.2 1.9						
40059	–106.8 1.8	–106.5 3.6	–111.0 3.2					
40063	–129.7 1.8	–134.6 5.0						
40064	–109.3 1.5	–112.8 2.3						
40066	–125.2 5.0	–126.6 5.4						
40070	–109.1 3.8	–123.1 6.0						
40071	–108.2 5.0	–105.5 8.4						
40076	–101.9 1.8	–103.8 4.1						
40078	–134.1 7.1	–136.9 5.9						
40080	–111.4 2.2	–114.8 8.7						
40082	–83.1 1.7	–80.5 5.0						
40088	–111.8 4.3	–105.7 5.4						
40089	–123.5 1.6	–118.5 2.1						
40090	–96.7 0.8	–96.4 1.2	–97.7 1.9					
40091	–106.0 2.1	–114.1 8.4						
40094	–116.0 1.3	–114.0 1.9						
40096	–102.4 1.9	–104.5 2.7						

TABLE 2—*Continued*

ID	$V_{\rm FP95}$	$V_{\rm FP94}$	$V_{\rm FP92}$	$V_{\rm FP91}$	$V_{\rm PSC}$	$V_{\rm FP98}$	$V_{\rm Druk}$	$V_{\rm Dub}$
40097	–123.9 2.9	–128.5 6.8						
40098	–100.1 1.2	–100.1 2.0						
40099	–102.1 1.2	–102.9 3.5						
40105		–127.6 1.6		–121.2 4.4				
40108	–104.1 3.3		–106.0 4.8					
40110	–102.7 3.5	–116.8 8.3						
40112	–102.7 1.2	–105.7 2.7						
40113	–124.3 1.7	–116.1 3.6						
40114	–104.2 3.4	–108.9 4.9						
40116	–83.9 3.5	–83.0 9.4						
40122	–100.3 1.9	–101.1 6.6						
40123	–110.0 1.2			–113.4 3.9				
40124	–96.8 2.1	–98.1 3.8						
40126	–98.6 1.2	–95.2 3.0						
40129	–108.7 4.4	–118.8 7.5						
40130	–95.7 2.0	–95.9 3.2						
40134	–118.3 2.3	–113.9 4.1						
40135	–103.9 1.1	–103.6 2.6	–111.7 2.3					
40136	–112.8 0.8	–113.9 0.9	–110.4 1.7					
40138	–124.0 1.2	–117.9 2.3						
40140	–107.6 0.8	–107.1 1.0	–105.5 2.0					
40141	–115.8 3.1	–109.7 5.8	–112.3 3.1					
40144	–96.8 3.2	–123.6 7.5						
40145	–118.9 0.7	–123.2 0.6	–114.2 1.8	–114.1 2.8	–116.6 0.8		–116.2 0.1	
40151	–114.0 1.5	–116.5 2.2	–116.7 4.8					
40152	–110.7 2.4	–110.0 6.2						
40156	–100.3 1.3	–96.7 2.7						
40157	–107.6 0.9	–108.1 1.5	–107.6 3.6					
40159	–112.9 0.8	–108.4 1.1	–109.8 2.0					
40161	–103.0 0.7	–100.5 1.0						
40166	–124.9 1.8	–121.5 3.3	–113.8 4.1					
40168	–92.8 0.6	–92.5 0.7	–92.5 1.8		–91.8 0.7		–92.9 0.1	
40169	–85.7 2.4	–87.8 8.1						
40171	–103.2 2.5		–93.9 3.4					
40174	–97.8 0.9	–99.5 1.2	–97.6 2.3					
40177	–97.0 1.0	–97.4 1.4	–99.8 2.2					
40178	–98.2 0.8	–97.7 1.6	–93.4 2.1					
40180	–84.2 6.9	–94.2 10.0						
40183	–96.1 0.6	–94.3 0.9	–93.4 1.9		–95.2 1.4		–95.9 0.8	
40185	–107.0 2.4	–107.4 7.8						
40186	–109.1 2.6	–107.4 8.6						
40192	–129.9 5.5	–129.1 7.7						
40194	–127.4 2.0	–123.0 3.2						
40201	–105.8 4.1	–106.7 8.0						
40203	–114.0 1.4	–112.1 2.4	–113.6 2.6					
40208	–122.8 6.1	–120.1 7.8						
40210	–123.7 1.6	–118.8 3.6						
40211	–119.1 1.0	–117.4 1.4	–111.9 3.0					
40212	–113.5 1.1	–115.5 1.8						
40213	–117.0 2.4	–114.5 6.0	–114.5 4.0					
40214	–110.0 0.7	–111.1 1.1	–110.3 1.6	–109.1 2.7				
40215	–97.7 2.3	–100.6 4.8						
40217	–118.1 2.5	–115.0 6.1						
40219	–100.6 2.6	–94.2 4.9						
40220	–105.3 1.4	–104.4 4.6						
40222	–111.7 3.7	–110.6 9.5						

TABLE 2—*Continued*

ID	V_{FP95}	V_{FP94}	V_{FP92}	V_{FP91}	V_{PSC}	V_{FP98}	V_{Druk}	V_{Dub}
40223	–116.1 1.4	–112.3 2.0	–109.9 2.5					
40225	–132.1 0.7		–125.1 1.3		–124.5 1.1		–119.9 0.8	
40226	–110.0 1.8	–105.6 3.3						
40228	–103.7 2.0	–110.1 4.3	–106.5 4.5					
40231	–120.3 1.5	–122.6 2.6	–114.9 4.0					
40233	–103.0 1.7	–96.2 5.6						
40234	–86.5 2.7	–89.8 5.8						
40235	–116.6 0.7	–108.8 0.6	–113.1 1.3		–113.1 0.9		–111.0 0.1	
40236	–114.3 1.1	–109.0 2.0	–111.4 2.6					
40242	–126.7 1.1	–123.6 1.7	–122.6 2.3					
40243	–118.0 1.4		–115.2 2.3					
40244	–104.2 2.4	–102.5 7.4						
40245	–129.4 1.5	–121.5 4.6	–120.6 3.3					
40251	–115.6 1.3	–112.8 2.1	–112.4 2.3					
40252	–101.6 0.8	–97.7 1.0	–99.6 1.6					
40258	–122.0 2.7	–98.2 8.8						
40261	–101.1 0.9	–100.8 1.7	–102.4 3.2					
40266	–108.3 0.8	–108.3 1.2	–108.0 2.1					
40267	–98.2 3.0	–114.7 5.0						
40273	–102.2 2.0	–102.5 5.4	–96.7 3.4					
40274	–104.1 0.7		–102.4 1.5		–101.7 1.1		–102.1 0.1	
40275	–104.9 4.7	–101.1 7.3						
40277	–111.0 1.3	–104.9 3.9	–112.9 3.0					
40278	–112.3 1.5	–114.4 4.1	–115.4 3.7					
40279	–108.0 0.8	–103.5 0.9	–106.1 2.7		–110.2 1.1		–106.1 0.1	
40285	–119.7 1.6	–116.2 3.4	–110.8 4.2					
40286	–114.0 3.9	–116.0 8.3						
40287	–132.7 4.2	–123.4 6.6						
40294	–118.8 1.1	–117.1 2.1	–113.5 2.4					
40295	–127.1 1.6	–123.4 4.1						
40297	–109.1 1.4	–113.2 2.3	–112.2 2.3					
40298	–104.8 1.3	–107.0 1.7	–109.3 1.9					
40299	–113.1 2.0	–111.3 4.5	–113.3 2.8					
40303	–117.6 1.5	–114.5 3.6						
40305	–94.7 1.2	–92.3 2.7						
40306	–120.4 5.5	–110.7 6.8						
40310	–107.9 3.2	–109.4 8.0						
40311	–99.9 3.4	–110.0 9.0						
40313	–100.1 2.6	–96.4 7.9						
40315	–94.8 5.4	–93.9 9.1						
40317	–107.6 0.8	–106.0 1.3	–110.0 1.9					
40318	–130.9 4.1	–124.4 7.0						
40319	–111.5 1.5	–112.3 4.2	–112.2 4.9					
40320	–107.4 3.4	–109.0 6.8						
40321	–106.9 5.7	–109.3 9.5						
40322	–122.5 1.5		–116.9 2.0					
40324	–112.1 0.7	–111.5 1.0	–113.3 1.8				–110.0 0.3	
40325	–97.4 0.8	–99.4 0.9	–97.3 1.7					
40329	–105.5 4.0		–101.7 3.7					
40330	–123.6 1.5	–124.0 4.5	–114.7 2.9					
40331	–105.2 7.6		–125.9 4.6					
40334	–125.1 1.4	–124.1 3.9	–119.1 3.3					
40336	–108.1 1.3	–109.0 2.9	–107.1 2.8					
40337	–116.8 1.4	–116.9 3.4	–116.2 1.7					
40342	–101.1 1.3	–99.8 2.6						
40343	–109.9 5.9	–107.8 9.1						

TABLE 2—*Continued*

ID	V_{FP95}	V_{FP94}	V_{FP92}	V_{FP91}	V_{PSC}	V_{FP98}	V_{Druk}	V_{Dub}
40350	–99.1 0.7	–98.5 0.9	–100.9 2.0					
40352	–106.0 1.9	–99.7 5.1						
40353	–113.9 0.7	–105.0 0.8	–112.8 1.8					
40360	–107.8 3.2	–113.3 9.3						
40361	–104.8 0.7	–104.0 1.2	–108.8 2.1					
40363	–110.9 3.5	–104.4 9.8						
40367	–97.9 1.6	–100.5 3.7						
40368	–115.6 6.2	–110.8 9.3						
40370	–96.8 3.5	–104.3 6.0						
40371	–116.2 0.9	–120.8 2.3						
40372	–103.1 1.1	–100.9 2.7						
40373	–117.9 0.7	–116.9 1.0	–119.7 1.5					
40375	–108.6 2.1	–106.1 4.7						
40376	–111.8 1.9	–110.5 4.3						
40379	–90.5 4.2	–80.3 7.8						
40383	–101.7 3.1	–101.0 3.1						
40388	–118.5 1.2	–116.3 1.5						
40393	–128.1 0.7	–119.7 0.8			–117.5 0.7		–118.5 0.1	
40394	–105.1 2.8	–88.1 6.2						
40396	–103.6 0.9	–104.5 1.7						
40405	–103.0 1.3	–109.2 5.2						
40406	–101.0 1.1	–102.6 2.1						
40409	–101.0 1.2	–99.1 3.3						
40410	–105.6 1.5	–105.2 5.6						
40412	–102.9 1.1	–101.6 2.1						
40413	–108.5 0.7	–108.5 1.2						
40414	–111.5 1.9	–109.7 4.6						
40417	–120.3 2.1	–126.8 3.1						
40419	–112.9 1.3	–115.9 4.6						
40421	–108.2 1.7	–109.4 4.2						
40422	–98.3 1.8	–104.3 5.5						
40423	–111.2 1.0	–112.1 1.9		–111.6 3.0				
40424	–102.3 1.4	–103.9 2.8						
40426	–96.6 0.8	–95.6 1.4					–95.5 0.7	
40436	–106.9 0.7	–107.4 1.2			–106.0 1.5		–105.0 0.1	
40439	–106.6 0.7	–105.9 0.8			–107.4 1.6		–104.1 0.1	
40441	–99.6 0.9	–100.7 1.6		–102.3 2.6				
40442	–106.2 1.9	–111.3 5.7						
40443	–110.2 1.3	–114.8 3.7		–114.0 2.6				
40444	–115.9 2.3	–121.1 4.2						
40446	–93.2 1.7	–102.5 3.6						
40447	–117.1 0.7	–118.0 0.7		–116.8 1.8	–115.8 1.3		–115.9 0.8	
40449	–111.6 0.9	–113.6 1.7						
40462	–113.5 1.9	–105.3 6.3						
40463	–111.8 0.7				–93.9 0.8		–96.5 0.8	
40465	–112.6 1.4	–115.0 2.4						
40467	–116.6 0.9	–119.0 1.5						
40468	–102.7 4.4	–113.8 9.1						
40469	–107.6 1.8	–111.5 4.6						
40470	–111.1 2.1	–113.3 6.1						
40471	–104.5 5.3	–107.7 9.7						
40472	–115.2 1.9	–118.7 4.9						
40474	–100.2 0.8	–103.9 1.0			–100.7 1.8		–97.7 0.8	
40475	–106.0 2.8	–126.7 5.5						
40477	–107.6 0.9	–109.8 1.5			–110.8 1.5			
40484	–108.8 1.1	–107.5 2.9						

TABLE 2—*Continued*

ID	V_{FP95}	V_{FP94}	V_{FP92}	V_{FP91}	V_{PSC}	V_{FP98}	V_{Druk}	V_{Dub}
40485	–111.6 0.9	–114.0 1.8						
40488	–104.0 0.7	–107.9 1.0			–103.2 1.2		–102.1 0.3	
40490	–95.3 0.9	–98.3 1.3			–96.0 0.9			
40491	–101.3 3.7	–109.6 8.4						
40493	–102.1 1.2						–97.6 0.8	
40494	–106.3 1.4	–110.6 4.0						
40497	–114.4 2.5	–107.7 8.7						
40499	–105.0 1.5	–104.5 3.2						
40502	–104.1 0.8				–104.8 1.0			
40514	–108.1 0.7	–107.7 0.9			–106.9 0.9		–105.4 0.8	
40522					–97.4 1.4		–98.4 0.4	
40524	–105.5 1.3	–103.1 2.8						
40528	–114.3 2.2	–117.3 6.7						
40532					–102.7 0.8		–101.6 0.2	
40535					–107.9 0.9		–108.3 0.8	
40536					–100.1 0.8		–99.0 0.1	
40537					–96.9 0.6		–96.6 0.8	
40539					–105.1 0.9		–104.3 0.8	
40540					–106.7 0.8		–106.9 0.8	
40547					–98.4 1.0		–99.3 0.2	
40551					–100.4 1.4		–98.7 0.5	
40560					–101.9 1.2		–104.7 1.1	
40562					–101.6 1.1		–100.3 0.4	
40565					–113.0 1.2		–110.5 0.4	
40567					–111.0 1.0		–110.2 0.2	
40568					–116.0 1.3		–113.9 0.2	
40572					–110.8 0.4		–109.6 0.0	
40575					–102.2 1.1		–101.4 0.6	
40576					–101.2 0.9		–99.3 0.1	
40578					–106.9 1.2		–107.0 0.6	
40582					–107.1 0.7		–107.2 0.1	
40587					–112.6 0.8		–111.3 0.9	
40588					–100.7 0.9		–100.5 0.1	
40589					–100.3 1.3		–101.6 0.3	
40592					–112.8 1.0		–112.8 0.1	
40593					–112.8 1.0		–112.0 0.2	
40595					–111.4 1.1		–110.6 0.2	
40596					–104.6 1.1		–101.4 0.3	
40598					–101.2 1.0		–99.4 0.0	
40600					–113.7 1.6		–111.1 0.5	
40605					–108.9 0.9		–108.5 0.2	
40607					–109.7 1.2		–109.8 0.3	
40611					–107.1 0.9		–106.6 0.4	
40613					–111.5 0.8		–110.2 0.8	
40615					–110.4 0.9		–110.6 0.1	
40616					–107.0 1.1		–105.0 0.1	
40617					–110.2 1.1		–110.6 0.2	
40619					–119.4 1.1		–116.9 0.3	
40620					–113.5 1.4		–113.6 0.2	
40622					–104.0 1.1		–101.9 0.6	
40626					–98.6 1.0		–100.7 0.1	
40630					–103.5 1.0		–103.7 0.2	
40638					–106.2 1.0		–105.2 0.1	
40642					–102.8 0.9		–102.0 0.2	

This figure "fig4.jpg" is available in "jpg" format from:

http://arXiv.org/ps/astro-ph/9912172v1

Draft version February 1, 2008
Preprint typeset using LaTeX style emulateapj v. 04/03/99

arXiv:astro-ph/9912172v1 8 Dec 1999

CFHT ADAPTIVE OPTICS OBSERVATIONS OF THE CENTRAL KINEMATICS IN M15

Karl Gebhardt[1,2]
University of California Observatories/Lick Observatory
University of California, Santa Cruz, Ca 95064
gebhardt@ucolick.org

Carlton Pryor[1], R. D. O'Connell[1], T.B. Williams
Department of Physics and Astronomy, Rutgers, The State University of New Jersey
136 Frelinghuysen Rd., Piscataway, NJ 08854-8019
pryor@physics.rutgers.edu,williams@physics.rutgers.edu

James E. Hesser[1]
Dominion Astrophysical Observatory
Herzberg Institute of Astrophysics, National Research Council of Canada
5071 W. Saanich Road, R.R.5, Victoria, B.C., V8X 4M6, Canada
James.Hesser@hia.nrc.ca

Draft version February 1, 2008

ABSTRACT

We have used an Imaging Fabry-Perot Spectrophotometer with the Adaptive Optics Bonnette on the Canada-France-Hawaii Telescope to measure stellar radial velocities in the globular cluster M15 (NGC 7078). An average seeing of 0.15″ full-width at half maximum, with the best-seeing image having 0.09″, allowed us to measure accurately the velocities for five stars within 1″ of the center of M15.

Our estimate of the second moment of the velocity distribution (i.e., the dispersion, ignoring rotation) inside a radius of 2″ is 11.5 km s^{-1}, the same value we find out to a radius of about 6″. However, the projected net rotation does increase dramatically at small radii, as our previous observations led us to suspect. The rotation amplitude inside a radius of 3.4″ is $v = 10.4 \pm 2.7$ km s^{-1} and the dispersion after removing the rotation is $\sigma = 10.3 \pm 1.4$ km s^{-1}, so $v/\sigma \simeq 1$ in this region. In addition, the position angle (PA) of the projected rotation axis differs by 100° from that of the net cluster rotation at larger radii. Current theoretical models do not predict either this large an increase in the rotation amplitude or such a change in the PA. However, a central mass concentration, such as a black hole, could possibly sustain such a configuration. The rotation increase is consistent with the existence of a central dark mass concentration equal to 2500 $M_\odot$.

The Strehl ratio is 1% in our worst images and 6% in our best. Despite these low values, the images allow us to resolve the brighter stars with an angular resolution close to the diffraction limit and to perform photometry on these stars accurate to a few percent. Thus, these adaptive optics observations provide us with crucial information on the central kinematics of M15.

Subject headings: globular clusters: individual (M15) — instrumentation: adaptive optics — stellar dynamics

1. INTRODUCTION

M15 (NGC 7078) was one of the first globular clusters known to have a steep central stellar density profile, inconsistent with isothermal models (King 1975, Djorgovski & King 1986). Its central structure is usually interpreted to be a product of "core-collapse" (e.g., Grabhorn *et al.* 1992)—a gravothermal instability that leads to a very small and dense core surrounded by a power-law cusp. Core-collapse predicts a specific density profile, about $r^{-2.2}$, and velocity dispersion profile, about $r^{-0.1}$ or nearly constant, in the cusp for the stellar component that contributes most of the mass (Cohn 1980, Spitzer 1987). However, the observed luminous component may have different profiles because of mass segregation. Thus, both photometric and kinematic observations are needed to estimate the profile of the gravitational potential and test the models.

The stellar density profile near the center has been measured by many authors; the best study comes from the HST analysis of Guhathakurta *et al.* (1996), who show that M15 contains a central cusp with a logarithmic slope around –1.8. This estimate is based on the deprojection of individual positions of the central stars. Although M15 has one of the highest surface brightnesses among the centrally-concentrated clusters, at the radii of interest these measurements still suffer from poor statistics due to the small number of stars. Thus, the uncertainty of the slope within a radius of 1″ is around 50%. Even more uncertain is the two-dimensional distribution of stars; i.e., whether the central isophotes are spherical or flattened.

Unfortunately, kinematical profiles are more difficult to measure than the light distribution and suffer from larger uncertainties. The central kinematics of M15 have been the subject of numerous studies (Newell *et al.* 1976, Peterson *et al.* 1989, Dubath *et al.* 1995, Zaggia *et al.* 1993, Gebhardt *et al.* 1994, 1995, 1997, Dull *et al.* 1997, Drukier *et al.* 1998). Measuring the central dispersion has been the primary goal in most of these studies. However, the central stellar density is so high that severe blending of the stellar images limits the number of stars that can be measured individually from the ground, while the large range of stellar luminosities on the giant branch limits the number of stars making significant contributions to the integrated light.

---

[1] Visiting Astronomer, Canada-France-Hawaii Telescope, operated by the National Research Council of Canada, the Centre National de la Recherche Scientifique of France, and the University of Hawaii.

[2] Hubble Fellow.

The improvements in our understanding of the central region have come from data taken under extremely good conditions (i.e., Guhathakurta's study of the stellar distribution using HST) or from the use of instruments designed to optimize the seeing profiles (i.e., Gebhardt *et al.*'s 1997 study using the fast-guiding Sub-arcsecond Imaging Spectrograph on the Canada-France-Hawaii Telescope (CFHT)). However, we have not achieved the optimal situation of equal angular resolution for the spatial and kinematic observations, primarily because the relatively small aperture of the HST makes spectroscopy very expensive. Combining adaptive optics (AO) observations, which yield the highest spatial resolution possible from the ground, with the two-dimensional velocity reconstruction enabled by Fabry-Perot (FP) observations should provide the most accurate measurements for the central kinematics.

Adaptive optics is one of the most powerful tools available to astronomers today, potentially allowing imaging at the diffraction limit of a ground-based telescope. AO is presently most efficient at near-infrared wavelengths. However, high-resolution spectrographs are only beginning to be used there, so most kinematic studies must still rely on optical wavelengths. Fortunately, in an overlap region near 9000 Å, spectrographs and CCDs are efficient, while AO systems still yield significant corrections. However, in this region the Strehl ratio – the ratio of the central intensity in the real stellar profile to that of a diffraction-limited profile – generally lies below 20%. This ratio is one of the most important numbers characterizing the quality of the corrected images. Values that low mean that careful measurements of the stellar point spread function (PSF) are required to interpret the results.

Globular clusters provide an ideal target for AO observations because the field is filled with stars that yield the PSF. Slit or aperture spectrographs do not lend themselves to AO kinematic studies because they do not generally allow an accurate measurement of the spatial PSF and because it can be hard to determine exactly where the slit was placed. Fabry-Perot imaging, in contrast, does provide both accurate spectral and accurate spatial information. In this paper we describe results from using the Adaptive Optics Bonnette (AOB) on the CFHT with an imaging Fabry-Perot.

The results from these data provide crucial information for the region within 3″ of the center of M15. They confirm the earlier results of Gebhardt *et al.* (1997) that the observed velocity dispersion profile remains flat inside a radius of a few arcseconds and that the net projected rotation profile rises in that region. The increase in the rotation is difficult to understand, but might be explained by the existence of a central massive dark object.

The rest of this paper is organized as follows. Section 2 describes how the FP AO data were taken and reduced, including a discussion of the impact that the small and variable Strehl ratio had on the accuracy of our photometry. Section 3 presents the profiles of the projected velocity dispersion and net projected rotation that result from these data, while Sec. 4 briefly revisits the mass density profiles derived with the techniques of Gebhardt *et al.* (1997). Finally, Sec. 5 summarizes the results and discusses how the large rotation at small radii in M15 might be understood in the context of the dynamical models of globular cluster evolution.

2. THE DATA

2.1. *Instrumentation*

In normal use, a Fabry-Perot étalon is placed in a collimated beam to avoid degradation of the spectral resolution. With the AO system on the CFHT at the time of our observations (see the description in Rigaut *et al.* 1998), this placement was not possible. In consultation with the CFHT staff, we chose to place our etalon in the f/40 converging beam behind the AOB focal expander. The STIS2 CCD then yielded 0.0305″ pixels and a 63″ field of view. However, the AOB optics are not telecentric – the optical axes of the converging beams were not perpendicular to the etalon away from the center of the field – and this caused additional loss of wavelength resolution. The converging beam caused a negligible degradation of the 2.0 Å intrinsic resolution of the etalon at the center of the field, but by a radius of about 6″ the resolution was worse by a factor of 1.4. Because our primary targets were the centers of clusters, this limitation of the usable field did not significantly compromise our scientific goals.

Our usual observing procedure is to scan across the Hα line, since it is a deep line that is not very sensitive to metalicity. With AO, we cannot obtain adequate correction at wavelengths that short. Fortunately, the coatings of the Rutgers etalon allowed us to work with the 8542 Å CaII triplet line. We employed our own filter to isolate the correct etalon order. It had a passband with a 30 Å full-width at half maximum (FWHM), centered on 8542 Å. A dichroic in the AO system sent the I-band light to the etalon and the CCD, and all other wavelengths to the wavefront sensor.

2.2. *Observations and Data Reduction*

We took data on June 15–19, 1998, observing M15 on three of the nights and obtaining a total of 26 usable 15-minute exposures for this cluster stepped across $\lambda\lambda$8536–8543 Å. We observed three other clusters (M13, M30, and M80) as well, which we will present in a later paper.

Due to the converging and non-telecentric beam, we could not use our standard wavelength calibration procedures and the result was increased uncertainty in the solution. Normally, a single exposure of a screen illuminated by an emission-line lamp produces a bright ring in the image because of the simple quadratic dependence of transmitted wavelength on distance from the optical axis. We measure the radii of these rings to calibrate the relation between etalon spacing and wavelength. However, in the present case, measurable rings did not exist due to a complicated dependence of both the mean wavelength and the spectral resolution on the distance from the optical axis. We were thus forced to take a sequence of images that scanned the etalon across the calibration line to measure the etalon spacing corresponding to the peak of the line. This procedure produced an adequate wavelength calibration (uncertainties < 0.1 Å), but required more time than usual.

We corrected for pixel-to-pixel sensitivity variations and the change in the transmission of the order-separating filter with wavelength using images of an internal incandescent flat field.

The CFHT AO system requires a natural guide star in the field to correct the wavefront. For the globular clusters studied, the choice was governed by a tradeoff between brightness and distance from the center. The central brightness cusps of M15 and M30 had too much structure to act as good guide stars. For M15, we used the star AC3 (Aurière & Cordoni 1981), which has V = 13.3 and is 6.7″ away from the center. The V-band magnitudes of the guide stars ranged from 13.3 to 15.5, with the best correction coming from the brighter stars.

2.3. *Photometry with AO*

The high stellar density near the center of M15 produces crowded frames that force us to use profile-fitting photometry as opposed to aperture photometry. Thus, errors in estimating the PSF directly affect the photometry and accurate photometry depends on understanding the PSF both as a function of position on the chip and as a function of time throughout the observations. AO in the optical complicates both of these matters; the small isoplanatic patch causes the PSF to vary significantly over the field and, since the AO correction is highly dependent on the native seeing, sudden changes in the seeing cause large temporal variability in the PSF. Some published reports suggest that these problems will limit the accuracy of stellar photometry in crowded fields with AO to be no better than 10% (Roberts *et al.* 1997, Esslinger & Edmunds 1998).

Estimating the PSF is a hard problem because the profile for a stellar source observed with the AO system is approximately a combination of an unguided profile – the natural site seeing – and the diffraction-limited profile, so the low Strehl ratios in the optical imply that most of the stellar light resides in the uncorrected PSF and very little in the diffraction-limited core. The fraction of the flux in the diffraction-limited core is approximately equal to the Strehl ratio. Therefore, we need to use very large PSFs to accurately measure all of the light at large radii, but, at the same time, we must finely sample the PSF to maintain the high-spatial-resolution information provided in the diffraction-limited core. Getting enough signal-to-noise to measure accurately the wings of the PSF is difficult.

Figure 1 shows Strehl ratios for the guide star in each M15 frame plotted as a function of FWHM of the star. The Strehl ratios range from 0.01 to 0.06; for our typical exposure over 90% of the light is in the broad component of the PSF. Although these Strehl ratios are low, accurate photometry depends *solely* on the ability to measure the PSF. Fortunately, the centers of globular clusters have bright stars scattered throughout the field, and so are well suited to measuring the PSF well into its wings with high-spatial resolution.

Because with FP observations we are building a spectrum from data that was taken over several days, the accuracy with which we measure the PSF in each individual frame is one of the most crucial aspects of the whole reduction. Previously, in these crowded fields, we have obtained photometry errors of roughly 2-3%; the errors are distributed among the following sources: crowding, the wings of the PSF, frame-to-frame normalizations for changing transparency, and wavelength calibration. With adaptive optics, we have to pay special attention to the PSF measurement. Photometry errors greater than 10% would render the data useless, since such errors would result in velocity uncertainties larger than 10 km s^{-1}, an unusable uncertainty for most globular clusters. We discuss below in turn the spatial extent of the PSF, the spatial variability of the PSF within a frame, and the temporal variability between frames.

2.3.1. *PSF Extent*

We determined the PSF for each frame with the normal DAOPHOT routines (Stetson 1994) and obtained the final photometry using ALLFRAME (Stetson *et al.* 1998). A quadratic variation with position on the chip provided an excellent fit for the PSF across the frame. We paid particular attention to the extent to which the PSF was both fitted and subtracted. For our observations, the diffraction limited core of the PSF is about 0.05$''$ across and the broader component is about 0.5$''$. This means that we must use a PSF that goes out beyond 1$''$ to contain most of the light. Given the pixel scale, we used a PSF radius of 50 pixels and a fitting radius of 20 pixels. The large PSF radius mandates using a large number of stars to overcome the low signal-to-noise in the wings of the PSF. Fig. 2 demonstrates the PSF's extent by plotting the flux of the guide star in each M15 frame versus radius. We truncate the logarithmic plot at a radius of 60 pixels (1.8$''$), but light is still present at these radii and our ALLFRAME photometry thus requires aperture corrections.

We can verify this extent for the PSF from data for an isolated standard star. Four consecutive 10s exposures of HD107328 (HR 4695; V=4.96) were taken in twilight on the fourth night. Conditions were mildly non-photometric; the Strehl ratios were about 0.03. The filled circles in Fig. 3 show the RMS scatter around the average aperture magnitude for apertures with radii between 3 and 150 pixels. The triangles are the uncertainties in the magnitudes expected from photon statistics. The RMS scatter in the magnitudes decreases with increasing aperture size until a radius of 50 pixels, after which it slowly increases. This scatter suggests that changes in the PSF caused by variations in the seeing and wavefront correction have become small at an aperture radius of 50 pixels. The amount of light within this radius is about 87% of that within a radius of 150 pixels for these data.

Problems caused by the extended PSF are shown in Fig. 4. This figure contains four images: (1) the best-seeing CFHT frame displayed with a linear stretch, (2) an HST frame of the same field as (1), (3) a slightly larger region of the same CFHT frame displayed with a square-root stretch, and (4) the same field as (3) with the stars subtracted. The CFHT image has a smaller FWHM than the HST image; however, the later image is preferable when one takes the tails of the PSF into consideration. The HST image essentially has no tails, whereas for the AO image most of the light is in the tails.[3] The bottom-left image demonstrates the amount of light in the tails since, with this stretch, stars separated by 1$''$ start to blend together. The bottom-right, star-subtracted, image shows residual light where there is a high density of stars because our estimate of the PSF does not contain all of the light. Since this light correlates with the brightness of the subtracted stars, it cannot be unresolved stellar light and is instead light from the unmodeled outer fringes of the PSF.

2.3.2. *PSF Variability*

We show the spatial dependence of the PSF in Figs. 5 and 6. Figure 5 overplots radial profiles of four PSFs at distances of 0, 10, 20, and 30$''$ from the guide star. The PSFs are normalized to have identical volumes. For each profile, the broad component – the uncorrected profile – is essentially unchanged, as we expect. What does change is the amount of light in the diffraction-limited core, as stars at the largest radii have almost no light in the core due to the AO correction. To demonstrate this effect with the FWHM, each line in the top panel of Fig. 6 shows the ratio of the FWHM of the PSF to the FWHM of the guide star as a function of CCD column number for the central row of an M15 frame. The ratio changes by a factor of two from the middle of the image to its edges. In addition, the change is

[3] In this regard our AO images are more like pre-COSTAR HST images.

similar for each frame. There is a slight dependence on the base FWHM; the bottom plot of Fig. 6 presents the FWHM ratio at the edge of each image as a function of the base FWHM. The smallest FWHM image has the largest variation across the field.

Figure 7 shows the temporal variation of the PSF by plotting the FWHM of the guide star as a function of frame number. The vertical lines mark the divisions between the three nights. Large, but smoothly varying, changes in the FWHM occur throughout the night. The greatest variation occurs for exposures during morning twilight, where the additional background begins to affect the AO corrections.

2.3.3. *Photometric Accuracy*

The ideal situation for determining the photometric accuracy of the observations would be to expose frame after frame using an identical setup. We obviously cannot employ this ideal method since we must scan across the absorption line in order to measure stellar velocities, but we can use our measured absorption line profile to estimate photometric accuracy. Fig. 8 plots the line profiles for four bright stars in our field. The line is a fitted Voigt profile (see Gebhardt *et al.* 1994 for details). The deviation of the points from the fitted line result from the photometric errors; the error bars for each point come from the standard DAOPHOT uncertainties. If the actual deviations divided by the expected uncertainties do not have a Gaussian distribution with unit standard deviation, the additional uncertainty is probably caused by our lack of understanding of the PSF. The points to which we fit Voigt profiles, such as those in Fig. 8, are already corrected on a frame-by-frame basis for the combined effects of transparency variations and the truncation of the PSF. As discussed in the beginning of Sec. 2.3, this last effect arises because our measured PSF does not include all of the light. Since we have many stars at different radial and spectral (i.e., different velocities) positions, these frame normalizations are unique and well-measured (see Gebhardt *et al.* 1994 for more discussion).

We average the fractional deviations from the fitted line profile for every star in each frame in order to estimate the true photometric uncertainties for each of the frames. Each point in Fig. 9 is the rms dispersion of the fractional differences between the fitted profiles and the data points in a frame as a function of the FWHM of the guide star in the frame. We estimate the dispersion from the biweight estimate of scale (Beers, Flynn, & Gebhardt 1990) using all stars with a velocity measurement and breaking the sample of stars into three groups according to brightness.

The photometric uncertainties indicated in Fig. 9 result from both photon statistics and any uncertainties due to particulars of the analysis—i.e., difficulties in measuring the PSF and the wavelength calibration. DAOPHOT provides an estimate of the photon noise through its reported uncertainty. For the brightest stars (the filled circles in Fig. 9), the typical DAOPHOT uncertainty is around 0.5% and, for the faintest stars, it varies from 6 to 10% (depending on the PSF FWHM). These typical uncertainties are smaller than the actual photometric scatter shown in Fig. 9 for both the faint and the bright stars. This difference does not suggest an additive uncertainty independent of brightness, such as that expected from PSF errors, but rather a multiplicative error in the DAOPHOT uncertainties—they are about a factor of 1.5 too small. Making such a correction brings the observed and predicted uncertainties of the faint and medium stars into reasonable agreement. However, the dispersion around the profiles of the bright stars shown in Fig. 9 is still larger than expected. This trend suggests the presence of an additive uncertainty of about 2%. We take this value as the upper limit to errors in our photometry caused by the difficulty of estimating the AO-corrected PSF.

2.4. *Velocity Zero-Point and Uncertainties*

In all of our Fabry-Perot runs we correct the zero-point of our velocities since it is difficult to get an accurate absolute wavelength calibration – we build up the spectrum over the course of a few nights and each frame has to be accurately calibrated. As discussed in Sec. 2.2, our current wavelength calibration is less accurate than for previous observations and, for this reason, we have an increased velocity zero-point uncertainty. However, we do not believe that we have systematic errors in our velocities as a function of velocity because we did not observe adjacent wavelength points at adjacent times.

To determine the velocity zero-point, we compare our velocities to the many previous datasets for M15: Gebhardt *et al.* (1994, 1997), Peterson *et al.* (1989), Dull *et al.* (1997), Drukier *et al.* (1998), and Dubath & Meylan (1994). The present data have been compared to each of these individually and to a combined dataset. All of the comparisons yield the same result: the required velocity offset is 5.7 km s^{-1}. In addition, one must increase the uncertainty for each AO velocity by adding 3.0 km s^{-1} in quadrature with the estimated uncertainty. Previous FP studies added 0.5–1.0 km s^{-1} in quadrature, which is consistent with the intrinsic velocity jitter of the giant stars (Gunn & Griffin 1979, Mayor *et al.* 1983). We attribute the larger errors in the present study to the difficulty of the wavelength calibration. Fig. 10 plots the difference between the 1995 CFHT/SIS and the shifted AO velocities as a function of the 1995 velocities. The two sets of data agree within their uncertainties, and give a reduced $\chi^2 = 1.2$ for 67 degrees of freedom.

We list the mean radial velocities in Table 1. For each star, we give the ID (Col. 1), the offsets in right ascension and declination (Cols. 2 and 3) from the center (as defined in Guhathakurta *et al.* 1996) in arc-minutes, the velocity and its uncertainty (Col. 4 and 5), the V-band magnitude from either HST or ground-based photometry (Col. 6), the probability (Col. 7) of the χ^2 from the multiple measurements exceeding the observed value by chance (blank if there is only a single measurement), and the ID (Col. 8) from Aurière & Cordoni (1981). The ID in Col. 1 is that of the HST WFPC2 photometry of Guhathakurta *et al.* (2000). When those did not exist we generated our own sequence numbers starting with 40001. The reported velocity is the classical mean of all of the measurements for that star, each weighted by the inverse of the square of the measurement uncertainty. The uncertainty in the mean is derived classically as well and will not be a good estimate of the true uncertainty when the χ^2 probability is low. Table 2 lists the individual velocity measurements from the eight epochs of data. The zero-point correction discussed above has been applied to the AO velocities, so all of the sets are consistent with the zero-point of PSC (we note that the Fabry-Perot velocities from 1991 to 1994 are the same as in Gebhardt *et al.* 1997; however, the 1995 FP velocities are 0.6 km s^{-1} larger due to a better estimate of the zero-point). There was no zero-point correction for either the Drukier or the Dubath data. In contrast, the additional uncertainties that we have adopted — 3 km s^{-1} for the present dataset, 1.5 km s^{-1} for FP95, 2.0 km s^{-1} for FP94, 1.5 km s^{-1} for FP92, 1.5 km s^{-1} for FP91, 0.7 km s^{-1} for PSC, 0.7 km s^{-1} for Drukier, and 0.7 km s^{-1} for Dubath — have not been included in the listed uncertainties. These additional uncertainties were used to calculate the velocity uncertainties and the χ^2 probabilities given in Table 1.

In Gebhardt *et al.* (1997), there is an inconsistency between the IDs of the stars in their Table 1 compared to those in their Table 2. For this reason we do not repeat those IDs in Table 1 here, instead introduce new IDs which are consistent between the two tables presented in this paper. Since all of the velocity data is provided in Table 2, there is no need for a cross-reference with previous papers.

3. RESULTS

The total velocity sample for M15 yields 1773 stars with a mean cluster velocity of -107.5 ± 0.2 km s^{-1}. Only the sampling uncertainty is included in the standard deviation. The AO dataset contains 104 stars with velocity uncertainties smaller than 10 km s^{-1}. Keeping only the best data based on visual inspection of the profiles provides a sample of 82 stars, but does not significantly alter the results; we thus use the full dataset in the following dynamical analysis. Given a total sample of 1773 stellar velocities, the 104 stars measured here only provide very modest gains in the total sample size. However, we stress that these measurements are in the central regions, where it is crucial to determine the kinematics accurately, as these regions are of the most importance for measuring the current dynamical state of the cluster.

In the central 1.5″ radius, there are five stars (the first five listed in Table 1) with velocities that the present dataset measured more accurately than previous datasets. The line profiles from the AO dataset for four of the five stars are shown in Fig. 11. One of these five stars, AC215 (number 5933 in Table 1 and Fig. 11), is a potential binary based on three epochs of observations; however, a detailed binary analysis will be the subject of a future paper. Another, AC214 (number 5831 in Table 1 and Fig. 11), is at least three stars (HST IDs 5831, 5846, and 5872) according to the photometry of Yanny *et al.* (1994) and Guhathakurta *et al.* (1996). These authors point out that this clump of stars is a candidate for the center of the cluster and note that the velocities of the stars should differ by $\geq$40 km s^{-1} if the center contains $\geq 10^3$ M$_\odot$ concentrated within the approximately 1000 AU projected extent of the clump. Since we have not separated AC214 into three components, we could only measure these velocity differences by a broadening of the average line profile. Our fitted profile for this object is not larger than what we measure for the other stars in the sample. However, one of the three stars, ID 5831, is 0.8 and 2.0 magnitudes brighter in the I band than the other two. It is also the reddest, hence the most strong-lined, of the three (which lie on the horizontal branch or its transition to the asymptotic giant branch; Guhathakurta *et al.* 1996), so it is likely that our measured profile mostly reflects that of this star. In any case, the signal-to-noise of the spectrum is very poor—likely due to the PSF fitting being confused by the three components and the variable seeing—making any firm conclusions impossible.

With only a small number of new velocity measurements compared to the previous study by Gebhardt *et al.* (1997), we do not present a complete dynamical analysis of M15. Since, however, all of the velocities in this study are in the central 20″, we present the kinematic state of the central regions of M15. The previous dataset for M15 contained 15 stars inside a radius of 2.5″. The present data adds eight new stars, and confirms the velocity measurements for most of the original 15 stars. With such small samples, it is important to have multiple measurements to secure the velocities. Two competing complications explain why we were not able to measure velocities for all of the stars in the previous samples: crowding and stellar flux. The AO system does allow for better separation of crowded stars; however, it requires more light due to the greater number of pixels over which a star is spread. Thus, our previous non-AO observations achieved fainter flux limits, whereas the AO system provided better separation in the most crowded regions. In total, there are 34 new velocity measurements from the AO system, all for stars at radii less than 17″.

3.1. *Kinematics Inside 20″*

Our goal here is to measure the moments of the velocity distribution as functions of radius to constrain the dynamical state of M15. The second moment about the mean cluster velocity represents a straight-forward quantity that can be directly compared to dynamical models. A more difficult measurement is determining the amplitude of the projected net rotation (v) and projected velocity dispersion (σ) separately; it is especially difficult for systems such as globular clusters, where v/σ is small. We estimate each of these quantities in turn below.

Fig. 12 plots the radial profile for the second moment of the velocity distribution for M15. The solid and dashed lines represent an estimate and its associated 90% confidence band obtained using the LOWESS technique described in Gebhardt *et al.* (1994). At around 2′, the density of points decreases drastically as we shift from Fabry-Perot data to other datasets. Due to the change in density, our LOWESS technique artificially biases the second moment in the lower density regions towards that in the higher density regions. This bias results from our windowing function, which includes a set number of data points rather than a specified radial range. For that reason, we do not use the LOWESS estimate at these radii and instead rely on radially binned values taken from Drukier *et al.* (1998, Col. 2 of Table 4). A bias may occur at small radii as well, if both the density of data and the value of the second moment change dramatically over a small radial range. We thus also estimate the second moment in a central bin containing the inner ten stars. The solid points in Fig. 12 and their 68% error bars are these binned values.

The value of the second moment for the central ten stars, with an average radius = 1″, is 11.7 ± 2.8 km s^{-1}. The second moment remains approximately constant out to a radius of 30″, a value and trend identical to those found previously (Gebhardt *et al.* 1997).

Gebhardt *et al.* (1997) suggest that the projected rotation increases within 3″ of the center of M15 and that the position angle of the projected rotation axis there differs by 100° from that at larger radii. This estimate came from the integrated cluster light, as there were too few individual stellar velocity measurements to constrain the rotation. With the additional velocity information from the AO dataset, we can measure the rotation from the stars alone. We are interested in looking for significant changes in the rotation over a small radial range. Smoothing techniques, such as the LOWESS technique, tend to wash out small scale features. Although techniques based on binning do not suffer from this particular effect, they are sensitive to the subjective choice of bin width and bin location. We have tried to preserve the better features of both techniques by using a hybrid approach: a variable-width data window in radius with lower weights for the points near the window edges. The variable-width window allows for recovery of sharp radial variations, and the weighting scheme is designed to lessen possible large variations due to discrepant datapoints.

We apply the data window to the velocities sorted into radial order. The window contains 251 points, except that it shrinks to a minimum of 25 points at the inner and the outer boundaries of the data. At each position of the window a maximum likelihood estimator determines the rotation amplitude, rotation position angle (PA), and dispersion about the rotation. Within each bin, the weight of a point varies as the cube of its distance from the bin center – i.e., $w_i = 1-(|i-n/2|)^3/(n/2)^3$, where n represents the number of points in the subsample and i is that point's rank in the sorted dataset. This weight multiplies that point's contribution to the likelihood function. The likelihood function minimizes the deviations of the velocities minus the cluster systemic velocity from a mean velocity that varies sinusoidally as a function of position angle. A sinusoidal variation is expected for solid-body rotation. However, for other rotation profiles, a sine function may not be optimal for measuring the rotation amplitude. The radius corresponding to each position of the window is the average of the linear radii of the included points.

Fig. 13 plots the results from the hybrid technique for the following four quantities, each with their 68% confidence bands: the projected rotation amplitude, the dispersion about the rotation, v/σ, and the PA of the projected rotation axis. Significant rotation exists at most radii in the cluster; only at $0.3'$ is the net rotation near zero, causing the PA estimate to fluctuate rapidly near that radius. Most surprising is the rotation seen at small radii. Inside of $0.05'$, the rotation amplitude rises significantly and, at $0.04'$, the rotational support equals the pressure support (i.e., $v/\sigma = 1$). Fig. 14 displays this rotation directly by plotting the offset from the mean cluster velocity for the 40 stars in the central $3.4''$ vs. azimuth. The rotation amplitude for these stars is $v = 10.4 \pm 2.7$ km s^{-1} and the dispersion after removing the rotation is $\sigma = 10.3 \pm 1.4$ km s^{-1}, so $v/\sigma \simeq 1$ in this region. The probability of measuring a rotation this high by chance when none is present is much less than 1%. Fig. 13 suggests that the rotation amplitude remains high into the center. Even for the five stars inside of $1''$, the rotation has the same position angle and an amplitude equal to 15.3 ± 6.2 km s^{-1}. For these five stars, a rotation amplitude this large is expected by chance only 5% of the time.

The confidence bands in Fig 13 result from a Monte-Carlo analysis. We create 100 realizations of the velocity sample by drawing points from the initial fit to the rotation as a function of radius. To each point we add random uncertainties that come from the data uncertainty distribution, determined by the velocity difference of the individual measurements relative to the rotation profile; this procedure includes both the velocity dispersion and the individual velocity uncertainties. To mimic the radial variation of dispersion and uncertainty in the data (the velocities at large radii primarily come from Drukier *et al.* (1998), which are on average more precise than the FP velocities), we have drawn the additive uncertainties from radial bins. For each realization, we estimate the radial variation of the kinematics as we did for the observed data. The scatter in the distribution of the kinematical properties at each radius provide the 68% confidence bands.

4. MASS MODELING

Since our dataset is not dramatically larger than in our previous analysis, we have not re-computed the mass density profile and the stellar mass function. Instead, we concentrate on the central dynamics and, in particular, black-hole models, since the most important changes in the dataset are at small radii.

Figure 15 plots both the actual second moment profile of the data from Fig. 12 and the expected second moment profiles for models with no rotation, an isotropic velocity dispersion tensor, a constant stellar M/L, and black holes of various masses. We construct the models from the surface brightness profile used in Gebhardt *et al.* (1997). The deprojection of that profile determines the potential, assuming a constant $\mathrm{M/L_V} = 1.7$. We add black holes of various masses to this potential and calculate the projected second moments using the isotropic Jeans equation. The model that best matches the data, given these assumptions, contains a 2000 $\mathrm{M}_\odot$ black hole. The full range of acceptable black hole masses is 0 to 4000 $\mathrm{M}_\odot$. Alternatively, the data are consistent with models with no black hole that have a stellar $\mathrm{M/L_V}$ that increases towards the center to a value of 5, possibly due to a central concentration of white dwarfs or neutron stars.

An additional, and probably more interesting, constraint to the dynamical models comes from our observed rotation profile. The AO data argue that net rotation exists inside of $3.4''$ (1.7 parsecs) with greater than 99% confidence and the best estimate of the rotation amplitude yields $v/\sigma = 1.0$. The innermost 40 stars have an average radius of $2.1''$ and a projected rotation amplitude of 10.4 km s^{-1}. Assuming pure rotational support, this amplitude implies a central mass concentration equal to 2500 $\mathrm{M}_\odot$. Net rotation this large at these small radii is surprising, but might be easier to explain with the presence of a few thousand solar mass black hole.

5. SUMMARY AND DISCUSSION

Two of the most obvious and interesting features of the M15 kinematics are the increase in the rotation amplitude at small radii, where $v/\sigma \simeq 1$, and the difference in the rotation axis PA at those same radii compared to the rotation of the rest of the cluster. The cluster 47 Tuc also shows more rotation than expected at small radii (Gebhardt *et al.* 1994), though less dramatically than M15. These two clusters have the largest velocity datasets presently available, suggesting that large central rotation may be a common feature among centrally-concentrated globular clusters. Can these features be understood in the context of dynamical evolution producing a collapsed core? Or does the rapid increase in net rotation suggest the presence of a central massive black hole? Unfortunately, few theoretical studies of cluster dynamical evolution include net rotation. Studies of the effects produced by central black holes in rotating systems are also rare.

5.1. *Rotation and Core Collapse*

The exchange of stellar energies and momenta caused by two-body relaxation acts to eliminate gradients in the mean velocity and, thus, to create solid-body rotation in a cluster with a net angular momentum (e.g., Ogorodnikov 1965). However, this equilibrium may not be stable, so the real evolution of a cluster can be more complex. Hachisu (1979) was one of the first to point out the gravo-gyro instability, where the central regions shrink and then spin up to maintain virial equilibrium as relaxation transports angular momentum outwards. This requires that the rotation supply significant support against gravity. N-body simulations of clusters with equal-mass stars by Akiyama & Sugimoto (1989) suggest that the random velocities eventually increase more rapidly than the net rotation, so that v/σ decreases and the cluster again tends towards solid body rotation. Similar N-body simulations by Arabadjis & Richstone (1998a) found that the flattening (and, presumably, the v/σ) of the central regions decreased more slowly when a spectrum of stellar masses was present. But it still decreased or, at best, remained constant.

The N-body simulations were unable to follow the collapse of the core very far because they only had N = 1000 and 3000, respectively. Einsel & Spurzem (1999) studied the dynamical evolution of a rotating globular cluster by numerically solving the Fokker-Planck equation to follow the change in the stellar distribution function. The clusters are tidally limited and contain stars of only a single mass. These simulations have much less noise than N-body models, though they are also too simple for confident comparison with real clusters. In their simulations, the net rotation velocity in the core increases rapidly at first, probably driven by the gravo-gyro instability, and then more slowly, at the same rate that the central velocity dispersion increases as the core collapses. However, there is only a small increase in v/σ in the core and certainly no steep gradient in this quantity near the center. The amount of rotation at large radii decreases, but the maximum mean rotation velocity always occurs at about the half-mass radius. This result is consistent with our data outside of the central few arcseconds, for which the maximum rotation velocity occurs at $0.9'$– approximately the half-mass radius for M15.

Preliminary multi-mass Fokker-Planck simulations (Einsel 1999) do show a larger increase in the net rotation for the most massive stars in the cluster center, perhaps similar to the results of Arabadjis & Richstone (1998a). These models need further testing, however, and are also being checked with additional N-body simulations (Spurzem, private communication). If the giants whose radial velocities we measure are the heaviest stars in the cluster and have been concentrated in the core by mass segregation, then we would expect the central mass-to-light ratio to be lower than that of the rest of the cluster. Figure 7 of Gebhardt *et al.* (1997) suggests that the mass-to-light ratio increases at small radii, though the uncertainties are large enough that a decrease can not be ruled out.

An argument against core collapse being the explanation for the rotation at small radii in M15 is the large change in the position angle of the apparent rotation axis. None of the simulations discussed above have any torque that could produce what is nearly counter-rotation. Tidal forces from our Galaxy can exert torques and will act differently on the inner and outer regions of the cluster. We would naively expect any resulting change in the rotation axis to occur at much larger radii. Perhaps gravitational coupling such as that in warped disks could align the rotation over most of the cluster, but the nearly spherical shape of M15 must make that weak and we see no reason that small radii would be exempted. Two-body relaxation also acts to align rotation throughout the cluster and should be most effective at small radii, where the relaxation time is short.

In summary, models of globular cluster dynamical evolution do not seem to produce the changing rotation axis position angle and the v/σ profile with a sharp central upturn that we observe in M15. The models might be more successful in explaining the more moderate departure from solid-body rotation in 47 Tuc. More simulations, particularly with models containing a range of stellar masses are needed, but we now turn to whether models with central black holes can explain the M15 data.

5.2. *Rotation and a Central Black Hole*

Whether M15 contains a massive black-hole remains a central question for black-hole demographics and has been the subject of much debate, starting with the discovery of a central x-ray source (Giacconi *et al.* 1974, Bahcall & Ostriker 1975) and revived more recently by the velocity dispersion measurements of Peterson *et al.* (1989). From dynamical studies of galaxies, Kormendy & Richstone (1995) and Magorrian *et al.* (1998) find a relation between the mass of the black-hole and the mass of the host galaxy. This relation is based on massive stellar systems (M32 being the smallest) and we have not yet explored its extrapolation to smaller systems. Possibly all hot stellar systems harbor a central massive black hole; this situation would have significant consequences in modeling these systems, and may even suggest that black holes act as a seed for hot stellar systems. Globular clusters are the natural targets to answer such a hypothesis due to their low mass. M15 is particularly well suited for these studies due to its proximity (9 kpc) and the high surface brightness of its cusp.

Bahcall & Wolf (1976) calculated the mass density and velocity dispersion profiles for the region of a non-rotating globular cluster influenced by a central black hole. The dispersion profile in Fig. 12 is consistent with their prediction, but we still do not have the spatial resolution necessary to choose between the models presented there. Detailed analysis by Sosin & King (1997) of the central stellar cusp in M15 found that neither the black hole model of Bahcall & Wolf nor pure core-collapse models are a good match to the light profile. More sophisticated dynamical models, perhaps combining a black hole with core collapse, are necessary.

Lee & Goodman (1989) demonstrated that the adiabatic growth of a central black hole in a rotating stellar system increased the projected v/σ within the region of gravitational influence of the black hole (where the mass of the stars approximately equals the final mass of the black hole). However, this study did not include the effects of two-body relaxation. The presence of the black hole reduces the mass density of stars that would otherwise be deduced from the velocity dispersion and this increases the relaxation time at small radii, perhaps helping to maintain a larger rotation. However, this time remains much shorter than the age of M15 at small radii.

Arabadjis & Richstone (1998b) followed the dynamical evolution due to two-body relaxation of a system that initially had solid-body rotation and stars of a single mass (the collisional coalescence of stars was allowed) and contained a central black hole. The rotation amplitude and dispersion both increased near the center as the system evolved, however, v/σ was essentially constant in time. The radial profile of v/σ at late times was flat. These conclusions are somewhat weakened by the noise in these N-body simulations (N = 3000), which makes it hard to determine kinematic quantities over a large range of radii.

Thus, while the models of Lee & Goodman (1989) are suggestive, Fokker-Planck simulations including a black hole and net rotation are probably needed to reach any definite conclusions. A central black hole with a mass of about 2500 $M_\odot$ is consistent with all of the dynamical data (we note that this mass is consistent with that from Phinney's (1993) estimate of the enclosed mass from pulsar timing measurements near the center of M15). However, this model also provides no clear explanation for the changing rotation axis position angle. Becoming (even) more speculative, stars formed in a disk of gas, accreted from outside of the cluster, might explain the rotation with or without a central black hole. The color-magnitude diagram for the inner region provides, at most, only a little evidence for a younger stellar population at small radii (Guhathakurta *et al.* 1996, De Marchi & Paresce 1995, Sosin & King 1997).

5.3. *The Potential of Adaptive Optics*

The high angular resolution provided by the Adaptive Optics Bonnette on the CFHT have strengthened some of the most surprising results in our previous M15 velocity samples. While the increase in the sample size was modest, the AO data provided crucial confirmation and, hence, better velocity uncertainties for many of the stars closest to the cluster center. Even more importantly, the AO observations increased the size of the velocity sample in this critical region. As adaptive optics systems become better understood and available on larger telescopes, and as the data analysis tools become better tailored to these observations (i.e., larger and better sampled PSFs), we will be able to greatly improve our measurements of the kinematics near the center of M15 and other core-collapse globular clusters.

Our AO observations have Strehl ratios of 2 – 6%. Even under these poor conditions for AO corrections, we were able to obtain photometry with errors less than 2%. Of course, our observations were the best of all worlds for photometry since we had bright stars everywhere in our field. The ability to extend this detailed understanding of the spatial and temporal variation of the PSF to observations where only a handful of calibration stars are present is not clear. Surely, present and future AO studies will deal with this concern.

We are indebted to the CFHT staff who spent long hours setting up a very difficult instrument configuration and who were able to provide us with 0.09″ FWHM images after 1 hour on the sky! KG thanks Jerry Nelson and Sandy Faber for many discussions about the AO observations and reductions. KG is supported by NASA through Hubble Fellowship grant HF-01090.01-97A awarded by the Space Telescope Science Institute, which is operated by the Association of the Universities for Research in Astronomy, Inc., for NASA under contract NAS 5-26555. The globular cluster research of TW and CP is supported by grant AST96-19510 from the National Science Foundation.

REFERENCES

Akiyama, K., & Sugimoto, D. 1989, PASJ, 41, 991
Arabadjis, J.S., & Richstone, D.O. 1998a, preprint astro-ph/9810192
Arabadjis, J.S., & Richstone, D.O. 1998b, preprint astro-ph/9810193
Aurière, M., & Cordoni, J.-P. 1981, A&A, 138, 415
Bahcall, J.N., & Ostriker, J.P. 1975, Nature, 256, 23
Bahcall, J.N., & Wolf, R.A. 1976, ApJ, 209, 214
Beers, T.C., Flynn, K., & Gebhardt, K. 1990, AJ, 100, 32
Cohn, H. 1980, ApJ, 242, 765
De Marchi, G., & Paresce, F. 1995, A&A, 304, 202
Djorgovski, S., & King, I.R. 1986 ApJ, 305, L61
Drukier, G., Slavin, S., Cohn, H., Lugger, P., Berrington, R., Murphy, B., & Seitzer, P. 1998, AJ, 115, 708
Dubath, P., & Meylan, G. 1994, å, 290, 104
Dubath, P., Meylan, G., & Mayor M. 1995, ApJ, 426, 192
Dull, J.D. *et al.* 1997, ApJ, 481, 267
Einsel, C. & Spurzem, R. 1999, MNRAS, 302, 81
Einsel, C. 1999, in “Dynamics of Galaxies and Galactic Nuclei” eds W.J. Duschl, C. Einsel, I.T.A. Series, No.2, Heidelberg, in press
Esslinger, O., & Edmunds, M. G. 1998, A&AS, 129, 617
Gebhardt, K., Pryor, C., Williams, T.B., Hesser, J.E. 1994, AJ, 107, 2067
Gebhardt, K., Pryor, C., Williams, T.B., Hesser, J.E. 1995, AJ, 110, 1699
Gebhardt, K., Pryor, C., Williams, T.B., Hesser, J.E., & Stetson, P.B. 1997, AJ, 113, 1026
Giacconi, R., Murray, S., Gursky, H., Kellogg, E., Schreier, E., Matilsky, T., Koch, D., & Tananbaum, H. 1974, ApJS, 27,37
Grabhorn, R. P., Cohn, H. N., Lugger, P. M., & Murphy, B. W. 1992, ApJ, 392, 86
Guhathakurta, P., Yanny, B., Schneider, D., & Bahcall, J. 1996, AJ, 111, 267
Guhathakurta, P. *et al.* 2000, in preparation.
Gunn, J.E. & Griffin, R. F. 1979, AJ, 84, 752
Hachisu, I. 1979, PASJ, 31, 523
King, I.R. 1975, in IAU Symposium No. 69, “Dynamics of Stellar Systems”, ed. A. Hayli (Dordrecht:Reidl), p.99
Kormendy, J. & Richstone, D. 1995, ARA&A, 33, 581
Lee, M.H., & Goodman, J. 1989, ApJ, 343, 594
Magorrian, J. *et al.* 1998, AJ, 115, 2285
Mayor, M. *et al.* 1983, A&AS, 54, 495
Newell, B., Da Costa, G.S., & Norris, J. 1976, ApJ, 208, L55
Ogorodnikov, K. F. 1965, Dynamics of Stellar Systems, translated from the Russian by J. B. Sykes (Oxford: Pergamon)
Peterson, R.C., Seitzer, P., & Cudworth, K.M. 1989, ApJ, 347, 251 (PSC)
Phinney, E.S. 1993, in Structure and Dynamics of Globular Clusters, eds. S.G. Djorgovski and G. Meylan, ASP Conf. Ser. No 50 (ASP, San Fransisco), p.141
Rigaut, F., Salmon, D., Arsenault, R., Thomas, J., Lai, O., Rouan, D., Véran, J. P., Gigan, P., Crampton, D., Fletcher, J. M., Stilburn, J., Boyer, C., & Jagourel, P. 1998, PASP, 110, 152
Roberts, L. C., Jr., ten Brummelaar, T. A., & Mason, B. D. 1997, AAS Meeting 191, #128.01
Sosin, C., & King, I.R. 1997, AJ, 113, 1328
Spitzer, L. 1987, Dynamical Evolution of Globular Clusters (Princeton: Princenton Univ.)
Stetson, P.B. 1994, PASP, 106, 250
Stetson, P.B. *et al.* 1998, ApJ, 508, 491
Yanny, B., Guhathakurta, P., Bahcall, J. & Schneider, D., 1994, AJ, 107, 1745
Zaggia, S.R., Capaccioli, M., & Piotto, G. 1993, A&A, 278, 415

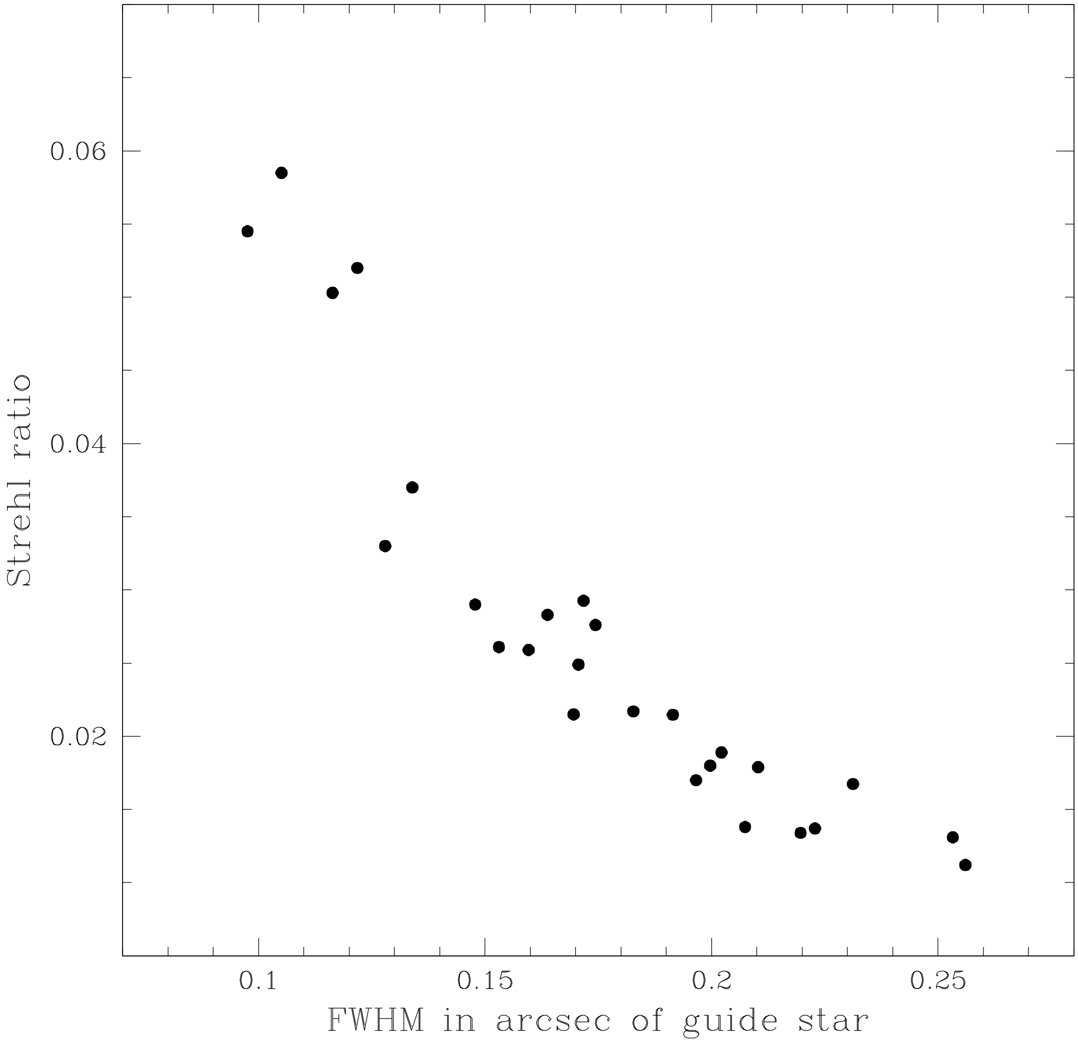

FIG. 1.— Strehl ratio of the guide star for each frame versus the FWHM.

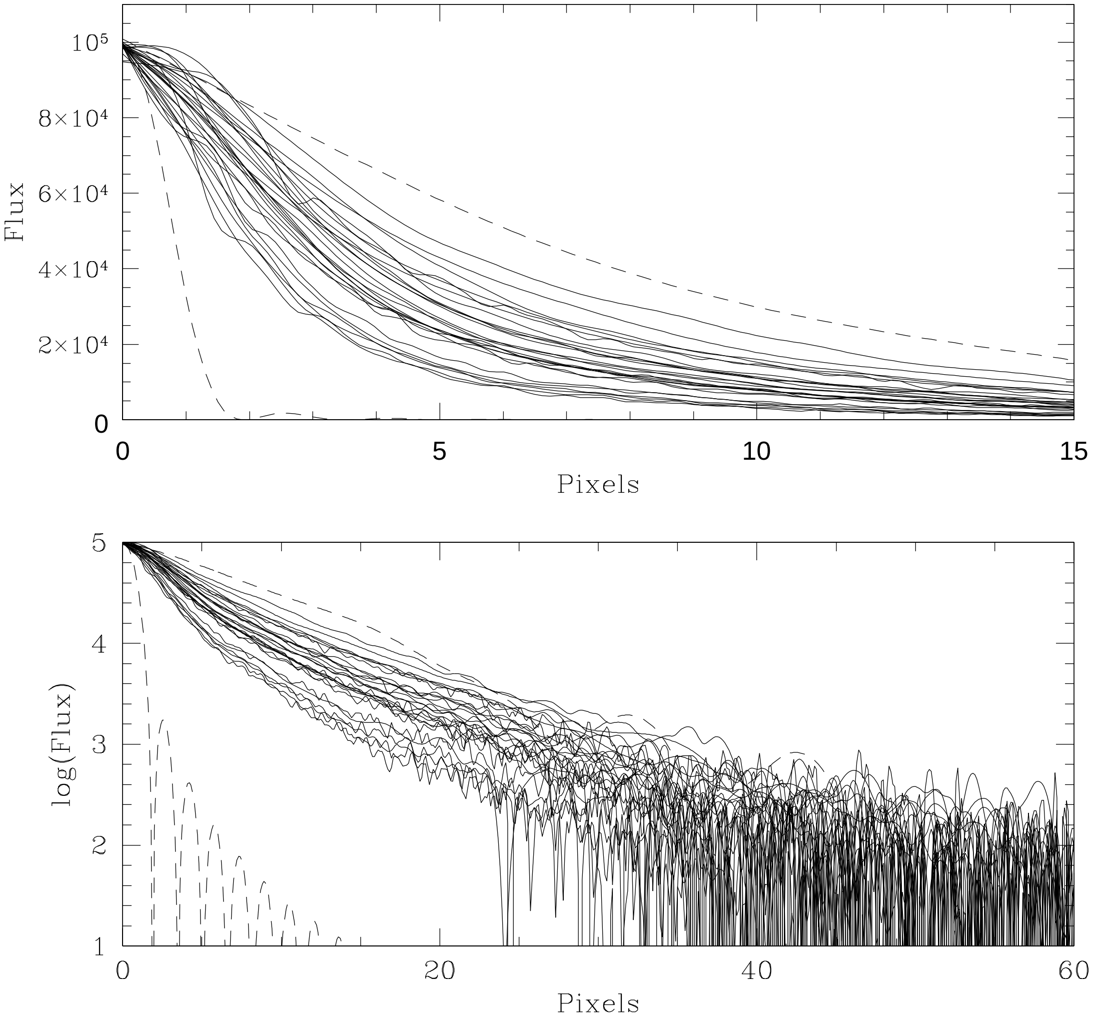

FIG. 2.— Flux of the guide star as a function of radius for each frame. The upper plot is linear and the bottom logarithmic. The solid lines represent the radial profile for the guide stars; the upper-dashed line represents an uncorrected profile (i.e., the AO system was turned off), and the bottom dashed line represents a diffraction-limited profile.

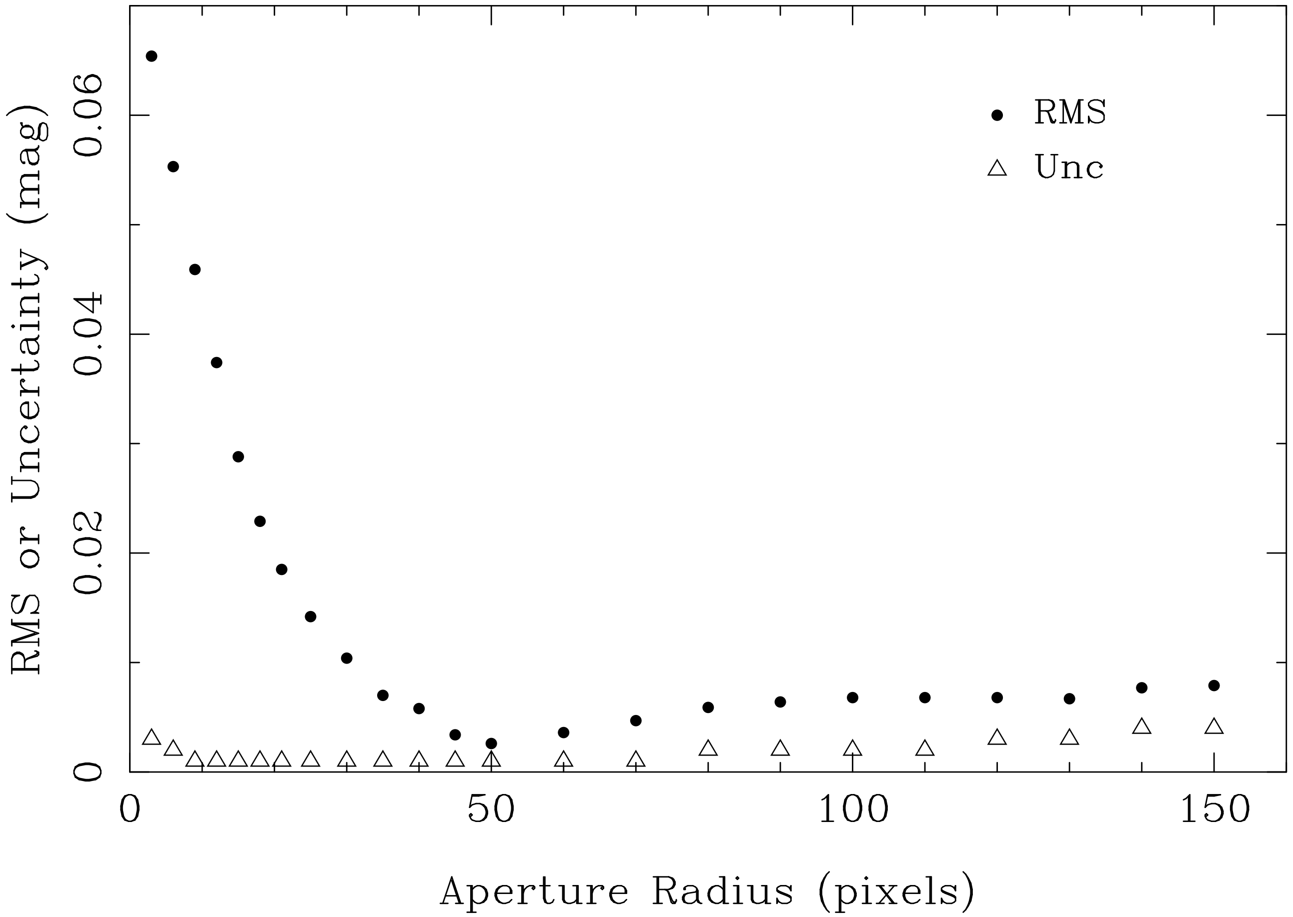

FIG. 3.— The filled circles are the RMS scatter around the average aperture magnitude for four consecutive 10 s exposures of HD107328. The aperture radii vary between 3 and 150 pixels (1 pixel = 0.0305″). The open triangles are the uncertainties in the magnitudes expected from photon statistics. Variations in the magnitudes due to variable seeing and wavefront correction contribute negligibly to the measurement uncertainties for apertures with radii larger than 50 pixels (1.5 arcsec).

fig4.jpg goes here

FIG. 4.— Four images of the central region in M15; the top two are the central $9''$ square and the bottom two are the central $15''$ square (North is up and East is to the left). The top-left image is the best-seeing CFHT/AOB frame with $0.09''$ FWHM displayed using a linear stretch. The top-right panel is an HST image taken from Guhathakurta *et al.* (1996). The bottom-left image is a larger region of the same CFHT image displayed with a square-root stretch to reveal the fainter signal levels. The bottom-right image is the star-subtracted version of its neighbor to the left, again displayed using a square-root stretch.

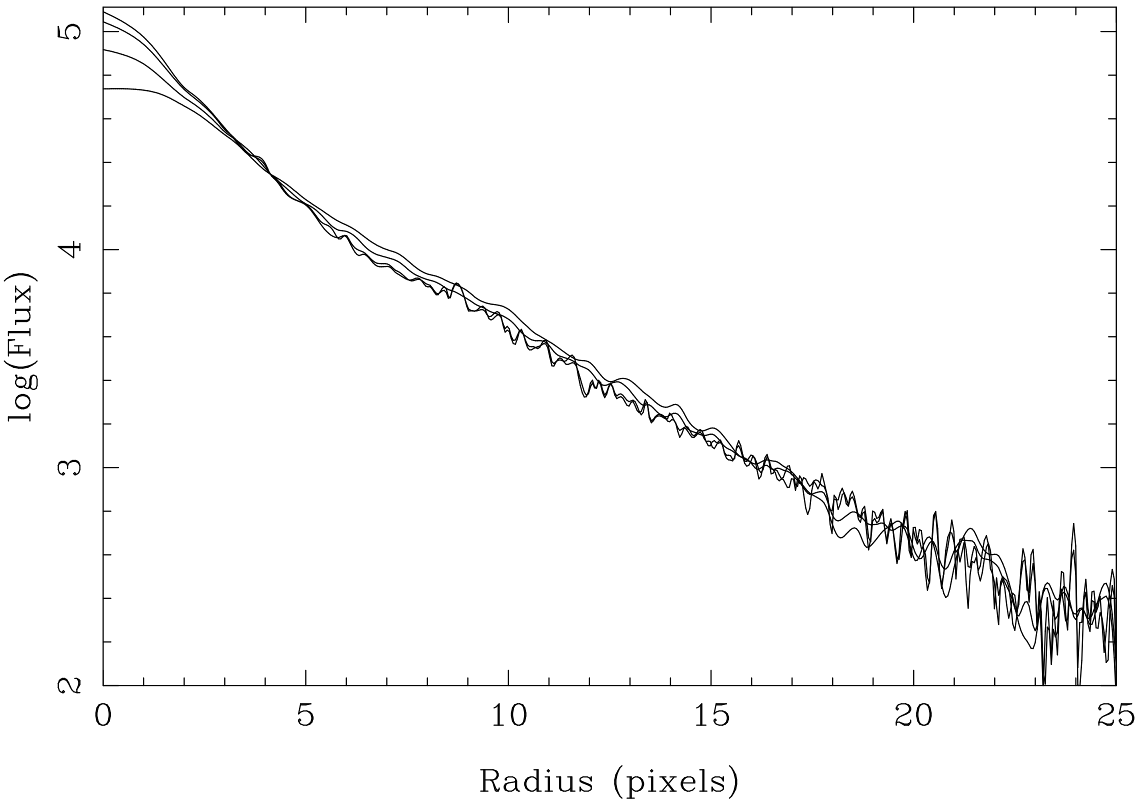

FIG. 5.— Radial profile of the PSF at four different radial positions in the frame. The PSFs are normalized to have identical volume.

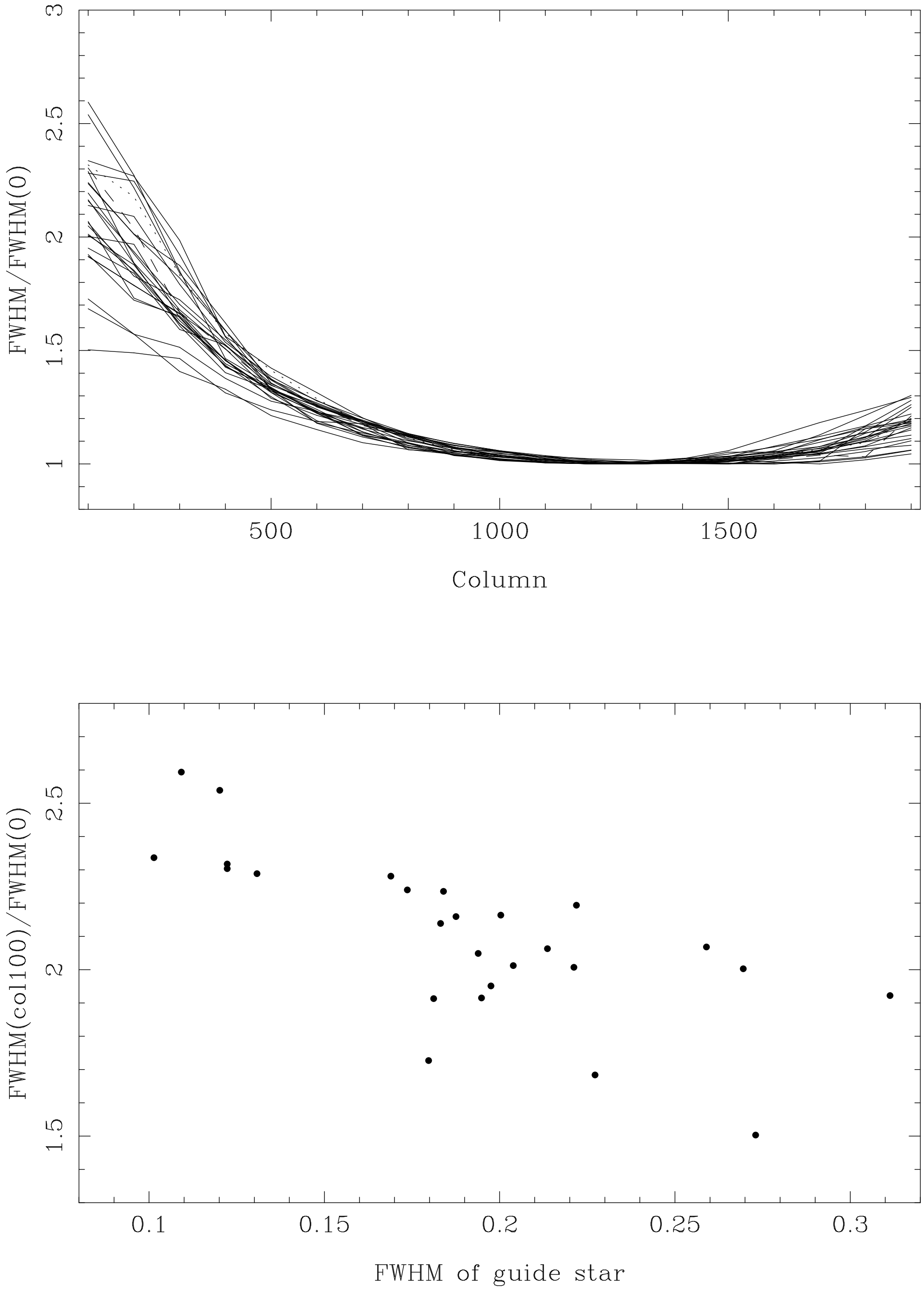

FIG. 6.— The top panel shows the variation the PSF width with CCD column number for the central row in the M15 frames. Each line is the the ratio of the FWHM of the stellar profile to the FWHM of the guide star for a frame. The bottom panel plots the FWHM ratio at the edge of each image as a function of the guide star FWHM. These points suggest that the image with the best FWHM has the largest variation across the field.

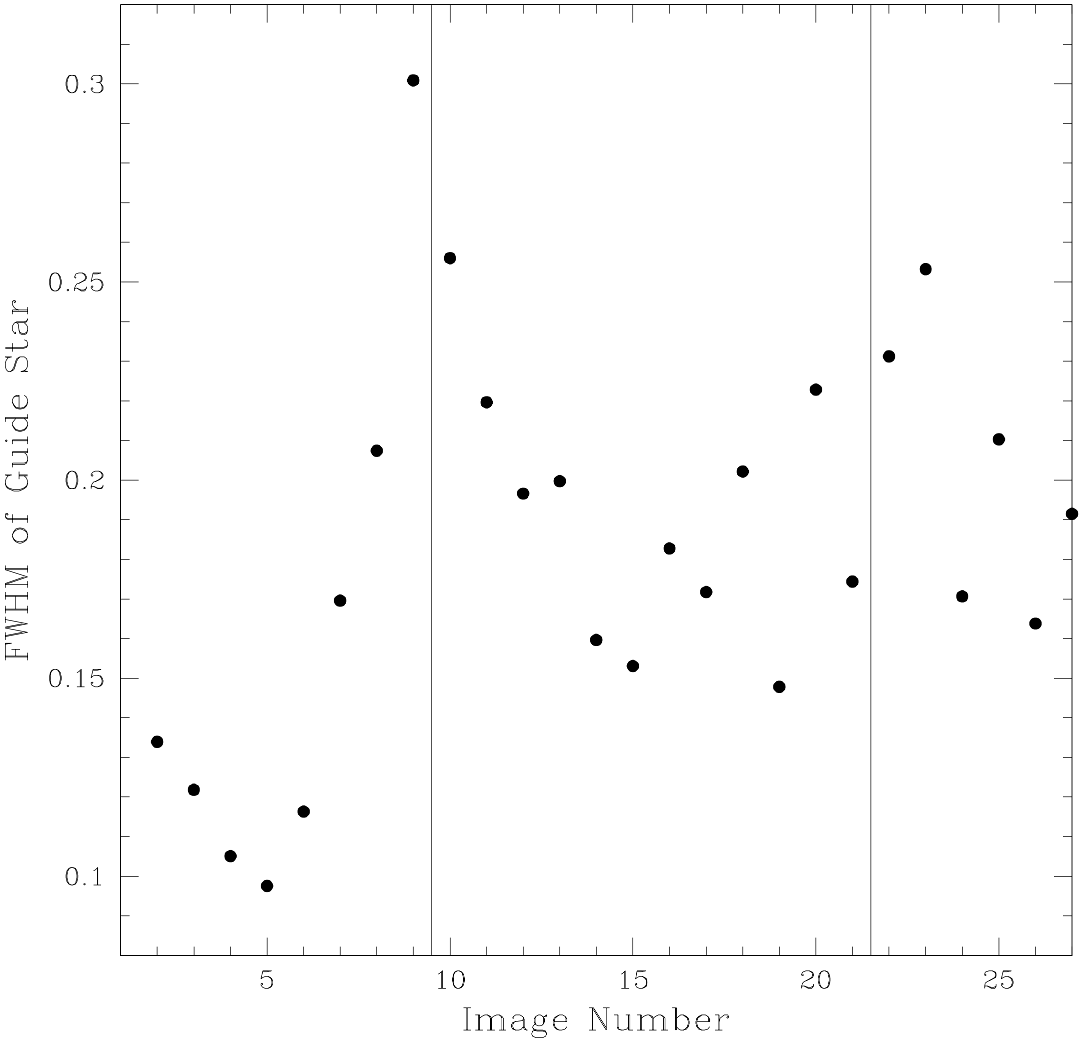

FIG. 7.— The temporal variation of the FWHM of the guide star from frame to frame. The vertical solid lines are the divisions between the nights during which we took M15 data.

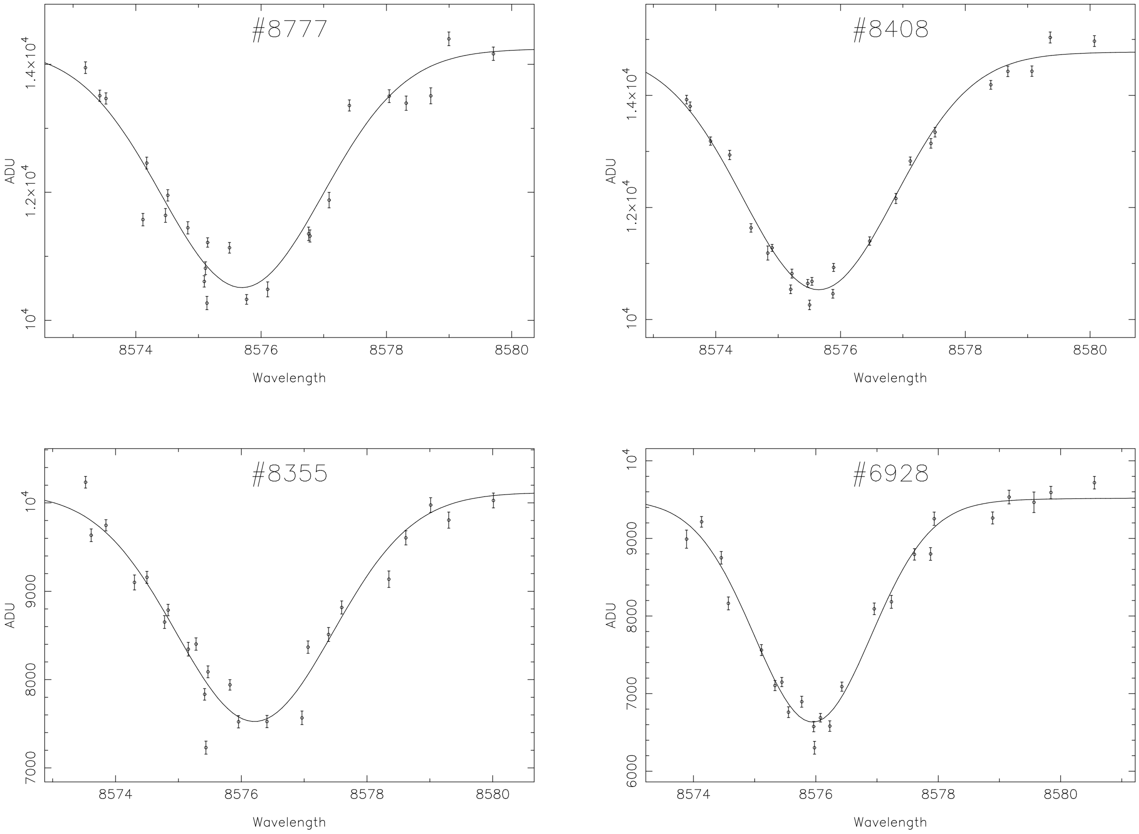

FIG. 8.— Line profiles for four bright stars for which we were able to obtain a reliable velocity measurement. The values and their error bars come from ALLFRAME and include the frame normalizations. The solid line is the fitted Voigt profile.

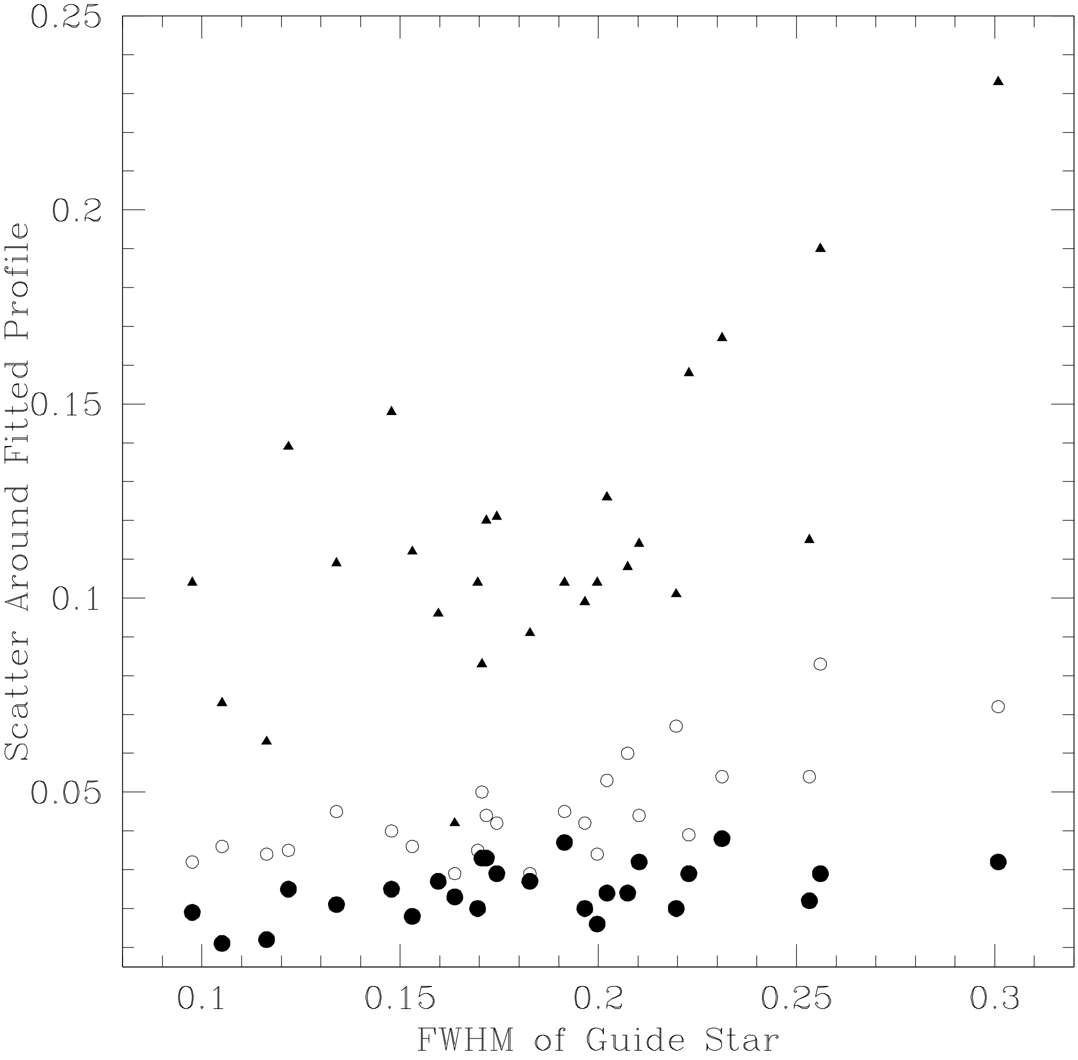

FIG. 9.— The dispersion in the fractional difference between the fitted line profile and the actual spectral data for stars in each M15 image, plotted versus the FWHM of the guide star in the image. Different symbols denote the dispersion for stars with different brightnesses: solid circles are the brightest third, open circles are the intermediate third, and solid triangles are the faintest third.

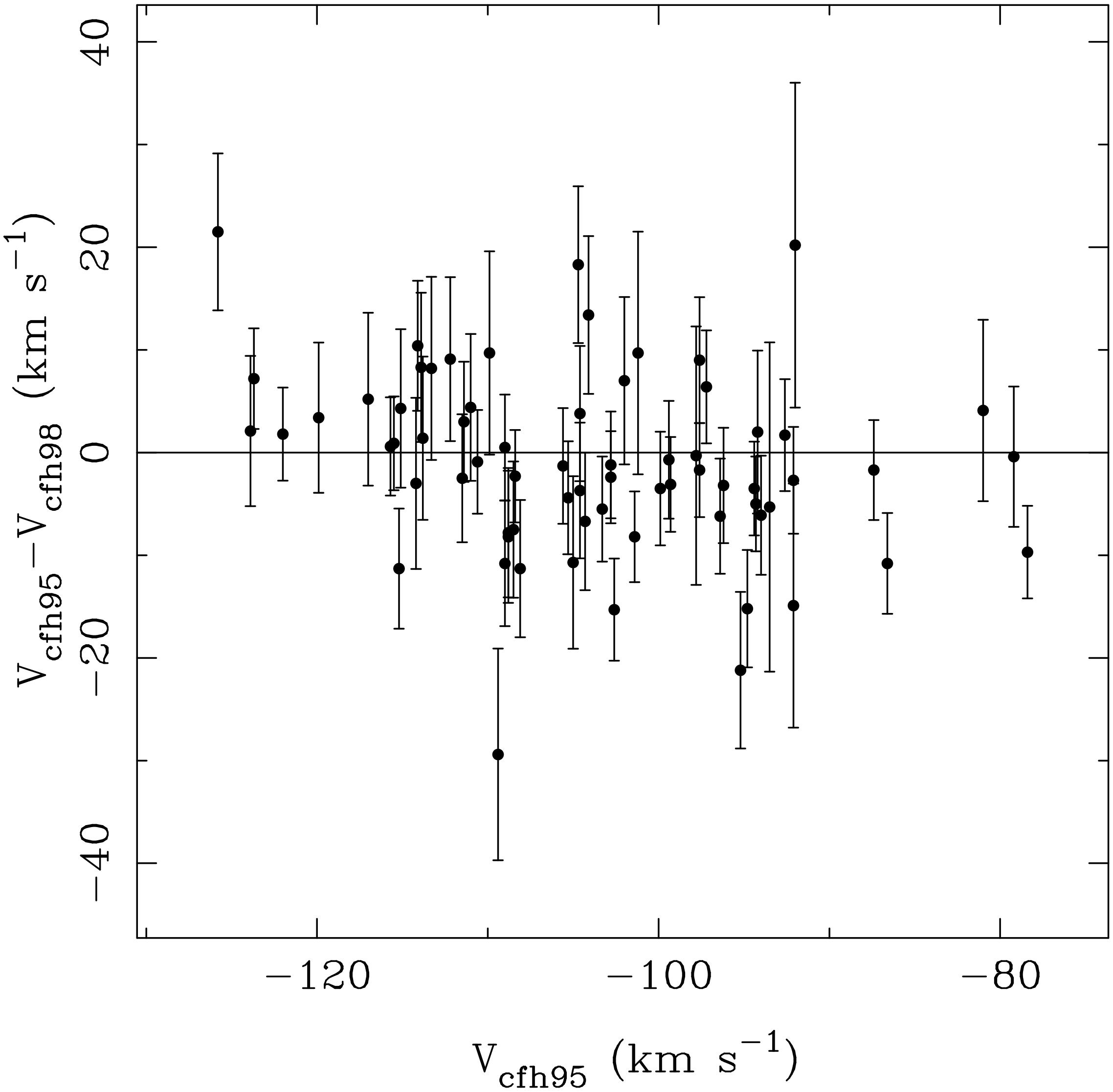

FIG. 10.— A comparison of our velocities taken at CFHT in 1995 and the velocities derived from the AO data.

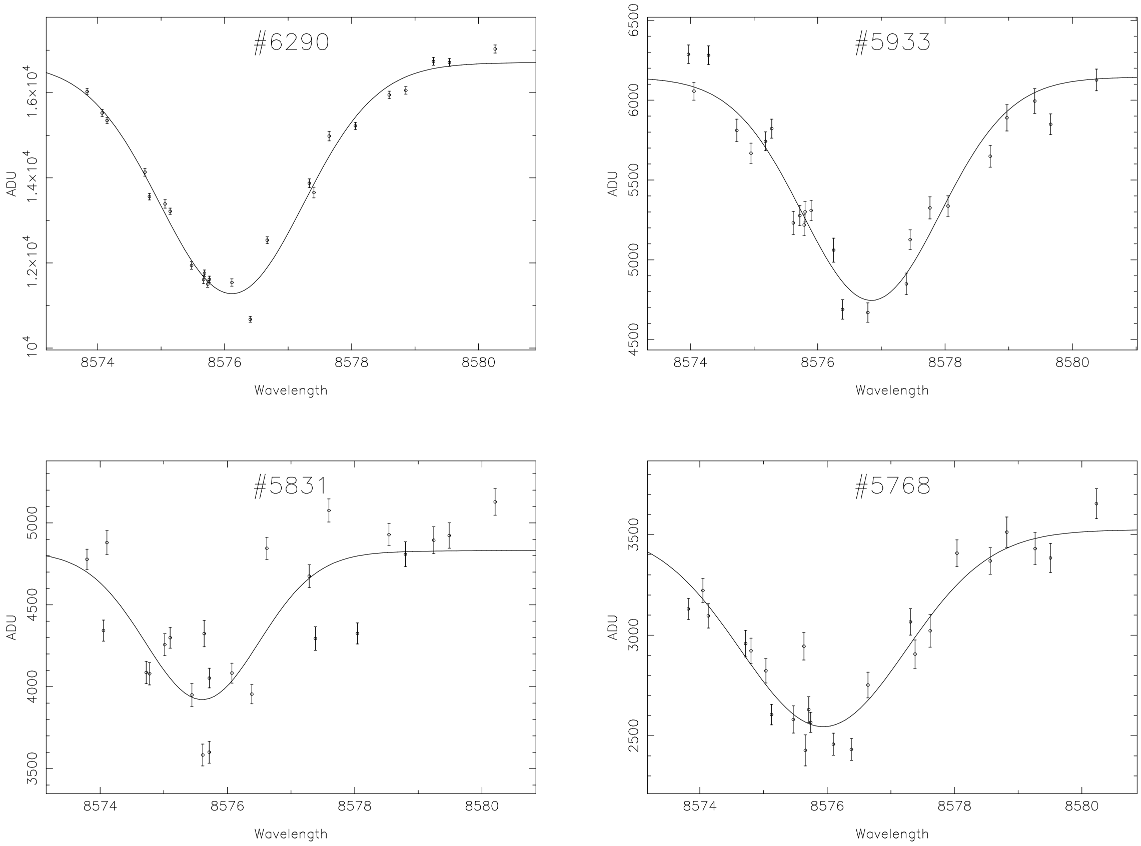

FIG. 11.— Line profiles for the four innermost stars for which we were able to obtain a reliable velocity measurement.

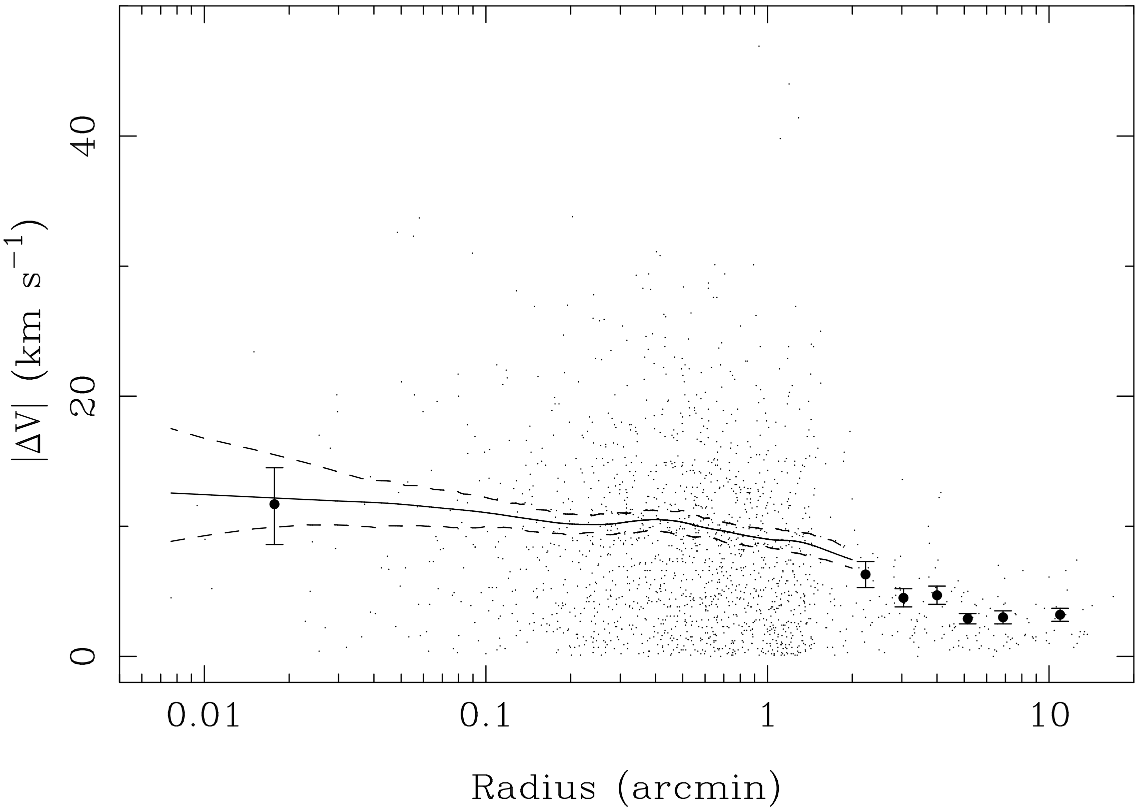

FIG. 12.— The velocity dispersion profile for M15. The small dots are the stellar velocity measurements. The solid and dashed lines represent the velocity dispersion profile and the boundaries of its 90% confidence band, respectively. At large radii, the solid points and their error bars are the binned dispersion estimates from Drukier *et al.* (1998). The inner solid point represents the dispersion measured from the innermost 10 stars of our sample.

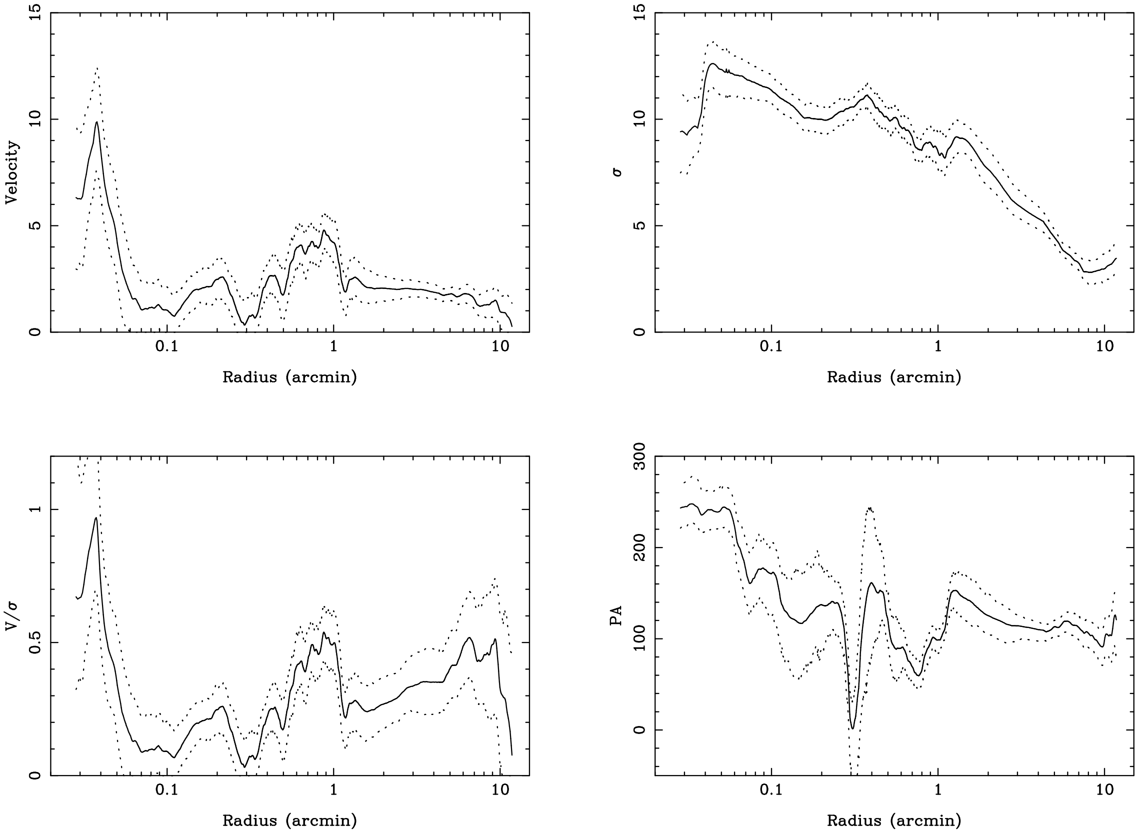

FIG. 13.— The projected rotation amplitude, velocity dispersion, v/σ, and the position angle of the projected rotation axis as functions of radius. The solid lines are the estimates and the dotted lines are the boundaries of the 68% confidence bands.

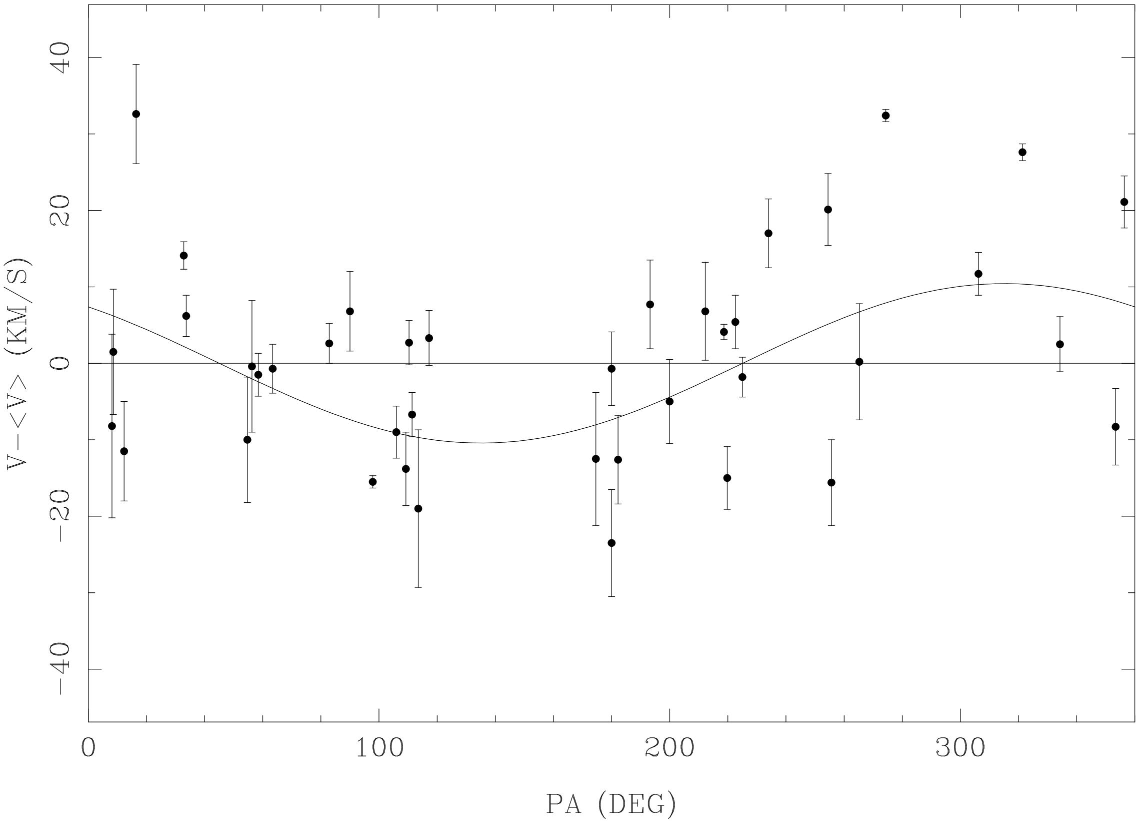

FIG. 14.— The net projected rotation for the stars in the central 3.4″. Each point is the offset of a star's velocity from the cluster mean and its uncertainty. The solid line is the best-fit sinusoid with amplitude= 10.8 ± 2.6 and PA_0 = 226 ± 14°. The dispersion around this curve is 11.9 km s^{-1}.

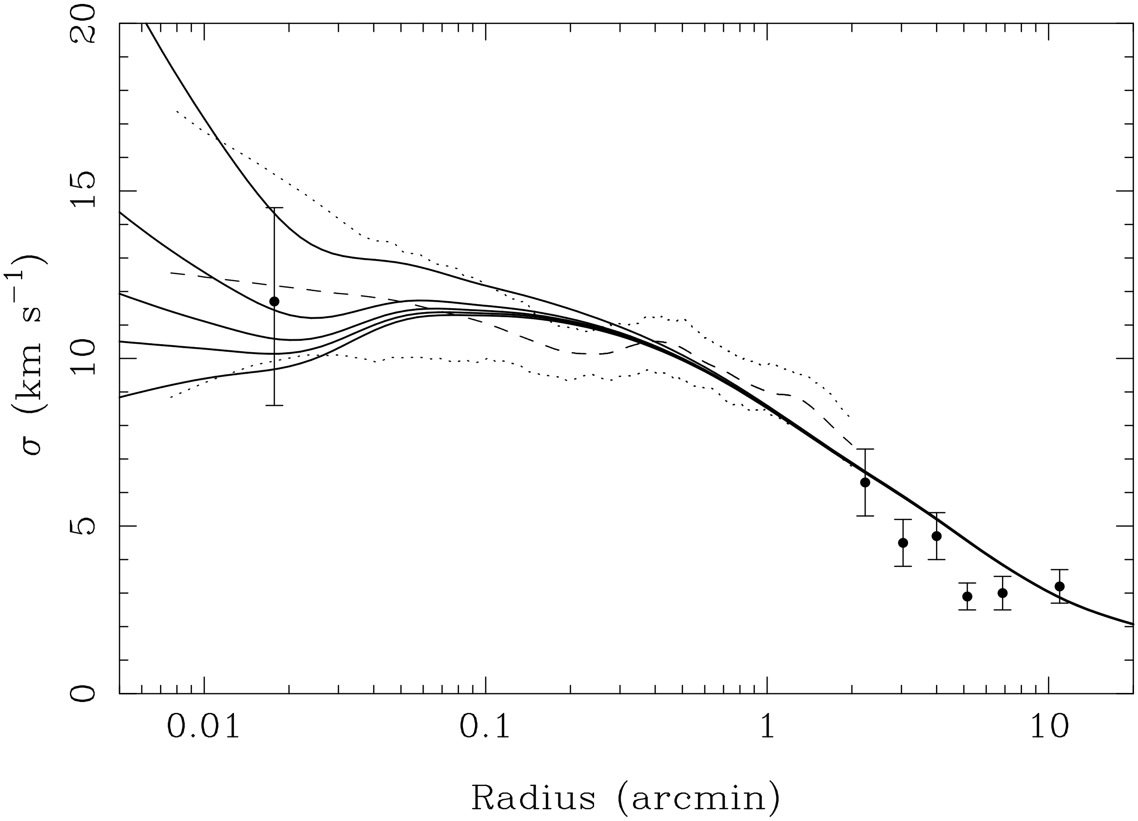

FIG. 15.— The same dispersion profile as in Fig. 12 (the dashed line) plotted with the profiles predicted by black hole models (the solid lines). The models assume isotropy, no rotation, and a constant stellar M/L$_V$ of 1.7. The masses of the black holes are equal to 0, 500, 1000, 2000, and 6000 M$_\odot$ in going from the lowest to the highest profiles.